Design and Optimization of a Micro-Aerial Vehicle

For Design/Build/Fly

Michelle Acevedo
Benjamin Andrews
Casey Brown
Christopher Cahill
Ruxandra Duca
Emily Dunham
Mitchell Lentz
Edson Novinyo
Luis Paredes
Emily Perry
Miles Schuler
Ashley Smith
Daniel Thiesse

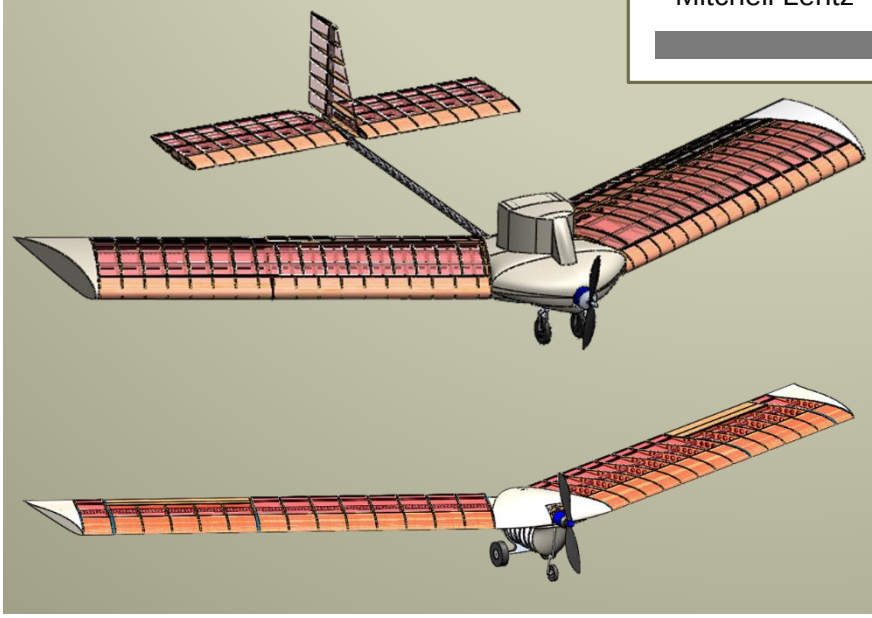

AL2-1601

Design and Optimization of a Micro-Aerial Vehicle

A Major Qualifying Project Report
Submitted to the Faculty of the
WORCESTER POLYTECHNIC INSTITUTE
In partial fulfillment of the requirements for the
Degree of Bachelor of Science
in Aerospace Engineering

by

Michelle Acevedo	_____	Edson Novinyo	_____
Benjamin Andrews	_____	Luis Paredes	_____
Casey Brown	_____	Emily Perry	_____
Christopher Cahill	_____	Miles Schuler	_____
Ruxandra Duca	_____	Ashley Smith	_____
Emily Dunham	_____	Daniel Thiesse	_____
Mitchell Lentz	_____		

April 26, 2016

Approved by: _____

Prof. Anthony B. Linn
Aerospace Engineering Program
Mechanical Engineering Department, WPI

_____

Prof. Seong-kyun Im
Aerospace Engineering Program
Mechanical Engineering Department, WPI

Abstract

AIAA's 2016 Design/Build/Fly Competition required the construction of two separate systems to complete distributive manufacturing missions. The team had to develop a production aircraft to carry a 1 kg payload and a manufacturing support aircraft which could carry the production aircraft internally. Aircraft designs were finalized using merit analyses and iterative design techniques to make quantitative decisions. The team selected a flying wing design for the production aircraft nested inside the wing of a conventional design manufacturing support aircraft as final configurations. The aircraft were manufactured and tested to ensure designs would complete mission requirements while maintaining the highest possible score by retaining minimal components and a low aircraft weight.

Executive Summary

The following report documents the efforts of Worcester Polytechnic Institute's 2016 AIAA/Cessna/Raytheon Design/Build/Fly competition team during the background research, design, analysis, manufacturing, and testing of their aircraft entries. The 2016 Design/build/Fly competition challenges teams to construct two remote controlled electrically powered aircraft that will fulfill mission requirements and receive the highest total score, which is calculated based upon the grading of the written report, the aircraft's flight scores, and the rated aircraft cost, a function which induces the total weight of both aircraft and the weight of the batteries used to power them.

The emphasis of this year's competition is to created aircraft optimized for distributed manufacturing, and requires the construction of two separate aircraft. The first, named the "Manufacturing Support (MS) aircraft", must be able to fly three laps around the DBF competition course within 5 minutes unloaded in mission 1. In mission 2, the MS aircraft must internally carry each of the components of the second aircraft from a loading to an unloading area within 10 minutes. The second, "Production" aircraft, must be made such that it can be repeatedly assembled and disassembled without using glue, tape, or screws. In addition to needing to fit within the MS aircraft during mission 2, the production aircraft is required to carry the payload of a 32oz Gatorade bottle for its only flight (mission 3) which requires the aircraft to fly three laps around the DBF competition track within 5 minutes.

Although decreasing the components of the production aircraft would increase the weight the MS aircraft had to carry during mission 2, a scoring analysis conducted by the team revealed that the winning aircraft tandem would consist of a production aircraft made up of no more than 2 components. Thus, the challenge for teams would be to create a production aircraft that was as light as possible to minimize the payload the MS aircraft must carry.

An initial trade study helped our team identify a flying wing configuration to be optimal for both of our aircraft. The high L/W this configuration yields will help us excel in mission 2 and 3 while simultaneously keeping our rated aircraft cost (RAC) low. Additionally, the ability of flying wings to "nest" within one another, similar to a Russian Babushka doll, was identified as a means to minimize the total components of the production aircraft. Subsequent trade studies helped us select a single tractor motor and tricycle-style landing gear. An analysis program was

written in MATLAB was used to determine thrust and power requirements for each leg of the mission. Battery packs and motors were selected based upon this data, and were sized to exceed the predicted specifications by a safety factor of 20%. The program also calculated the distance each aircraft needed to take off, ensuring they would be airborne within 100ft, one of the mission requirements. Numerous iterations were run using different combinations of airfoils, batteries, and motors, and the most efficient configuration was selected.

To increase the stability of the production aircraft, the Gatorade bottle was slung under the main frame. Its housing was 3D printed and reinforced with carbon fiber roving to increase its structural integrity without adding excess weight. The production aircraft is loaded into the manufacturing support aircraft upside-down through a hinged flap in the top of the MS aircraft's airfoil. This flap is secured through the use of Velcro. A foam faring covers the fuselage and landing gear of the production aircraft. A tail was added In order to counteract the large moment created by the MS aircraft's think airfoil. The tail also houses the MS aircraft's control surfaces. Each subsystem of our aircraft were tested, and the results were compared to the predicted values, resulting in small changes to optimize results. Due to heavy winds at the competition, flight of the MS aircraft was only briefly achieved, whereas the production aircraft did not fly.

Acknowledgements

We would like to thank the following individuals and groups for their help and support throughout the entirety of this project:

Project Advisor	Professor Anthony B. Linn
Project Advisor	Professor Seong-kyun Im
Project Advisor	Professor Nikhil Karanjgaokar
WPI Faculty	Professor Raghvendra V. Cowlagi
WPI Students	Jean Furter, Johnathan Griffin, Zachary Ligham, Austin McCalmont, John O'Neill, Kelley Slabinski,
Club	Millis Model Aircraft Club

Table of Authorship

Section	Author(s)
1. Introduction	
1.1 – 1.2	ED, ML
2. Conceptual Design	
2.1, 2.4	CB
2.2, 2.4	AS
2.3, 2.5	ML
2.5	MA, MS
2.6	BA
2.7	CB
3. Aircraft Design	
3.1 – 3.4	CC, EP, DT
3.5 – 3.6	DT
3.7	BA, ED, EN
3.8	AS, CB
4. Detailed Design Models	
4.1	DT
4.2	CB, AS
4.3 – 4.8	RD, LP
4.7	BA
4.9 – 4.10	ML
5. Manufacturing	
5.1	CB, LP
5.2	MA, CB
5.1 – 5.3	AS
6. Testing	
6.1	CB
6.1 – 6.4	AS
6.2	DT
6.3	BA, ED, EN
6.5	MS
7. Final Results	
7.1 – 7.2	AS
8. Conclusion	
8.1 – 8.2	MA
Appendices	
A – D	CC, EP, DT
E	ML
F	RD, LP
Final Edits	
References	CC
Editing and Formatting	RD

Table of Contents

Table of Figures

List of Tables

1. Introduction

Unmanned aviation dates back to the early nineteenth century models used in the development of manned flight. Today, unmanned aerial vehicles are used for both military and civilian purposes, with applications ranging from disaster recovery missions to delivering online purchases. The term “unmanned aerial vehicle” refers to a robotic aircraft that operates either autonomously or via remote control. Unmanned aerial vehicles are particularly attractive due to their implementation capabilities in high-risk circumstances. [1]

The purpose of this project was to design, manufacture, and test two unmanned aerial vehicles for entry in the 2016 AIAA Foundation/Cessna/Raytheon Missile Systems Student Design/Build/Fly competition. The AIAA Foundation invites university students from around the world to participate in this competition and have the opportunity to construct a radio-controlled aircraft to meet specific mission requirements that vary each year. [2] The 2016 Design/Build/Fly competition required teams to simulate distributed manufacturing through the development of two aircraft: one aircraft optimized for assembly into a production aircraft and another optimized for moving the production aircraft components to a centralized assembly location. [3]

This project aimed to develop two aircraft to meet the mission requirements established by the AIAA Foundation. The primary objectives were to minimize the weight of both aircraft and the number of components used to construct the production aircraft. This report describes the analysis, design, and manufacturing processes used to develop the two unmanned aerial vehicles entered by the Worcester Polytechnic Institute 2016 Design/Build/Fly team.

1.1 Team Organization

The WPI team adopted a business structure and project timeline to aid in the delegation and timely completion of project objectives. As a method of optimizing each group member’s skill set, the team was separated into five subgroups: Project Manager, Aerodynamics, Propulsion, Design, Structures/Materials and Manufacturing. This business structure was flexible, as all team members collaborated together to reach deadlines, share viewpoints and learn the various disciplines. The team layout can be seen below in figure 1.1-1.

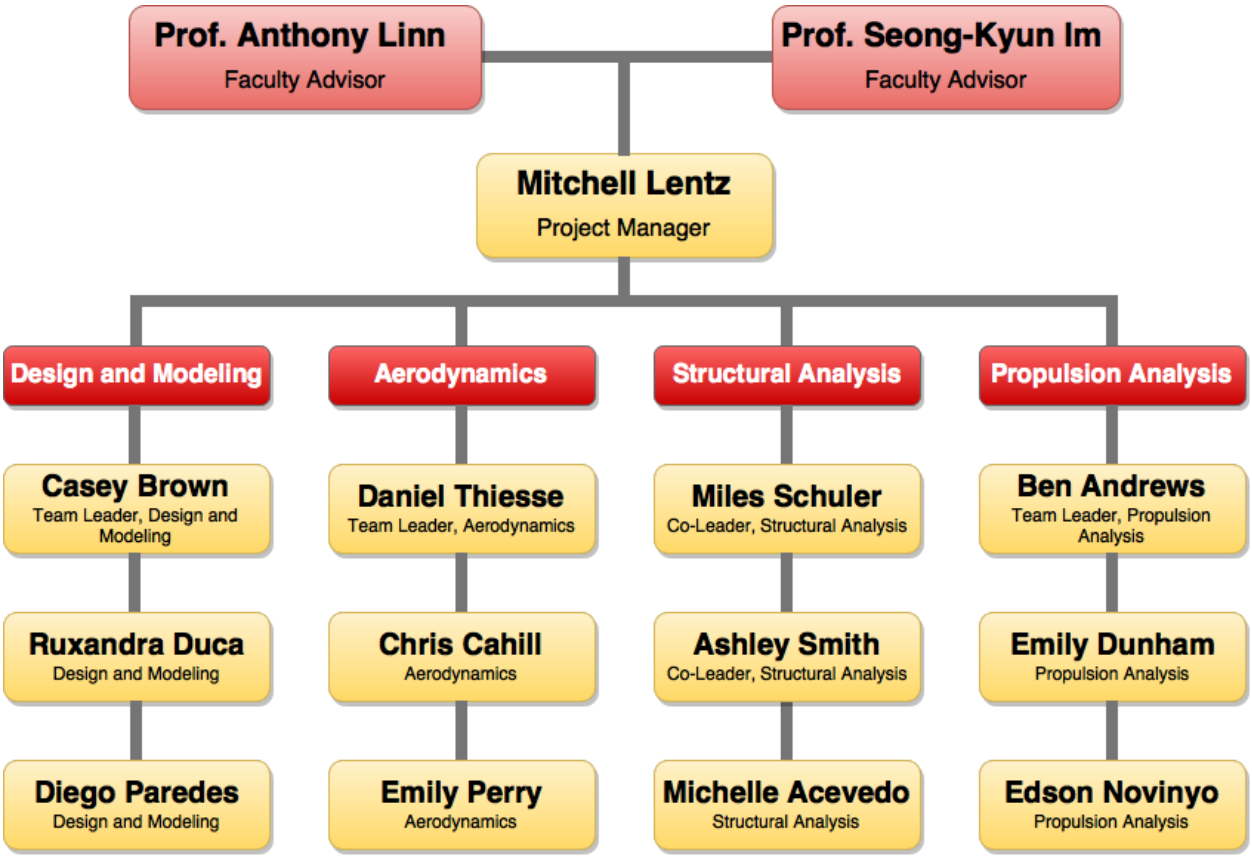

Figure 1.1-1 Group Organizational Structure

Each subgroup was led by one person, who was in charge of their respective assignments and delegating the workload to the group. As the needs of the team changed throughout our first and second semesters, additional subgroups were formed and existing subgroups were disbanded. All team members fully participated in the writing of reports. The roles of each group are as follows:

- **Project Manager**: The project manager was responsible for organizing and leading team meetings, corresponding with the AIAA, analyzing and confirming results from subgroups, and delegating work at meetings. This position required planning, organizing, delegating, and communication skills, as well as the ability to be flexible and manage setbacks.

- **Aerodynamics Team**: The aerodynamics team was responsible for selecting airfoils, sizing, performing stability analyses, and designing the control surfaces of both the Production and the Manufacturing Support Aircraft. The skills required were a deep knowledge of both incompressible fluid and aircraft dynamics, and the ability to use and interpret XFLR5.

- **Propulsion Analysis:** The propulsion analysis team was responsible for selecting the motor, battery, propeller, speed controller, and receiver for the aircraft. The skills required included an understanding of electrical components, propeller thrust equations, and battery types.

- **Design Team:** The design team was responsible for researching and strategizing innovative RC designs and structures that would call for a successful aircraft. The skills required were a blend of knowledge from multiple disciplines as well as the use of Computer Aided Design software such as SolidWorks.

- **Structural and Material Analysis**: This team was responsible for researching, testing, and acquiring the materials needed to build the aircraft. They also identified necessary manufacturing techniques and equipment. The skills required included a background in structural analysis and materials science.

- **Manufacturing Team**: This team was responsible for the implementation of the model created by the Design Team. This consisted of the purchasing of materials, the manufacturing of test sections, structural testing and actual building of the Production and Manufacturing Support Aircraft.

1.2 Project Gantt Chart

To stay on schedule throughout the project, a Gantt chart was used. This chart shows the progress of all activities that occurred since the start of the project. The chart is color coded for both the production aircraft and the manufacturing support aircraft.

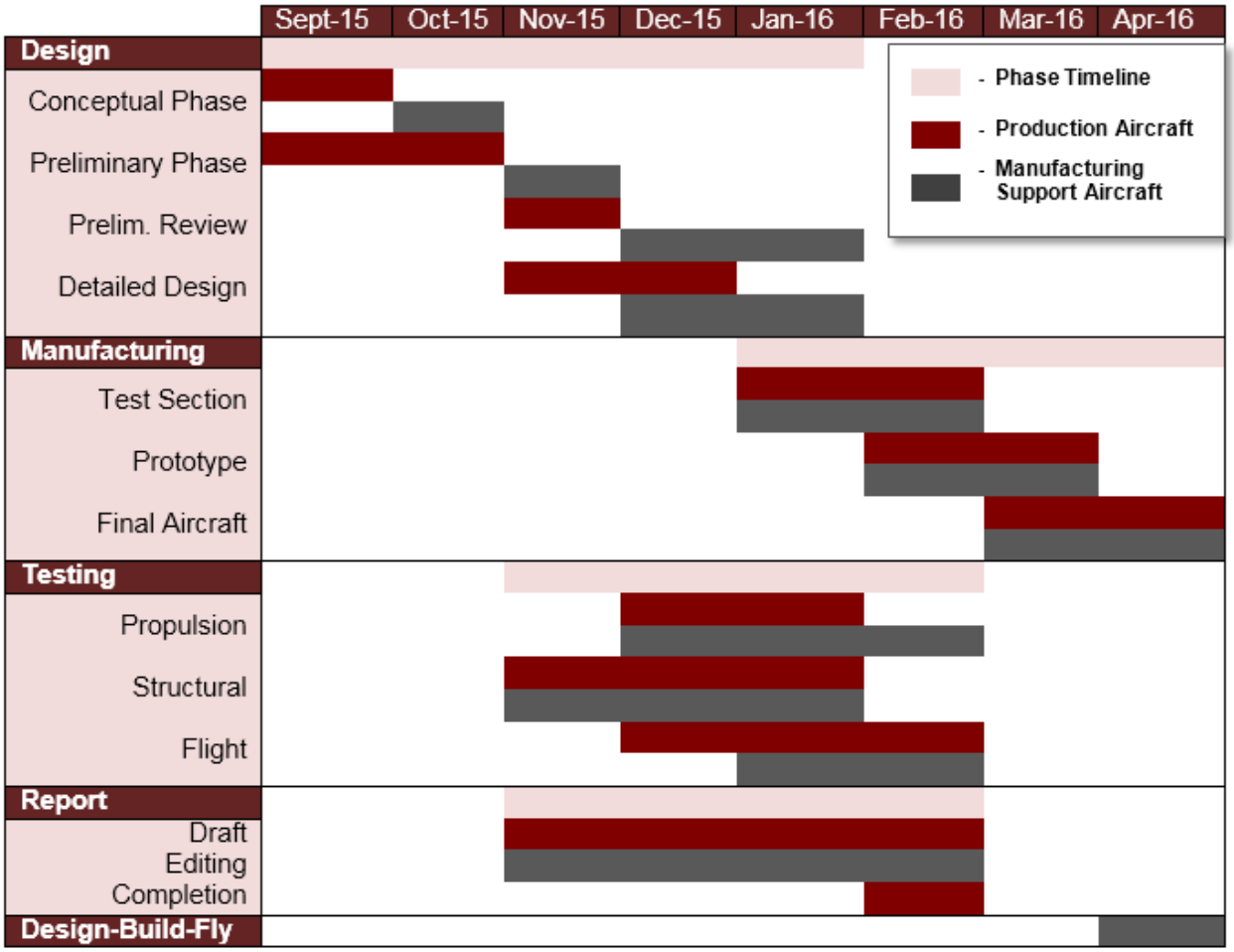

Figure 1.2-1 - Project Gantt Chart

2. Conceptual Design

The objective of the conceptual design phase was to identify possible configurations which would meet the requirements of the 2016 Design/Build/Fly competition. Merit analyses were used to vet the possible solutions and to determine the optimal configuration for each aircraft.

2.1 Design Constraints

Analysis of the contest rules yielded the following requirements for this year's aircraft

- The aircraft can be of any design except rotary wing or lighter-than-air.
- The batteries must be either NiCD or NiMH, and the on-board battery packs must be the only power source assisting the aircraft's takeoff.
- The aircraft must be propeller driven and electric powered.
    - The propeller must be bought from a manufacturer and cannot be built by the team.
    - The motor must be available over-the-counter and remain unmodified by the team.
- The payloads must be secured in place during flight.
- The Manufacturing Support Aircraft must carry the Production Aircraft internally as a payload. The Production Aircraft may be disassembled and transported internally one component at a time.
- The Production Aircraft must be transported within the Manufacturing Support Aircraft.
    - This can be done by dissembling the Production Aircraft into sub-assemblies. Each sub-assembly must be transported alone without any other components.
    - The Production Aircraft must be capable of being taken apart and reassembled multiple times. Therefore, the aircraft may not undergo any cutting or gluing as methods of breakdown and reassembly.
- The Production Aircraft must carry an unopened 32-ounce Gatorade bottle internally as a payload.

2.2 Mission Sequence

The 2016 DBF competition consists of three flight missions and one bonus ground mission. All three flight missions must be flown in order; a new mission cannot be attempted until a score has been received for the previous mission. The bonus ground mission will then be completed after completing all the above missions successfully. Before beginning the first of the three missions, the aircraft must first pass the wing tip load test with the intended payload for each mission. The bonus ground mission will be completed in an area separate from the flight area immediately after the final flight. For the bonus mission, the team will bring all Production Aircraft sub-assembly groups flown to the designated area and must assemble the Production Aircraft from the sub-assemblies within 2 minutes, including re-installing the payload. The completed aircraft must then pass the wing tip lift test and a controls systems check for a score to be given. [3]

The staging box is only for the pilot, pilot assistant and assembly crew members. After pre-flight checkout, the crew members may be swapped out if the team desires. The aircraft is limited to a 30.48 m (100-ft) takeoff field length and the aircraft must use ground rolling takeoff and landing. For the turn on the first lap on any mission, the turn will not be permitted until the judge gives a signal The pilot will have unaided visual control of the aircraft at all times. Finally, to receive a score on any mission, the plane must successfully land. [3]

2.2.1 Mission 1: Manufacturing Support Aircraft Arrival

This mission only requires the Manufacturing Support Aircraft. There is no payload for the arrival flight and the aircraft has a 30.48 meter takeoff requirement. The goal of this mission is to complete three laps within the time limit of five minutes. Time is started when throttle is advanced for takeoff. A lap is measured when the aircraft passes the start/finish line. The aircraft must land successfully to get a score. The aircraft can receive 1 of 2 scores for this mission [3]:

- MF1 = 2.0 - if aircraft completes the mission
- MF1 = 0.1 - if aircraft does not attempt or complete the mission

2.2.2 Mission 2: Manufacturing Support Aircraft Delivery Flight

In Mission 2, both the Manufacturing Support Aircraft and Production Aircraft will be used. The Production Aircraft will be disassembled into sub-assemblies to be carried internally by the

Manufacturing Support Aircraft. The mission will begin when the first sub-assembly is installed. The Manufacturing Support Aircraft must take-off within the 30.48 m field length, fly one lap with the sub-assembly installed then return and land. After each lap, the aircraft will taxi to the designated payload change area where the ground crew will "safe" the aircraft propulsion system, remove the installed sub-assembly group, install and secure the next sub-assembly group and re-enable the aircraft propulsion system. The aircraft will taxi to a location before the Start Line and take-off for the next lap. Time ends when the aircraft passes the start line in the air at the end of the final flight. The goal of this mission is to complete the required task within 10 minutes. The aircraft must complete a successful landing on each flight to obtain a score. The Production Aircraft sub-assemblies do not include the Production Aircraft flight battery or payload. The aircraft can receive 1 of 3 scores for this mission [3]:

- MF2 = 4.0 – Aircraft completes all sub-assembly group transport flights successfully within the time window.
- MF2 = 1.0 - Aircraft completes less than all the sub-assembly flights within the designated time allowance but at least 1 group is successfully transported
- MF2 = 0.1 – Aircraft does not attempt or complete a successful flight

2.2.3 Mission 3: Production Aircraft Flight

This is mission requires the Production Aircraft to carry a payload internally. The load is a 32 oz. Gatorade bottle with approximate specifications: height 20.8 cm, max diameter 9.4 cm, weight 1.02 kg. The goal of this mission is to complete three laps within the time limit of five minutes. A lap is complete when the aircraft passes over the start/finish line in the air. The aircraft can receive 1 of 3 scores for this mission [3]:

- PF = 2.0 – Aircraft completes the required flight within the time period carrying the full payload
- PF = 1.0 – Aircraft completes less than the required laps or exceeds the time period
- PF = 0.1 – Aircraft does not attempt or complete a successful flight

2.2.4 Mission 4: Bonus Mission

Each team may attempt the bonus mission after completing all three missions. The bonus mission will be completed in an area separate from the flight area immediately after the final flight as the team will bring all Production Aircraft sub-assembly groups flown to the designated area. The ground crew must assemble the Production Aircraft from the sub-assemblies including re-installing the payload. The goal of this mission is to complete the required tasks in

under two minutes. The completed aircraft must pass the wing tip lift test and a controls systems check. The aircraft can receive 1 of 2 scores for this mission [3]:

- Bonus = 2.0 – Aircraft assembled in specified time and passes wing tip lift test
- Bonus = 0.0 – Any other result

2.2.5 Mission Model

A mission model was created to aid in the determination of power and energy requirements as well as the ideal flight path for each mission. The model can be seen below:

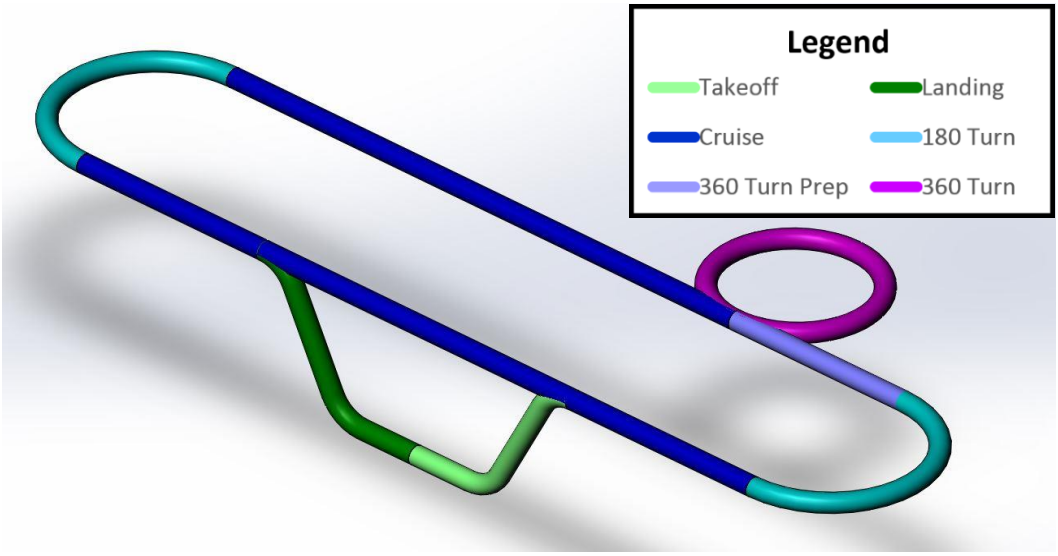

Figure 2.2-1 - Mission Model

- Takeoff roll - Starting at a standstill, the aircraft will begin to accelerate to takeoff speed
- Liftoff - Before the aircraft begins to climb, the aircraft will continue to throttle up to the climb velocity
- Climb - Aircraft will increase in altitude in order to commence the mission
- Cruise - Ideal velocity of operating the aircraft during the missions
- Turn - The turns will be executed dependent on the wing loading of the aircraft. Each turn will be mission dependent.
- Assumptions - Velocity, climb rates and turns were determined assuming no winds during the flight. Also, no immediate pitch angle change is assumed. Finally, the model was determined with no pilot error.

2.3 Scoring Formula

Once all of the missions are completed the team's total score can be calculated. The total score is a function of all of the mission scores, the total weight of both aircraft, the battery weight of both aircraft, the number of components of the Production Aircraft, and the written report score. The equations that are used to calculate the total score can be seen below [3]:

$$Score = \frac{Written\ Report\ Score * Total\ Mission\ Score}{RAC} \quad (1)$$

$$Total\ Mission\ Score = MF1 * MF2 * PF + Bonus \quad (2)$$

$$Rated\ Aircraft\ Cost\ (RAC) = EW1 * Wt_{Battery1} * N_{Components} + EW2 * Wt_{Battery2} \quad (3)$$

EW1 and EW2 are the empty weights of the Production and Manufacturing Support Aircraft respectively, and $N_{Components}$ is the number of subassemblies that the Production Aircraft is broken into to be delivered by the Manufacturing Support Aircraft. As seen from the equation, aircraft weight has a significant factor in the final score. This will necessitate an aircraft design with a strong enough structure to withstand the forces of flight and landing that is also as light as possible. The number of components in which the Production Aircraft must be broken into to be delivered is also a factor in the denominator of the overall score equation, which means that it will have a large effect. To minimize the number of components, clever packaging designs for the Production Aircraft within the Manufacturing Support Aircraft will need to be employed. Since the aircraft or the sub-assemblies must be completely enclosed, the design of the Production Aircraft will significantly affect the design of the Manufacturing Support Aircraft.

2.4 Sensitivity Analysis

2.4.1 Aircraft Configuration Selection

Four types of aircraft were considered: traditional (fixed wing), canard, biplane, and flying wing. Although the canard configuration allows for good stall characteristics and stability, it is difficult to choose a forward wing of the correct size, and to make sure it stalls before the wing. Additionally, the wing twist distribution can distort the load distribution, leading to the elimination of this type of aircraft from our list of choices. Similarly, the biplane was not considered due to

the added weight of a second airfoil and the increased number of components, a key feature that the team wished to minimize.

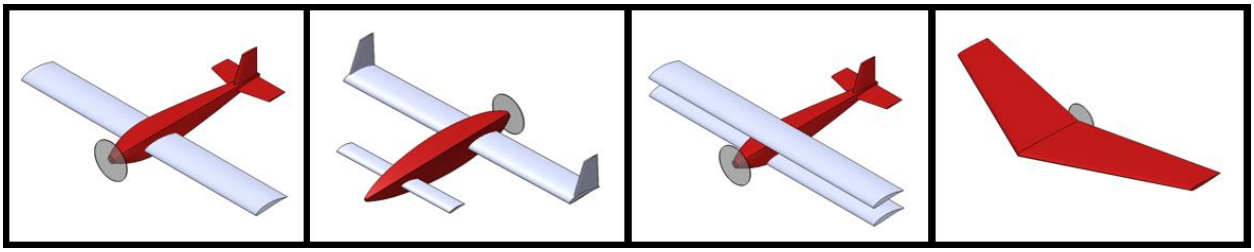

Figure 2.4-1 - Aircraft Configurations

After narrowing the research down to the flying wing and the traditional configurations, two concepts were drawn as shown in the figure below:

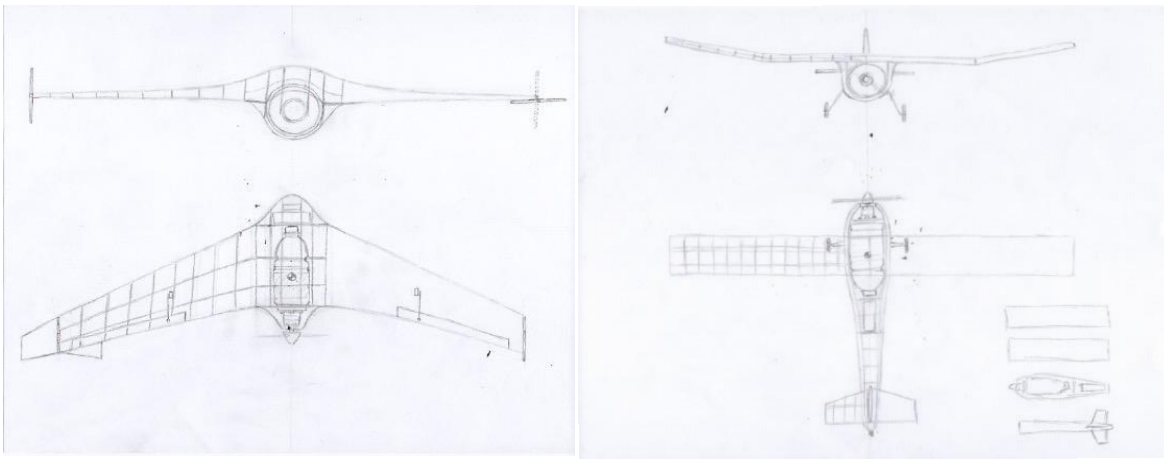

Figure 2.4-2 Concept Drawing of Flying Wing and Traditional Production Aircraft

Then, a comparative analysis between them was performed as presented below:

Table 2.4-1 Comparative Analysis of Aircraft Configurations

	Weight of score	Conventional	Flying wing
Weight	0.35	0	1
Number of components	0.25	0	1
Payload abilities	0.05	1	0
Drag	0.10	0	1
Ease of Manufacture	0.15	1	0
Power Needed	0.10	0	1
TOTAL		**0.20**	**0.80**

In the table above, 1 represents the preferred performance in the given category. The preferred performance is defined as the smaller value for weight, number of components, drag, and power needed. Overall, the multiple advantages of low weight/number of components as well as the high lift provided by the flying wing led us to choose this configuration for our Production Aircraft.

2.4.2 Payload Configuration

The Production Aircraft must carry the payload (Gatorade bottle) during two of the events of the competition: tech inspection and mission three. During tech inspection, the Production Aircraft is required to undergo the wing tip lift test with the design payload installed. During mission three, the Production Aircraft must takeoff within a prescribed field length and fly three laps within five minutes while carrying the payload internally. For our team's payload configuration, we determined the best possible way to carry our payload internally was to position our payload along the central axis of the Production Aircraft fuselage and ensure it was properly secured during the two events. This configuration is beneficial as it is much easier to maneuver an aircraft which possesses a balanced load distribution. Similarly, during tech inspection, an even load distribution reduces the possibility of irreparable damage to the aircraft. The detailed design was performed later in the project.

2.4.3 Propeller Configuration

When designing the aircraft, five propeller configurations were considered: single tractor, single pusher, tractor/pusher, double tractor, and double pusher. A tractor configuration produces thrust using propellers that pull in air from the front of the aircraft. A pusher configuration produces thrust using propellers that push air from the back of the aircraft. A tractor/pusher configuration uses one tractor propeller and one pusher propeller and a double tractor or double pusher configuration uses one propeller on each wing. Our research focused on airflow through the propeller and over the aircraft body, aircraft stability, and takeoff/landing clearance.

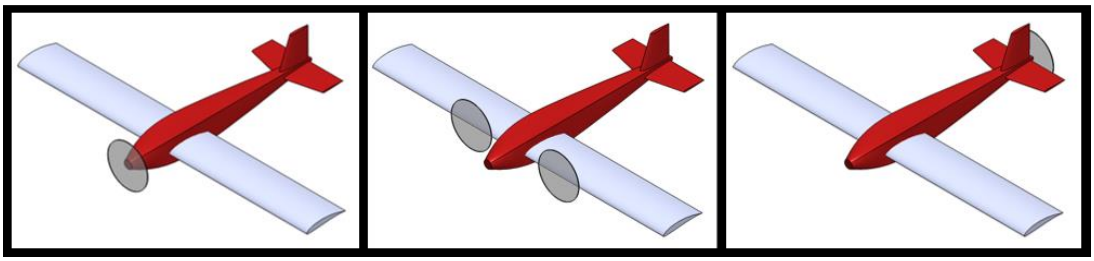

Figure 2.4-3 Propeller Configurations

It is generally known that for Radio Controlled aircraft tractors are significantly more efficient than pushers because a tractor propeller will intake clean, undisturbed air, while a pusher propeller will intake turbulent air that has already passed over the body of the aircraft. However, it was also noted that because the air travelling over the main aircraft body will be turbulent from the propeller, tractor propellers cause the body to create more drag. It was concluded that for low speed applications, the efficiency of the motor will be of greater effect than any induced drag.

From a stability standpoint, pusher propeller aircraft tends to be more stable, particularly in the yaw and pitch axes. The propeller improves stability by acting as a vertical tail surface that moves the center of lift toward the back of the plane. A tractor propeller has the opposite effect, bringing the center of lift forward and improving maneuverability but lessening the aircraft stability. For our aircraft, stability carries more importance than maneuverability due to the nature of the flight missions this year.

Takeoff, landing, and ground maneuverability all favor a tractor setup. Pusher propellers require very careful takeoff and landing because it is possible for the propeller to clip the ground during the nose up of a takeoff or during the flare of a landing trajectory. Pusher configurations are also less maneuverable than tractors during taxiing on the runway. Pictured below is a weighing chart of each of these factors for the various propulsion system configurations.

Table 2.4-2 Comparative Analysis of Propeller Configurations

Criteria	Weight	Single Tractor	Single Pusher	Tractor/ Pusher	Double Tractor	Double Pusher
Weight	0.3	2	2	1	1	1
Stability	0.15	0	2	1	1	3
Efficiency	0.25	2	1	3	2	1
Takeoff/Landing Clearance/Control	0.2	2	1	1	2	0
Compactability	0.1	2	2	1	0	0
Total		***1.7***	***1.55***	***1.5***	***1.35***	***1***

This table gives different weight to each of the important criterion that affect our aircraft's performance in the given missions. A higher positive value given to a configuration indicates a more favorable outcome. The total score of each configuration is printed in bold at the bottom of their respective columns. From these results, we selected a single tractor configuration.

2.4.4 Landing Gear Configuration

Three landing gear configurations were considered in the design of both aircraft: tricycle gear, taildragger gear, and bicycle gear. The tricycle gear configuration uses two main gear wheels aft of the CG and a steerable nose wheel forward of the CG, resulting in excellent ground handling but high drag due to the length of the gear legs. The taildragger configuration uses two main gear wheels forward of the CG and a small steerable tail wheel mounted on the tail of the aircraft. Since the tailwheel is aft of the CG, this configuration is unstable during ground handling and requires proper rudder input to maintain control during taxi. However, this configuration creates less drag than the tricycle gear configuration since the tailwheel is small and remains close to the fuselage. The bicycle configuration allows most of the weight of the aircraft to be transferred to a main wheel and a secondary wheel closer to the tail, but requires two additional wheels mounted on the wings to remain balanced during taxi, which adds drag.

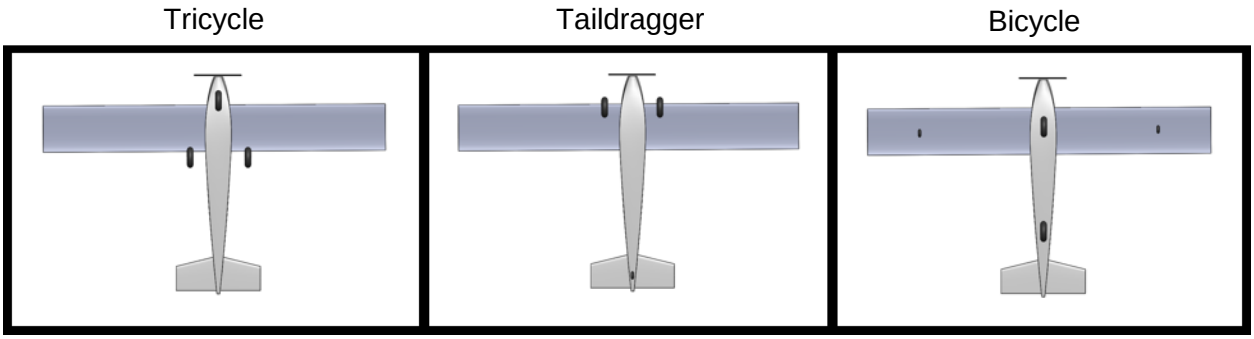

Figure 2.4-4 Landing Gear Configurations

For the Production Aircraft, we decided to use a tricycle gear since the flying wing design does not include a tail and therefore eliminates the possibility of a taildragger or bicycle configuration. This setup requires a third servo to control the steerable nose wheel during ground handling and allows us to place the wheels as closely as possible to the fuselage to minimize the Production Aircraft's profile as it is transported in the Manufacturing Support Aircraft.

A taildragger configuration was selected for the Manufacturing Support Aircraft since the boom tail allowed for the presence of a lightweight tail wheel while most of the aircraft's weight is transferred to sturdy main gear legs. A taildragger configuration also allows a steerable tailwheel to be connected to the aircraft's controllable rudder, eliminating the need for an additional servo to steer the aircraft during taxi.

2.5 Material Analysis

To gain an understanding of the materials that should be utilized when creating the two aircraft, preliminary tests were performed on a 0.22'' diameter aluminum tube,1/8''x3''x38'' balsa, 2/8'' thick balsa, and ½'' diameter carbon fiber tube. We found that the ½'' diameter carbon fiber tube withstood the most weight of 20lbs without breaking. The 2/8'' thick balsa did not break under 18lbs; this makes it a good thickness for constructing the spar of the aircraft. At 10lbs the 1/8''x3''x38'' balsa cracks and breaks at 12lbs. The 0.22'' diameter aluminum tube proved to be the weakest in the test and it started to bend at 8lbs.

Table 2.5-1 Materials Properties

	Price (USD/Kg)	Density (Kg/m3)	Modulus (GPa)	Yield Strength (MPa)	Tensile Strength (MPa)	Flexural Modulus (GPa)	Flexural Strength (MPa)
Balsa (Longitudinal)	~8	190	4.7	12.5	20	3.8	20
Balsa (Transverse)	~8	190	0.17	0.8	0.9	0.16	0.95
Polystyrene Foam	~3	30	0.01	0.225	0.4	0.01	0.45
Carbon Fiber	~45	1800	380	2000	2400	380	3500
Polyolefin Film	~2.5	880	0.02	15	15	0.03	28

2.6 Battery Selection

Two types of batteries, Nickel-Metal Hydride and Nickel-Cadmium, were researched for the application of the aircraft. Research shows that NiMH can outperform NiCd battery in long duration applications. It was found that NiMH batteries store twice as much energy as standard NiCd batteries. Therefore there is a higher power/weight ratio from NiMH than NiCd batteries. Also, NiMH batteries can be charged many times at different battery charge levels without affecting the life cycle of the battery while NiCd batteries have to be charged only after they

have been fully discharged. This improved life cycle of NiMH over NiCd increases its applications. NiCd batteries can discharge with about twice the current of NiMH batteries. However, batteries can be connected together in parallel to increase the max current if needed, but this increase in battery pack weight would lower the rated aircraft cost. The chart below is a weighing chart illustrating each of the factors for the battery requirements.

Table 2.6-1 Comparative Analysis for Battery Selection

Criteria	Weight	NiMH	NiCd
Power/Weight	0.6	2	1
Ease of Use	0.1	2	1
Max Current	0.3	1	2
Total		***1.7***	***1.3***

As with previous weighing illustrations, a higher positive value represents a more favorable outcome. From the different weights on the chart, the highest score would provide an aircraft with the best performance in the given mission. Based on the total scores shown at the bottom of the chart, we selected NiMH batteries.

2.7 Conceptual Design Summary

The analyses performed ultimately favored a flying wing design for the Production Aircraft and a flying wing with a boom-mounted tail configuration for the Manufacturing Support Aircraft. The final Production Aircraft design is a constant chord, swept flying wing with a single tractor propeller, and tricycle landing gear which allows for adequate ground handling on a tailless aircraft. The final Manufacturing Support Aircraft design is essentially a larger version of the Production Aircraft flying wing with the addition of a boom-mounted tail to help counteract a large moment from a thick, cambered airfoil. These two aircraft were designed in tandem to ensure a high score at the competition.

3. Aircraft Design

3.1 Aerodynamic Analysis

Initial sizing and design of the aircraft began with rough weigh estimates and an initial chord length. The weight estimates were based on historical empty weight ratios from RC aircraft from similar competitions, as well as the weight of the payload. The chord length was initially estimated based on the size of the payload, specifically the height of the Gatorade Bottle. Aerodynamic calculations were then made to determine initial sizing of the aircraft. The calculated aerodynamic data was sent to the design team to determine a more precise weight estimate. With the values of lift and drag from the aerodynamic analysis, a MATLAB program was written to determine the power requirements of each leg of the mission. Additionally, the program determined the load factor on the airplane and the time each plane would require to complete three laps of the course. Based upon results obtained from this program, the initial propulsion subsystem elements were selected. This became an iterative process until the team achieved a final weight, design and size of both aircraft.

3.2 Aerodynamic Analysis for Production Aircraft

3.2.1 Initial Approach

The first number needed was a rough weight estimate for the production aircraft only as the weight of the production aircraft would be needed to have a weight estimate for the manufacturing support aircraft. To make sure there was a buffer with the amount lift needed, a 2:1 ratio of aircraft weight to payload of used. As the bottle weighed about 1 kg, the aircraft would need to be 2 kg for a grand total of 3 kg.

Airfoils commonly used for flying wing aircraft were researched and four airfoils were observed to appear most frequently. The airfoil selected to be further investigated were MH 64, MH 114, SD 7062, and the NACA 4412. These airfoils all have different characteristics that made them viable options for the design.

After selecting these four airfoils, a standard chord of 12 inches or 0.3046 meters was set so there was enough room for the bottle itself as well as any critical components. All the airfoils were to be analyzed at 0 degrees angle of attack and 15 m/s for cruise conditions as a minimum velocity to complete three laps in five minutes. The four airfoils were then analyzed in XFLR5's two-dimensional program. The velocity was required for the Reynolds number equation to put into XFLR5 and was calculated to be 311,150. The Reynolds number equations is as follows [4]:

$$Re = \frac{\rho * V * c}{\mu} \tag{4}$$

From XFLR5, the coefficients of lift and moment were obtained for all four of the airfoils. From here, the span of each airfoil was calculated using the lift equation. As this was the cruise condition, the lift equaled the weight of the aircraft, which came out to 31.2 Newtons. The equation used is as follows [4]:

$$L = 0.5 C_l \rho V^2 bc \tag{5}$$

The results for the span can be seen in the picture below. From here, the Aspect Ratio (AR) was calculated for each airfoil was used by using the following equation [4]:

$$AR = \frac{b^2}{S} \tag{6}$$

The results are seen in the image below. Lastly, using the coefficient of lift, the aspect ratio, and a set Oswald efficiency of 0.8, the induced drag was calculated for each airfoil. The equation for induced drag is as follows [4]:

$$C_{di} = \frac{C_l^2}{\pi A R e} \tag{7}$$

The results of the induced drag are seen in the table below.

Table 3.2-1 Induced Drag Results

Airfoil	Cl	b	AR	Cdi	Cm, L=0
SD 7062	0.45	1.600	5.249	0.01535	-0.08
MH64	0.15	4.790	1.572	5.69e-4	-0.02
MH114	0.85	0.847	2.779	0.1035	-0.19
NACA 4412	0.50	1..439	4.721	0.2107	-0.11

After calculating all these values, a merit analysis was performed on all four airfoils. The coefficient of lift was given a point value of 40, the coefficient of moment and aspect ratio both at 25 points, and induced drag coefficient was at 10 points. Each of the airfoils was then ranked 1 through 5 in increments of 0.2, with 1 being the best.

Table 3.2-2 Airfoils Initial Ranking

Parameter	Weight	SD 7062	MH 64	MH114	NACA 4412
Cl	40	0.4	0.2	1	0.6
AR	25	0.6	0	0.6	0.8
Cdi	10	0.8	1	1	0.4
Cm, L=0	25	0.6	0.8	0	0.4
TOTAL:	**100**	**270**	**190**	**285**	**290**

The merit analysis revealed that the NACA 4412 was the best, followed by the MH 114, the SD 7062, and lastly the MH 64. The area of the NACA 4412 was calculated to be 0.438m^2. The last image is an XFLR5 model of the NACA 4412 with winglets to improve yaw stability.

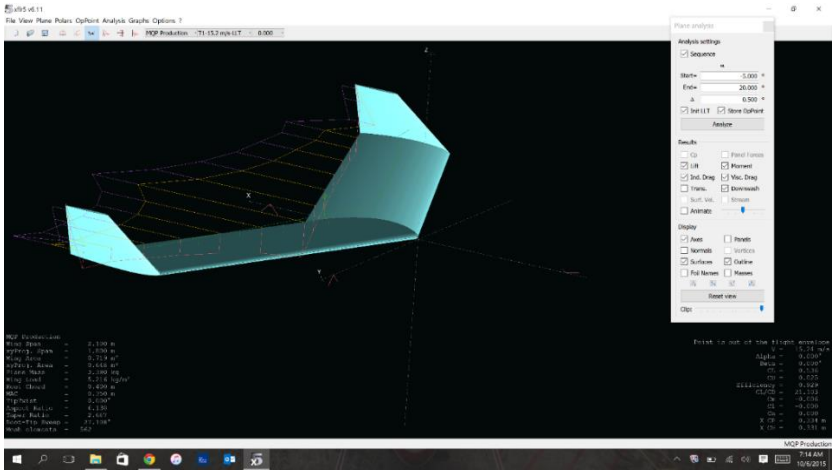

Figure 3.2-1 XFLR5 Initial Model for Production Aircraft

A second approach was pursued in which the analysis was expanded over a variety of speeds and angles of attack to find the critical wing area needed at the lowest speed and highest angle of attack. This provided a more accurate wing area required for each leg of the aircraft's mission.

3.2.2 Second Approach: Weight Estimate

The same weight estimate method was used to try a second approach. This entailed estimating an empty production aircraft weight to payload weight ratio of 2:1. With a payload weight of approximately 1 kg the weight estimate for the production aircraft was 3 kg.

3.2.3 Second Approach: Airfoil Analysis

For the airfoil analysis, a wide variety of airfoils were analyzed rather than just the four airfoils from the first approach, which all had similar aerodynamic characteristics. Using the

UIUC airfoil database, five additional low thickness airfoils were found with moment coefficients close to 0 and low drag coefficients. Based on those characteristics, the following were analyzed: the S 1223, NACA 4424, MH 45, MH 83 and Lissaman 7769 in addition to the NACA 4412, MH 64, SD 7062 and MH 114 which were previously investigated.

After selecting these airfoils, an XFLR5 analysis was performed at five different airspeeds, ranging from 5 m/s to 25 m/s. To do so, the Reynolds Number corresponding to each airspeed was first calculated since XFLR5 cannot analyze airfoils with just airspeed. For each airfoil, XFLR5 produced graphs of coefficient of lift vs alpha, coefficient of moment vs alpha, coefficient of drag vs. alpha, coefficient of lift vs. coefficient of drag and lift to drag vs. alpha graphs. When analyzing the graph data, the focus was on the values that corresponded to a cruise angle of attack of 0 degrees and a take-off angle of attack of 10 degrees. The take-off angle of attack used for the analysis was arbitrarily chosen based on the take-off angles of attack of previous competition teams. The graphs and resulting data for NACA 4412 airfoil can be seen below. The results from the other airfoils can be seen in Appendix A.

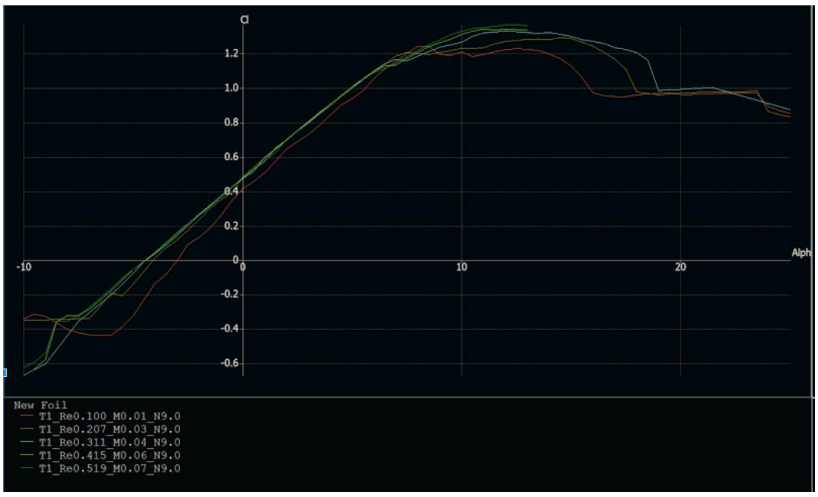

Figure 3.2-2 NACA 4412 Coefficient of Lift vs. Angle of Attach

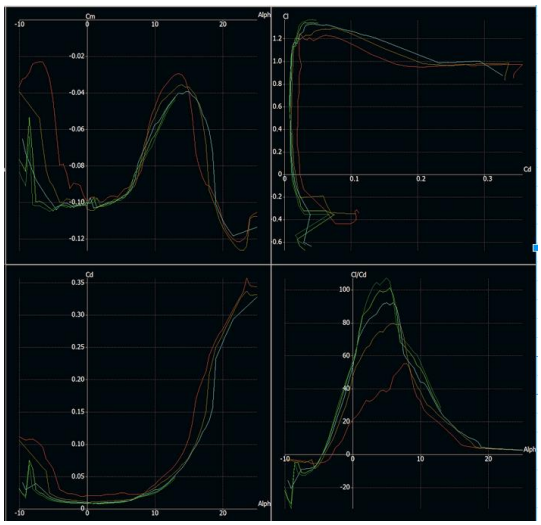

Figure 3.2-3 NACA 4412 Moment, Drag, and Lift-t-Drag Graphs

Table 3.2-3 NACA 4412 Aerodynamic Coefficients Based on Airspeed

	Cruise Angle of Attack (α=0°)					Take-off Angle of Attack (α=10°)				
Airspeed	**5 m/s**	**10 m/s**	**15 m/s**	**20 m/s**	**25 m/s**	**5 m/s**	**10 m/s**	**15 m/s**	**20 m/s**	**25 m/s**
C_l	0.40	0.50	0.50	0.50	0.50	1.20	1.25	1.30	1.30	1.30
$C_{m,o}$	-0.10	-0.11	-0.10	-0.10	-0.10	-0.05	-0.05	-0.06	-0.07	-0.07
C_D	0.02	0.01	0.01	0.01	0.01	0.04	0.03	0.03	0.03	0.03
L/D	21.00	47.00	55.00	55.00	57.00	32.00	37.00	45.00	55.00	58.00

The Lissaman 7769 was the only airfoil selected that XFLR5 was unable to analyze. The only data that could be collected was the necessary airfoil characteristic data at an angle of attack of 0 degrees and at 15 m/s from graphs available online:

Table 3.2-4 Results for Lissaman 7769 Airfoil

Parameter	Value
C_l	0.25
$C_{m,o}$	-0.0325
C_D	0.2
L/D	1.25

Since no other pertinent information could be collected for the Lissaman 7769, this airfoil was excluded from further research.

3.2.4 Second Approach: Initial Sizing

Using the airfoil characteristic data collected from XFLR5, the initial sizing of the aircraft was calculated at each of the five airspeeds and two angles of attack for each airfoil. The initial sizing calculations included dimensions such as wing span, wing area, aspect ratio, thrust to

weight ratios and wing loading ratios. For these calculations, the chord length was set at 0.3048 m which was based on the length of the Gatorade bottle, the payload to be carried by this aircraft. The following equations were used in an excel spreadsheet to aid the calculations [4]:

$$Span\ b = \frac{2W}{\rho c C_l V^2} \tag{8}$$

$$S = b * c \tag{9}$$

$$Aspect\ Ratio\ AR = \frac{b}{c} \tag{10}$$

$$Thrust\ to\ Weight\ Ratio\ \frac{T}{W} = \frac{1}{L/D} \tag{11}$$

$$Wing\ Loading\ \frac{W}{S} = \frac{W}{b * c} \tag{12}$$

In these equations, W was the estimated weight of the loaded production aircraft, ρ was the air density at sea level and c was the set chord length. The variable C_l was the coefficient of lift that corresponded with the airspeed, V. The ratio L/D was the lift to drag ratio taken from the XFLR5 data. The initial sizing calculations were made using the collected airfoil characteristic data and the above equations. The results for NACA 4412 can be seen in the table below. The results for all other airfoils are in Appendix B.

Table 3.2-5 NACA 4412 Updated Aerodynamic Coefficients Based on Airspeed

	Cruise Angle of Attack (α=0°)					Take-off Angle of Attack (α=10°)				
Speed	**5 m/s**	**10 m/s**	**15 m/s**	**20 m/s**	**25 m/s**	**5 m/s**	**10 m/s**	**15 m/s**	**20 m/s**	**25 m/s**
b (m)	16.03	3.21	1.42	0.80	0.51	5.34	1.28	0.55	0.31	0.20
S (m^2)	4.88	0.98	0.43	0.24	0.16	1.63	0.39	0.17	0.09	0.06
AR	52.58	10.52	4.67	2.63	1.68	17.53	4.21	1.80	1.01	0.65
T/W	0.05	0.02	0.02	0.02	0.02	0.03	0.03	0.02	0.02	0.02
W/S	6.13	30.63	68.91	122.50	191.41	18.38	76.56	179.16	318.50	497.66

An airfoil could have been selected based on the smallest area at 5 m/s during take-off. The size of the aircraft, however, seemed inappropriate at the angle of attack of 10 degrees. Additionally, the take-off angle of attack should vary with the airfoil. Therefore, a third approach to the aerodynamic analysis was pursued, using more accurate methods.

3.2.5 Third Approach: Changes from the Previous Approach

For the third and final approach, a more accurate weight estimate was used after the concept was developed using Computer Aided Design. With an estimate of 3.6 kg, not including

epoxy, tape, and other components, was rounded up to 4.0 kg for an added 10% safety factor in the weight calculation. This was a significant increase in weight that was not accounted for in the previous approach.

3.2.6 Third Approach: Methodology

The following steps were taken to properly analyze and select airfoils for use on the production aircraft. Each airfoil was analyzed at four different airspeeds (10; 15; 20; and 25 m/s) along with their corresponding Reynolds Numbers (207,000; 311,000; 415,000; and 519,000). We removed 5 m/s because of the large required area needed for take-off.

Using the selected airfoils in approach two, we calculated the corresponding lift-curve slopes for each airfoil. This equation was used as the standard for all baseline lift data. The lift-curve slope equations can be found in each corresponding graph.

$$C_l = m\alpha + b \tag{13}$$

Where C_l is the coefficient of lift; m is the slope of the lift-curve; α is the angle of attack; and b is the y-intercept.

Step 1:

We needed to ensure that we would have the largest amount of lift at takeoff conditions so that the aircraft could takeoff at a low velocity. To do this, we set each takeoff angle of attack (AoA) at the airfoils critical AoA for 10 m/s. Then, using the lift-curve equation for each airfoil, we were able to calculate the minimum area needed for takeoff at that specific airfoils AoA and associated coefficient of lift using the following equation [4]:

$$S = \frac{L}{0.5\rho V^2 C_l} \tag{14}$$

Where L is the required lift, which is equal to the weight of the aircraft.

This approach allowed us to normalize each airfoil about the surface area required for takeoff. All following calculations would be completed using the calculated surface area at takeoff.

Step 2:

By rearranging the preceding equation, we were able to calculate the new coefficient of lift needed for flight at the remaining set airspeeds of 15, 20, and 25 m/s.

$$C_l = \frac{L}{0.5\rho V^2 S} \tag{15}$$

Step 3:

Using the lift-curve equation we could calculate the necessary AoA to achieve the minimum coefficient of lift that is required for flight. [4]

Step 4:

Using the surface area and set chord length of 0.2785 m, we could calculate the span and aspect ratio of the aircraft. [4]

$$b = \frac{S}{c} \tag{16}$$

$$AR = \frac{b^2}{c} \tag{17}$$

Step 5:

At this point we had the necessary angles of attack for each airfoil, at four different airspeeds. Using this data and the data generated by XFLR5 (shown in approach two), we identified the coefficient of drag, coefficient of the moment, and the lift/drag at each airspeed with the required AoA. [4]

Step 6:

We calculated the total drag on the aircraft, power, thrust to weight ratio, and wing load ratio using the following equations [4]:

$$D = 0.5\rho V^2 S C_D \tag{18}$$

$$Power = D * V \tag{19}$$

$$\frac{T}{W} = \left(\frac{L}{W}\right)^{-1} \tag{20}$$

$$Wing\ Load = \frac{W}{S} \tag{21}$$

3.2.7 Third Approach: Results

From our research of small flying wing style UAV's, we found that an appropriate wing load ratio is between 5-10 N/m^2. All airfoils except the S 1223 fit this requirement. Therefore, we eliminated the S 1223 as a potential airfoil. We also eliminated the Lissaman 7769 because of the drag coefficient, the SD 7062 for the high pitching moment, and the MH 64 for a lower stall AoA than the MH 45. The remaining four airfoils were analyzed in the power requirements MATLAB program to see the power needed to complete the missions, the time to takeoff, and

the distance to takeoff. This resulted in the MH 45 being selected as the airfoil for the production aircraft. Tables 3.2-6 and 3.2-7 show the summary of aerodynamic requirements for all airfoils and the detailed results for NACA 4412. The detailed results for the other airfoils are in Appendix C.

Table 3.2-6 Summary of Aerodynamic Analysis for Production Aircraft Potential Airfoils

	NACA 4412	MH 114	SD 7062	MH 83	MH 64	S1223	MH 45	Lissaman 7769
Max. Lift Coeff	1.2	1.8	1.6	1.8	1	1.6	1.2	1.4
Coeff of Lift at Zero AoA	0.5	0.8	0.4	0.45	0.15	1.2	0.1	0.3
Min. Drag Coeff	0.01	0.01	0.01	0.01	0.01	0.01	0.01	0.02
Max L/D at Cruise Speed	82	135	105	100	80	100	82	70
AoA at Max L/D	5	4	5	8	5	6	5	5
Zero Lift Angle	-1	-10	-5	-4	-2	-5	-1	-3
Critical AoA	11	15	12	12	10	11	11	11
Lift Slope	0.08	0.09	0.08	0.09	0.1	0.07	0.092	0.1
Coeff of Moment at Zero AoA	-0.01	-0.19	-0.08	-0.065	-0.02	-0.08	-0.01	-0.03
Distance to Takeoff (meters)	22	19		24			17	
Time Until Takeoff (sec)	3.2	2.9		3.4			2.8	

3.2.8 Control Surfaces Analysis

After researching designs of small UAV flying wings, we discovered that there is no definitive way to design elevens for a flying wing. Instead, it is a trial and error iteration process to obtain the required size of the elevon to be able to pitch and roll the aircraft. We used the report of a Major Qualifying Project team from previous years [5] which was also a flying wing design to help us design our control surfaces. We calculated the wing surface area and the control surface area of the 2013 MQP aircraft, and determined the ratio of control surface area to wing surface area.

To calculate the control surface area required for our aircraft, we implemented the same ratio from the 2013 aircraft. For the aircraft to obtain a certain pitch rate at takeoff, we used a control surface chord equal to the quarter chord of the main wing, 0.0762 m. Then used the ratio of the 2013 aircraft to calculate a span of the control surfaces. [5]

Table 3.2-7 Summary of Aerodynamic Results for NACA 4412

NACA 4412						
Weight = Lift	40	N	4	kg		
Density of air	1.225	kg/m^3			Coeff of lift linearization	
Chord	0.3048	m			Cl = mx +b	
Area required at low speed	**0.60**	m^2			Cl = 0.08x +0.5	
Frontal Area	0.07	m^2				

			Velocity (m/s)			
Parameter	**Notation**	**Units**	**10**	**15**	**20**	**25**
Reynolds Number	Re		207,000	311,000	415,000	519,000
Coeff of Lift Min	Cl		1.20	0.48	0.27	0.17
Angle of Attack	AoA	degrees	8.75	-0.19	-2.84	-4.07
Span	b	meters	1.96	1.96	1.96	1.96
Aspect Ratio	AR		6.44	6.44	6.44	6.44
Coeff of Drag	Cd		0.03	0.01	0.01	0.01
Coeff of Moment	Cm		-0.07	-0.10	-0.10	-0.10
Lift/Drag	L/D		50.00	60.00	55.00	55.00
Drag	D	Newtons	0.92	0.83	1.47	2.29
Power	P	Watts	9.17	12.38	29.33	57.29
Thrust/Weight Ratio	T/W		0.02	0.02	0.02	0.02
Wing Loading Factor	W/S	N/m^2	6.68	6.68	6.68	6.68

3.3 Aerodynamic Analysis for Manufacturing Support Aircraft

For the Manufacturing Support aircraft, we were able to use the same process as the final approach of the Production aircraft. We again were able to get a final weight estimate of 7.5kg. This is to account for the weight of the Production aircraft as cargo. The airfoils selected ranged in thicknesses between 12 and 18 percent and increased camber than the production aircraft to provide more lift. The moment caused by the camber will be corrected by a vertical and horizontal tail. The following tables shows a summary of results for all airfoils analyzed.

Table 3.3-1 Summary of Results for Manufacturing Support Aircraft Potential Airfoils

	NACA4412	MH 114	MH 104	NACA2414	S8036	NACA 4418
Max. Lift Coeff	1.5	1.8	1.2	1.25	1.25	1.5
Coeff of Lift at Zero AoA	0.5	0.9	0.1	0.25	0.2	0.5
Min. Drag Coeff	0.08	0.01	0.01	0.01	0.01	0.01
Max L/D at Cruise Speed	110	107		100	110	
AoA at Max L/D	6	7.5	5	7	8	
Zero Lift Angle	-4.5	-9	-1	-2.5	-2	-4.5
Critical AoA	15	14	12	15	16	11
Lift Slope	0.08	0.09	0.11	0.077	0.059	0.09
Coeff of Moment at Zero AoA	-0.01	-0.19	0.025	-0.049	-0.028	-0.095
Min. Surface Area for Takeoff (m^2)	0.58	0.41	0.58	0.56	0.56	0.56
Takeoff Distance	16	16				

Table 3.3-2 shows the results for NACA 4418. Tables for other airfoils are in Appendix D.

Table 3.3-2 Summary of Aerodynamic Results for NACA 4418

NACA 4418						
Weight = Lift	75	N	7.5	kg		
Density of air	1.225	kg/m^3			Coeff of lift linearization	
Chord	0.4826	m			Cl = mx +b	
Area required at low speed	**1.08**	m^2			Cl = 0.09x +0.5	
Frontal Area	0.10	m^2				

			Velocity (m/s)			
Parameter	**Notation**	**Units**	**10**	**15**	**20**	**25**
Reynolds Number	Re		207,000	311,000	415,000	519,000
Coeff of Lift	Cl		1.25	0.51	0.28	0.18
Angle of Attack	AoA	degrees	8.33	0.06	-2.40	-3.54
Span	b	meters	2.23	2.23	2.23	2.23
Aspect Ratio	AR		4.63	4.63	4.63	4.63
Coeff of Drag	Cd		0.02	0.01	0.01	0.01
Coeff of Moment	Cm		-0.08	-0.09	-0.09	-0.09
Lift/Drag	L/D		62.50	50.51	28.41	22.73
Drag	D	Newtons	1.32	1.49	2.64	3.30
Power	P	Watts	13.20	22.28	52.80	82.50
Thrust/Weight Ratio	T/W		0.02	0.02	0.04	0.04
Wing Loading Factor	W/S	N/m^2	6.96	6.96	6.96	6.96

3.4 Stability Analyses

Flying wing aircraft are renowned for their high lift-to-drag ratios as the whole aircraft acts as a lifting body. It was critical that the Production Aircraft was pitch stable as there would be no tail to counteract any moments. This problem was easily resolved on the Manufacturing Support Aircraft as it had a vertical and horizontal stabilizer.

As seen in the graphs below, the MH 45 had the lowest lift of the airfoils chosen; however, the drag and moment coefficients for the MH 45 were also the lowest. As described in the sensitivity analysis, weight would play the biggest role in our score. The battery was the heaviest component of the aircraft, so minimizing the weight of the battery reduced the weight of the overall aircraft. Trade studies showed that reducing the weight of the battery would play a more significant role than reducing the weight of the wing. It was also discovered that the lower the moment about the quarter chord, the easier it would be to achieve pitch stability without a horizontal stabilizer. Therefore, we chose the MH 45 as the airfoil for the Production Aircraft.

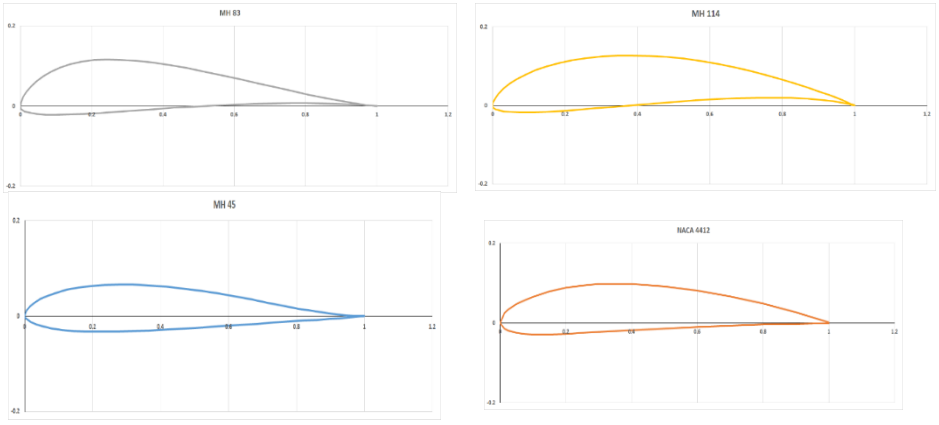

Figure 3.4-1 Production Aircraft Airfoil Profiles

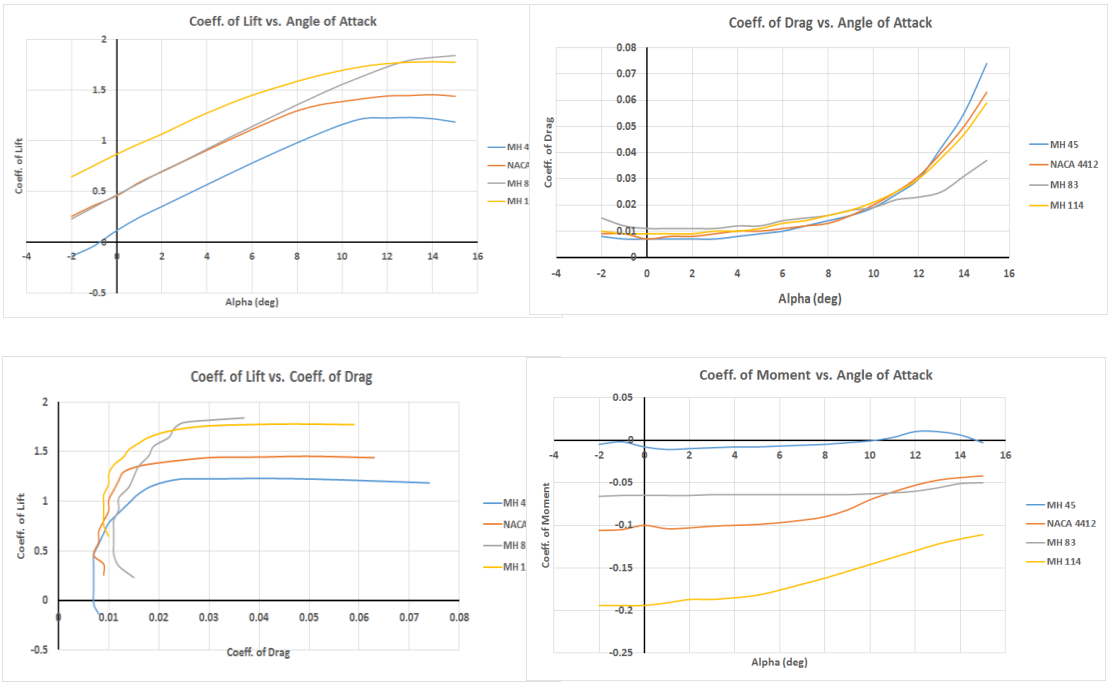

Figure 3.4-2 Production Aircraft Aerodynamic Graphs

Similar to the MH 45, the NACA 4418 did not produce the most lift of the chosen airfoils, but did have low drag features to reduce the required power of the motor. Despite the large pitching moment of the NACA 4418, it was chosen because of the high thickness (needed to nest the Production Aircraft inside), high lift, and low drag. The pitching moment would be corrected using a horizontal stabilizer.

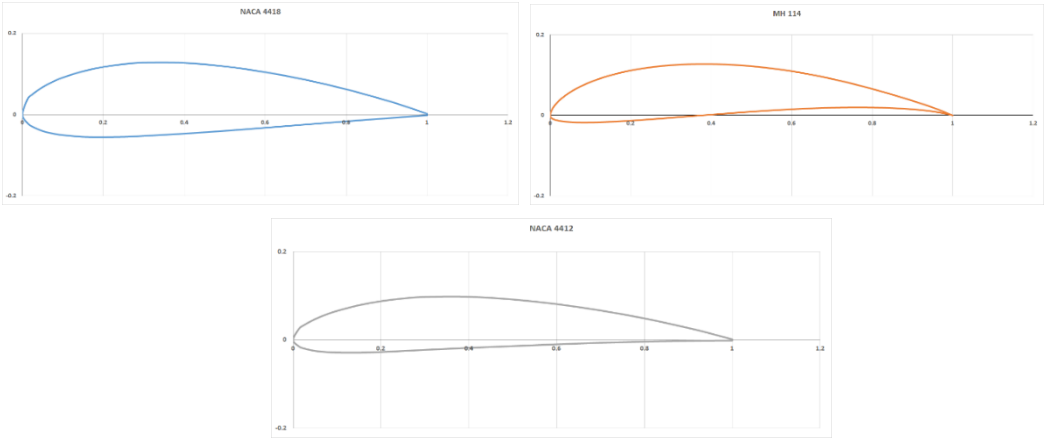

Figure 3.4-3 Manufacturing Support Aircraft Airfoil Profiles

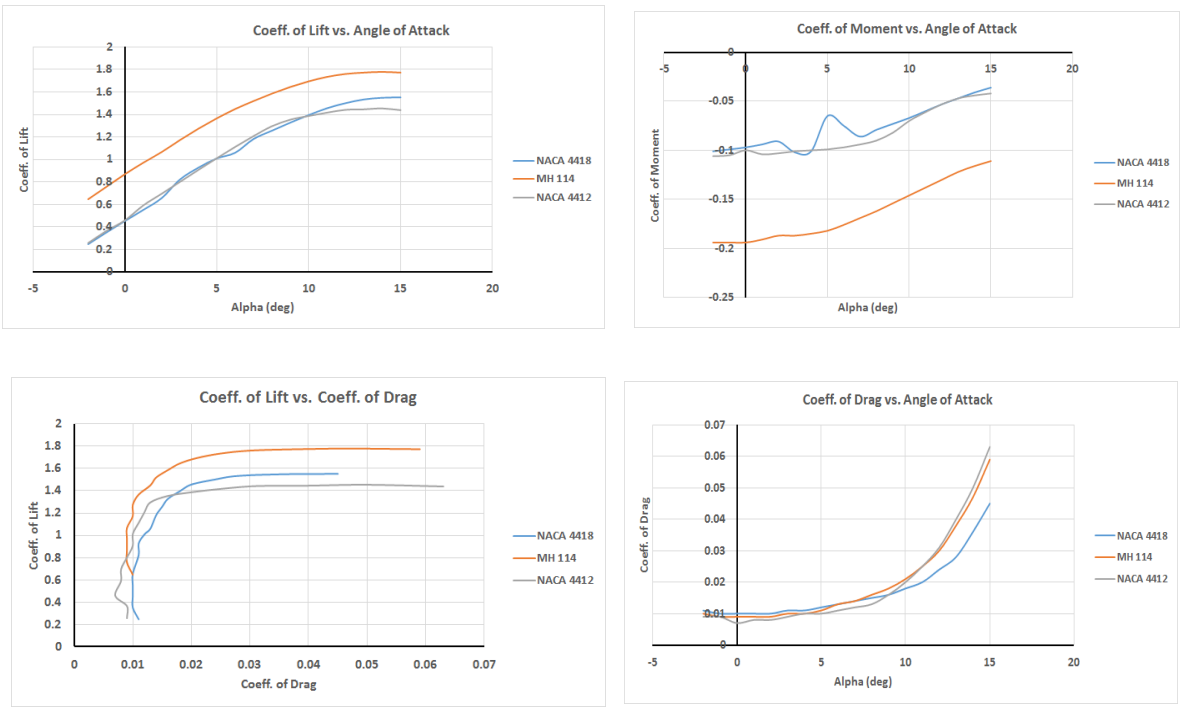

Figure 3.4-4 Manufacturing Support Aircraft Aerodynamic Graphs

To determine the stability of both the Production Aircraft and the Manufacturing Support Aircraft, the built in stability and control analysis tool in XFLR5 was used. After entering each aircraft's geometry and center of gravity, XFLR5 was able to produce longitudinal and lateral stability eigenvalues and stability derivatives. Using preliminary weights, aircraft geometry and center of gravity, a model of the Production Aircraft was created in XFLR5.

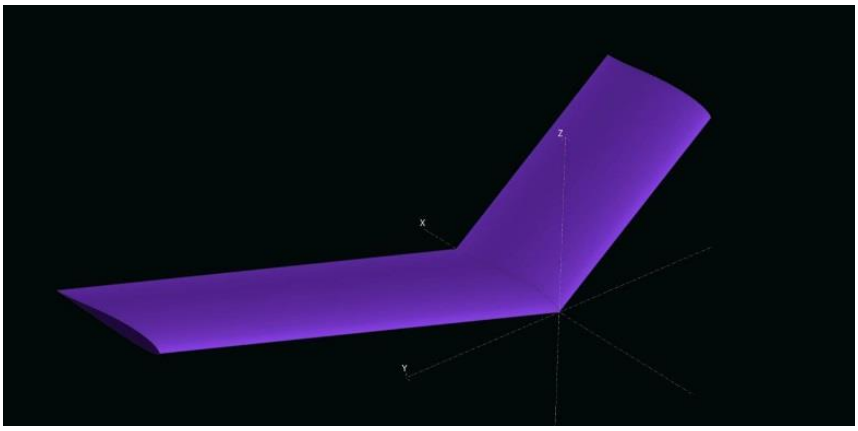

Figure 3.4-5 Production Aircraft Stability Analysis in XFLR5

The software then took the aircraft data and calculated the aerodynamic performance of the aircraft as well as the stability and control derivatives. The tables below summarizes the eigenvalues calculated in the flight simulation.

Table 3.4-1 Production Aircraft Initial Stability Results

Longitudinal		Lateral		
Phugoid	Short Period	Spiral Mode	Dutch Roll	Roll
-0.000 +/- 0.125i	-96.680 +/- 137.700i	-0.0002 + 0.000i	-0.017 +/- 4.239i	-36.875 + 0.000i

As indicated by the corresponding negative eigenvalues, the Production Aircraft was stable in all five modes. The same process was used to analyze the Manufacturing Support Aircraft's stability and control. After entering preliminary weights, aircraft geometry, and center of gravity, a model of the Manufacturing Support Aircraft was created in XFLR5.

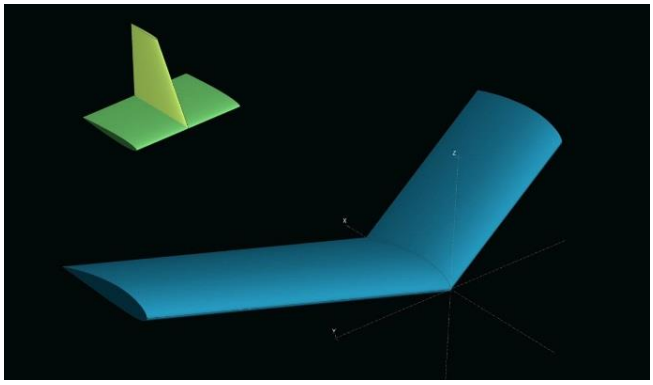

Figure 3.4-6 Manufacturing Support Aircraft Stability Analysis in XFLR5

Likewise, the negative values prove that the Manufacturing Support Aircraft was also stable in all five modes. This was only possible with a horizontal tail deflection angle of -4 degrees at the trim condition. Therefore, the aircraft would have to maintain tail deflection during the course of the flight.

3.5 Wing Tunnel Testing

To test the 3 dimensional lift characteristics, two wing test sections were constructed and placed in the 2ft x 2ft test section of a wind tunnel. The lift force was calculated at -5, 0, 3, 6, 9, 12, and 15° angle of attack at 10, 15 20, and 25 m/s airspeed.

Production Aircraft

Angle of Attack (degrees)	Back Scale Baseline (grams)	Front Scale Baseline (Grams)	Back Scale reading (grams)
-5	0	0	415.2
0	0	0	49
3	0	0	226.7
6	0	0	468.9
9	0	0	602.3
12	0	0	727.7
15	0	0	XXXX

	Front Scale reading (grams)	Difference in reading(Lift in grams)	Newtons	Entire wing Lift	Coeff of Lift for test
2	-143	-272.2	-2.66756	**-11.89287167**	-0.1501886882
9	323.1	372.1	3.64658	**16.25766917**	0.1408136606
7	499.3	726	7.1148	**31.72015**	0.3365404189
9	740.6	1209.5	11.8531	**52.84507083**	0.5747868622
3	1115.2	1717.5	16.8315	**75.0404375**	0.563484252
7	1347.7	2075.4	20.33892	**90.677685**	0.6809055118
X	XXXX	#VALUE!	#VALUE!	**#VALUE!**	#VALUE!

The measured lift and the theoretical lift were plotted on the same graph. It was evident that the actual lift produced was not going to be enough to keep the aircraft in flight, therefore a 10% increase was added to the wing area on the production aircraft.

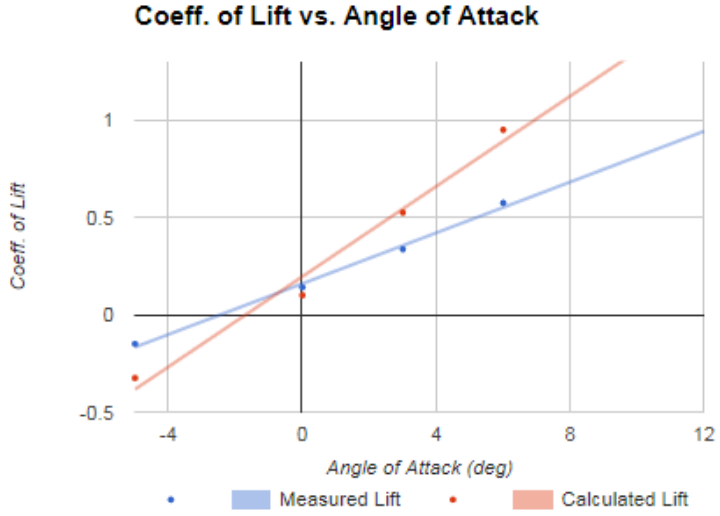

Figure 3.5-1 Theoretical/Actual Lift for Production Aircraft

Manufacturing Support Aircraft

Angle of Attack (degrees	Back Scale Ba	Front Scale B	Back Scale reading (grams)	Front Scale reading (grams)
-5	0	0	296.9	118.6
0	0	0	780.8	758.1
3	0	0	855.2	904.9
6	0	0	1261.5	2192.8
9	0	0		
12	0	0		
15	0	0		

Difference in reading(Lift in grams)	Newtons	Entire wing Lift	Coeff of Lift Test
-415.5	-4.0719	**-18.1538875**	-0.05605100568
1538.9	15.08122	**67.23710583**	0.4280142488
1760.1	17.24898	**76.9017025**	0.5532728459
3454.3	33.85214	**150.9241242**	0.9342606097
0	0	**0**	
0	0	**0**	
0	0	**0**	

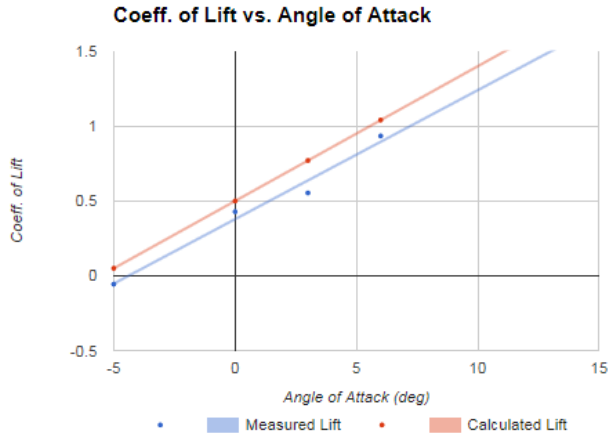

Figure 3.5-2 Theoretical/Actual Lift for Manufacturing Support Aircraft

The Manufacturing Support Aircraft produced enough lift because it was already designed larger than needed, in order to fit the Production Aircraft inside.

3.6 Final Design Parameters based on Aerodynamic Analyses

The final production aircraft used a MH45 airfoil with a span of 2.15m, a chord of 0.279m, and a sweep of 27 degrees. Though this airfoil did not produce as much as lift as its competitors, it produced the least amount of drag and requires the least amount of power to meet mission requirements. Moreover, the MH 45 had the smallest pitching moment of all the airfoils and was stable both laterally and longitudinally. As a result, the production aircraft did not require vertical or horizontal stabilizers. The Manufacturing Support Aircraft used a NACA 4418 airfoil. The camber of the NACA 4418 provided more lift than the MH45 but it also had a pitching moment that could not be corrected without a tail. Since a tail was needed, the

horizontal stabilizer had elevators and the vertical stabilizer had a rudder for pitch and yaw control. These stabilizers were both NACA 0009. The NACA 4418 airfoil was thick enough to contain the MH45 airfoil within itself while also providing structural support. The summary of all design results can be seen in the tables below:

Table 3.6-1 Final Design Parameter for Both Aircraft

PA Main Wing:		
Airfoil Chosen	MH45	
Span	2.150	m
Chord Length	0.279	m
Surface Area	0.600	m^2
Aspect Ratio	7.720	
Sweep Angle	27.00	deg
Taper Ratio	1.000	
Mean Aero Chord	0.279	m
Control Surfaces:		
Elevon Length	0.373	m
Elevon Width	0.064	m
Aerodynamic Characteristics:		
Coeff of Lift	0.191	
Coeff of Lift Max	1.11	
Coeff of Drag	0.008	
Coeff of Moment	0.033	
Critical AoA	15	

M/S Main Wing:		
Airfoil Chosen	NACA 4418	
Span	2.150	m
Chord Length	0.483	m
Surface Area	0.980	m^2
Aspect Ratio	4.210	
Sweep Angle	27.000	deg
Taper Ratio	1.000	
Mean Aero Chord	0.483	m
Total A/C Weight	4.750	kg
X-CG	0.611	m
Z-CG	0.006	m
Horizontal Tail:		
Airfoil Chosen	NACA 0009	
Span	0.535	m
Chord Length	0.300	m
Surface Area	0.161	m^2
Aspect Ratio	1.783	
Sweep Angle	0.000	
Taper Ratio	1.000	
Mean Aero Chord	0.300	
Vertical Tail		
Airfoil Chosen	NACA 0009	
Span	0.309	m
Chord Length Root	0.309	m
Chord Length Tip	0.150	m
Surface Area	0.070	m^2
Aspect Ratio	2.640	
Sweep Angle	0.000	deg
Taper Ratio	2.060	
Mean Aero Chord	0.240	m

Control Surfaces:		
Elevators	0.1122	m
Rudder	0.103	m
Aileron Length	0.535	m
Aileron Width	0.1143	m
Aero Characteristics:		
Coeff of Lift	0.369	
Coeff of Lift Max	1.22	
Coeff of Drag	0.02	
Coeff of Moment	0.18	
Critical AoA	15	

3.7 Propulsion Analysis

There are three major components within the propulsion subsystem in both aircraft: the motor, propeller, and battery. The motor and propeller were selected together as most motor specification sheets recommend a propeller for the most effective and efficient use. Once the motor and propeller were selected, the battery pack configuration could be determined from motor and mission requirements.

3.7.1 Motor and Propeller

The first step of the design process for the propulsion system was to select the appropriate motors. The motor had to be capable of taking off in the allotted runway size and generating enough thrust in order to complete the mission requirements in the allotted time. From dynamic thrust calculations and preliminary design parameters, we decided to first select an AXI Gold 2820/12 Outrunner Motor with specifications that can be seen in the table below:

Table 3.7-1Motor and Propeller Specifications

	AXI Gold 2820/12 Outrunner Motor
Motor Diameter	35 mm
Shaft Diameter	5 mm
KV	990 Kv
Voltage Range	9.6 – 18.5 V
Max Current	37 Amps
Weight	5.3 oz.

Based on the motor specification sheet, an 11x7 propeller was recommended for use with the motor to achieve the best efficiency.

3.7.2 Battery

From our analysis shown in section 2.6, NiMH batteries were decided to be used for both aircraft. With the motor was selected we were able to choose a battery back that met the mission requirements. A 10 cell, 12V, 3300mAh battery pack was decided for use. This would meet the voltage output required by the motor and the capacity to run the motor for the duration of each mission.

3.8 Structural Analysis

In an effort to use less total material, components that would be able to support high bending moments and fracture toughness for the wing tip test were analyzed. The loads of the aircraft were divided into three categories:

- Aerodynamic loads: This included all the wing and control surfaces that created lift, drag and moment that would translate to the main SUPPORT of the structure. Balsa is a good material since is lightweight and able to support sizeable loads applied in a perpendicular direction to its grain.
- Propulsion loads: This included propulsive torque, thrust and continuous vibrations that would transfer to the fuselage structure. A firm material was needed to absorb the motor vibrations and to properly secure all fasteners.
- Ground loads: This included aircraft weight and landing impact. The truss consists of metal components since it must have a high flexural strength that can withstand impact without breaking.

Since all the loads acting on the aircraft need to be transferred to the major load bearing components, all impact parts were designed to connect to the central spar or the wing spar. To maximize the strength against bending moments at the fuselage, the wing spars were connected as close as possible and secured with aluminum fittings and pins, thus allowing the loads to be transferred along the fuselage truss.

4. Detailed Design Models

After the optimization process, and mission profile analysis, a prototype of the Production Aircraft was constructed. The prototype was designed to test the flying characteristics of the fully loaded Production Aircraft and validate the aircraft design. After the design for the Production Aircraft was completed, a detailed design of the Manufacturing Support Aircraft was created to conform to the size and shape of the Production Aircraft so it could be efficiently transported inside the Manufacturing Support Aircraft. After these designs were successfully created using Computer Aided Design software, they were built and tested to validate that the designs accomplished each mission profile.

4.1 Summary of Final Specifications

The preliminary aircraft dimensions selected by the Aerodynamics team changed minimally after the structural, layout, material and weight-balance analyses were done. Having the final dimensions listed in the following tables, the wing design was carefully designed to allow adequate thickness for manufacturability. The Production Aircraft and Manufacturing Support Aircraft were designed for structural efficiency, simplicity and flight stability.

Table 4.1-1 Summary of Final Specifications

Production Aircraft Main Wing	Value	Units
Airfoil Chosen	MH 45	
Span	2.150	m
Chord Length	0.279	m
Surface Area	0.600	m^2
Aspect Ratio	7.720	
Sweep Angle	27.000	deg
Taper Ratio	1.000	
Mean Aero Chord	0.279	m

Propulsion Systems Production	Value	Units
Motor Type	Axi 2820/12	
Weight	0.15	kg
Kv	990	rpm/V
Power	300	W
Max RPM	11,880	
Propeller	11x7	in

Electrical System – Production Aircraft	Unit
Speed Controller	Eflite 40A Brushless ESC
Radio Receiver	Airtonics 92224
Number of Servos	3
Servo Type	HS-225BB

Batteries - Production Aircraft	Value	Units
Type	NiMH	
Capacity (each)	1,400	mAh
Range	5	min
Weight (each)	0.227	kg
Number of Batteries	2	

Manufacturing Support Main Wing	Value	Units
Airfoil Chosen	NACA 4418	
Span	2.150	m
Chord Length	0.483	m
Surface Area	0.980	m^2
Aspect Ratio	4.210	
Sweep Angle	27.000	deg
Taper Ratio	1.000	
Mean Aero Chord	0.483	m

Manufacturing Support Horizontal Tail	Value	Units
Airfoil Chosen	NACA 0009	
Span	0.535	m
Chord Length	0.300	m
Surface Area	0.161	m^2
Aspect Ratio	1.783	
Sweep Angle	0.000	
Taper Ratio	1.000	
Mean Aero Chord	0.300	

Vertical Tail	Value	Units
Airfoil Chosen	NACA 0009	
Span	0.309	m
Chord Length Root	0.309	m
Chord Length Tip	0.150	m
Surface Area	0.070	m^2
Aspect Ratio	2.640	
Sweep Angle	0.000	deg
Taper Ratio	2.060	
Mean Aerod Chord	0.240	m

Propulsion Systems Manufacturing Support	Value	Units
Motor Type	Axi 4120/14	
Weight	0.32	kg
Kv	660	rpm/V
Power	672	W
Max RPM	14,400	
Propeller	13x11	in

Electrical Systems Manufacturing Support	
Speed Controller	Turnigy AE-65A
Radio Receiver	Airtronics 92164
Number of Servos	3
Servo Type	HS-225BB

Batteries Manufacturing Support	Value	Units
Type	NiMH	
Capacity (each)	2,200	mAh
Range	5	min
Weight (each)	0.34	kg
Number of Batteries	2	

4.2 Weight Balance

Weight and balance tables were created for both aircraft to calculate the fore/aft position of the Center of Gravity (CG) and help to determine the stability of the aircraft. The tables feature the weight, arm, and moment for all the major components of the aircraft whose locations can be changed, as well as the weight, arm and moment for aircraft's structure itself to compute the aircraft's CG location. The arm length of each component was measured from a datum located at the tip of the central carbon spar running down the middle of both aircraft. The moment of each component is equal to the weight of the component multiplied by the arm, and the sum of the weight, arm, and moment for each component is shown at the bottom of each table. The CG position aft of the datum line was calculated by dividing the total moment by the total weight of all the components in each in table.

The battery and the Gatorade bottle were the heaviest components in the production aircraft, and both were placed near the center of the root chord to keep the CG closer to the nose for stability purposes and ensure that the aircraft's CG was within the footprint of the tricycle landing gear.

The weight and balance of the Manufacturing Support Aircraft needed to be evaluated for flight with and without the Production Aircraft loaded since the Production Aircraft was not placed directly at the CG during transportation. Since the Manufacturing Support Aircraft used a taildragger landing gear configuration, the CG has a large range longitudinally to prevent a landing gear tip-over, but it had to be ensured that the aircraft did not become unstable with or without the Production Aircraft loaded. For this reason, the Production Aircraft's location for transportation was kept as close to the CG as possible to limit the change in flight characteristics between missions, and the battery location for the Manufacturing Support Aircraft would be slightly different for each mission in an effort to keep the CG at a constant location.

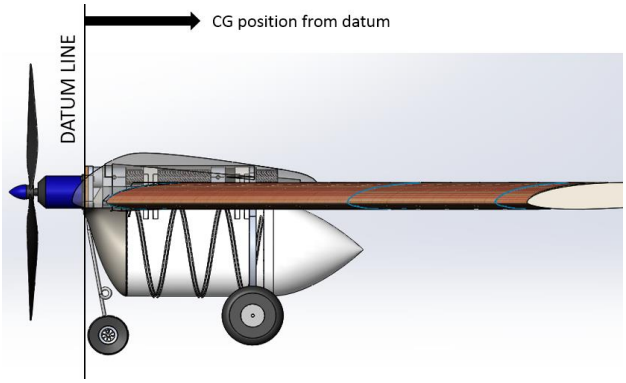

Component	Weight (kg)	Arm (m)	Moment (kg-m)
Motor	0.150	-0.003	0.000
Propeller	0.011	-0.054	-0.001
Motor Batteries	0.454	0.094	0.043
Reciever Battery	0.043	0.028	0.001
ESC	0.014	0.028	0.000
Reciever	0.008	0.037	0.000
Gatorade Bottle	0.599	0.058	0.035
Bottle Case	0.108	0.109	0.012
Tail Cone	0.047	0.196	0.009
Nose Gear	0.018	0.018	0.000
Main Gear	0.074	0.174	0.013
Aircraft Structure	0.998	0.248	0.248
Totals:	2.523	0.934	0.360
CG position aft of datum line:		0.1428671561	(m)

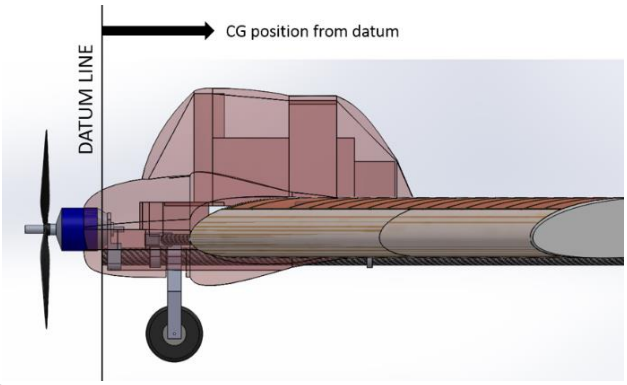

Component	Weight (kg)	Arm (m)	Moment (kg-m)
Motor	0.320	-0.032	-0.010
Propeller	0.018	-0.081	-0.001
Motor Batteries	0.680	0.218	0.149
Reciever Battery	0.043	0.126	0.005
ESC	0.014	0.133	0.002
Reciever	0.008	0.056	0.000
Main Gear	0.242	0.096	0.023
Tailwheel	0.025	1.721	0.044
Empennage	0.546	1.568	0.856
Aircraft Structure	2.750	0.016	0.045
Production A/C	1.461	0.340	0.496
Totals:	1.350	1.312	0.212
CG position aft of datum line:		0.1568055027	(m)

Figure 4.2-1 Weight Balance

4.3 FUSELAGE - PRODUCTION AIRCRAFT

The entire Production Aircraft design wa based on the integration of optimized subsystems into a lightweight assembly. The following subassemblies were analyzed with greater detail: fuselage, payload arrangement, wings, propulsion system, and landing gear.

To obtain an aircraft that wa as lightweight and simple as possible, yet still strong enough to sustain all aerodynamic forces, a central Carbon Fiber tube was initially considered as the main structural component. The wings were attached to it through two aluminum fittings, while the landing gear and payload arrangement were designed to have slots and could slide forward and backward on the central spar until a desired Central of Gravity (CG) was obtained.

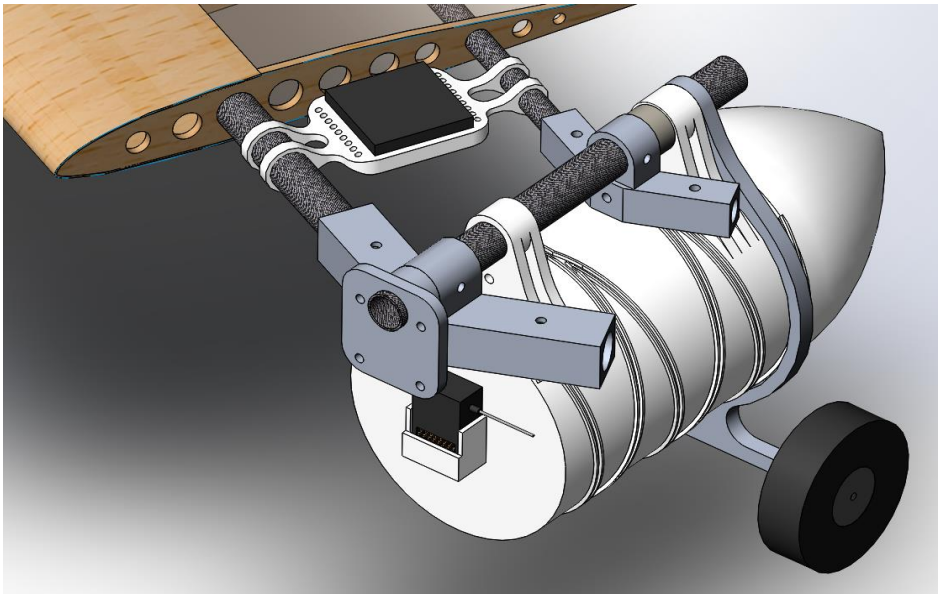

Figure 4.3-1 Production Aircraft Initital Fuselage Design

The aluminum fittings were designed to allow both front spars of the wing and the aft spars to be connected as close as possible in the center of the aircraft, thus ensuring the fundamental structural capability. A shorter tube was placed inside the wing spars in the fittings area to add extra strength. The spars were secured to the fittings through pins.

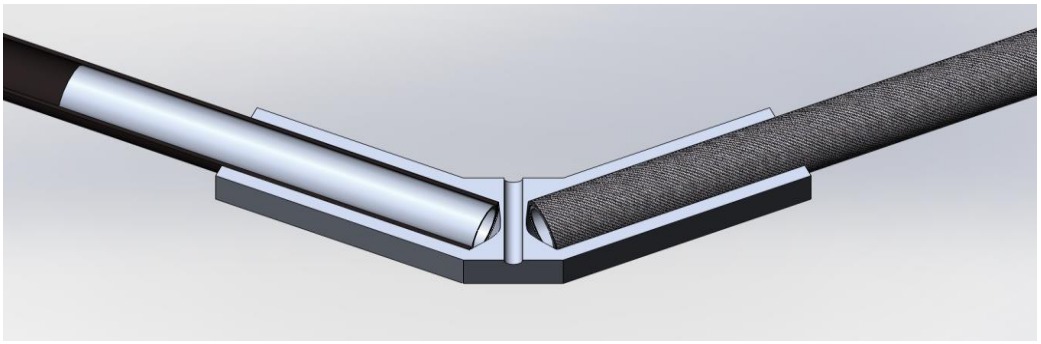

Figure 4.3-2 - Section View of Aluminum Fitting Showing Wing Spar and Reinforcing Tubes

Upon further propulsion analysis, using two separate batteries placed inside the wings was not possible. Rather, a single larger and heavier battery had to be used. The placement of this battery was not favorable with the current configuration. Therefore, a new setup with two central carbon fiber spars was chosen, so the battery could be places between them. This updated model can be seen in the following figure:

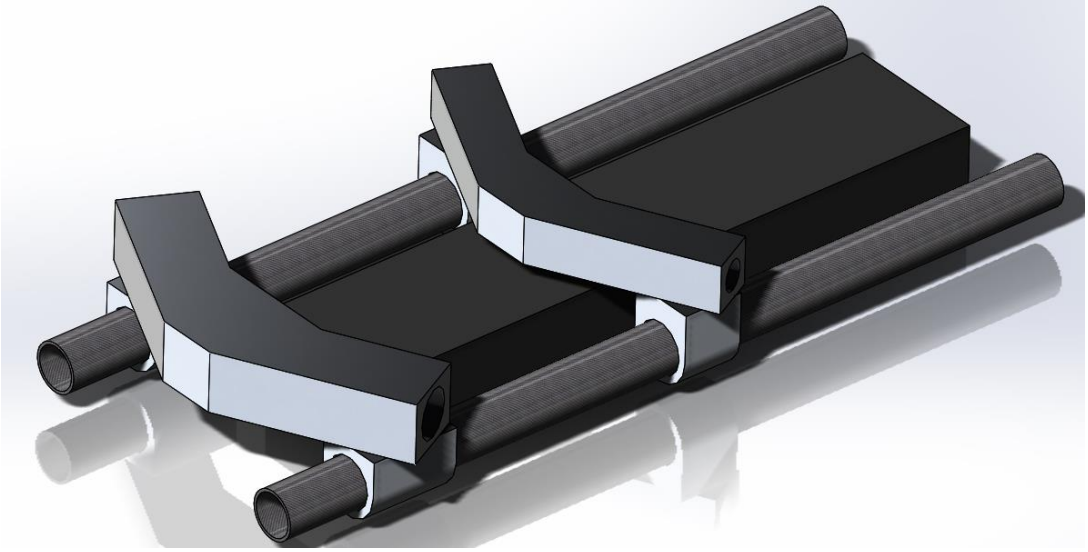

Figure 4.3-3 Updated Structure of Production Aircraft Fuselage

To give the fuselage an aerodynamic shape, two foam fairings were used to enclose the front side of the aircraft, one at the top and one at the bottom.

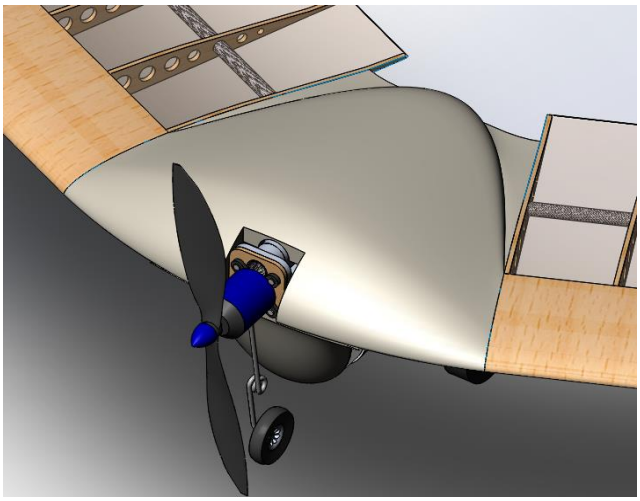

Figure 4.3-4 Foam Fairing Fuselage an Aerodynamic Shape

4.4 FUSELAGE – MANUFACTURING SUPPORT AIRCRAFT

Similarly the Manufacturing Support Aircraft used a Carbon fiber spar as the main structural component. The wings were attached to the central spar with two aluminum fittings like in the Production Aircraft to keep the manufacturing process consistent and to reduce the

building time. The landing gear was designed to move forward and backward on the central spar until a desired Central of Gravity (CG) is obtained.

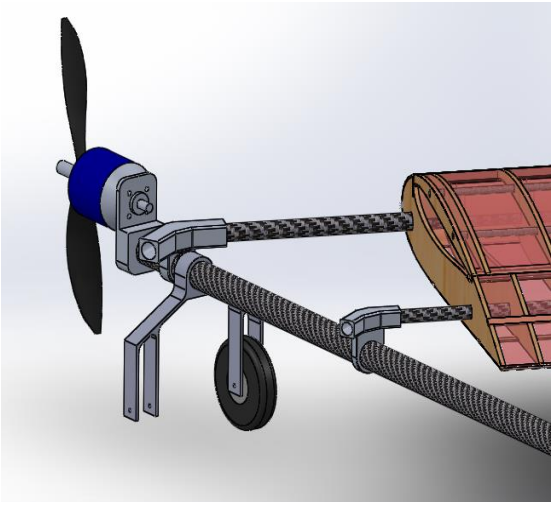

Figure 4.4-1 Fuselage Strength Given by Central Carbon Fiber Spar

In order to secure the tail, the central carbon fiber was extended all the wail to the tail. Two aluminum fittings were used to attach the horizontal tail wing, and a wooden block was used to attach the vertical stabilizer and the tail wheel bracket.

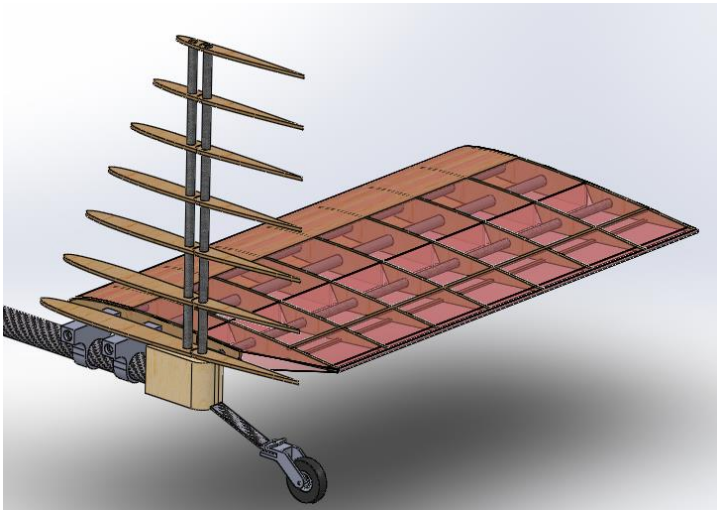

Figure 4.4-2 Tail Fittings Connected to Central Carbon Fiber Spar

The aluminum fittings for the Manufacturing Support aircraft were designed in the same manner as those for the Production Aircraft. Additionally, a shorter tube was be placed inside the wing spar similar to the method used in the Production Aircraft as shown in Figure 4-2.3

To give the fuselage an aerodynamic shape and enclose the Production aircraft and other components, two foam fairings were used, one at the top of the fuselage and one at the bottom.

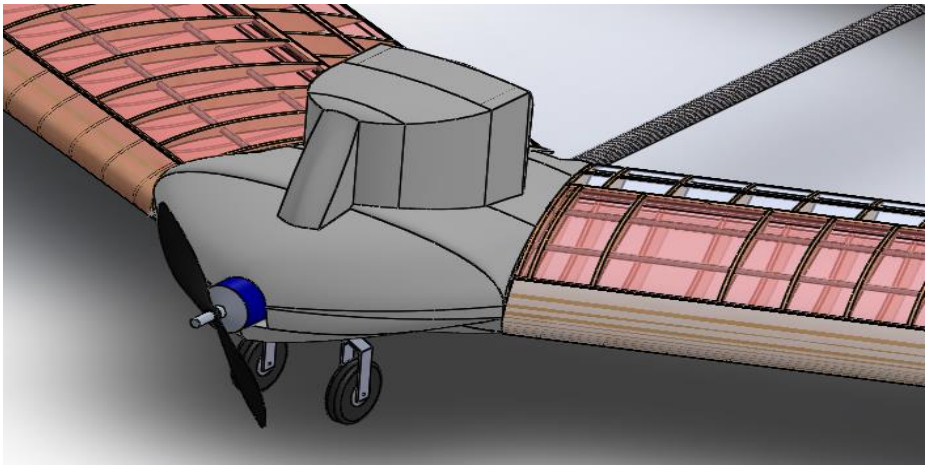

Figure 4.4-3 Foam Fairing for Manufacturing Support Aircraft

4.5 Payload Arrangement

For the Production Aircraft, a thin 3D printed cylindrical case reinforced with Carbon Fiber roving was used to hold the Gatorade bottle. A conical lid was designed to secure the bottle in place and give the fuselage an aerodynamic shape in the rear, where the foam covers ended. Initially this case connected to the central spar and was restricted from rotation and translation using pins. The case was initially a support for the receiver as well.

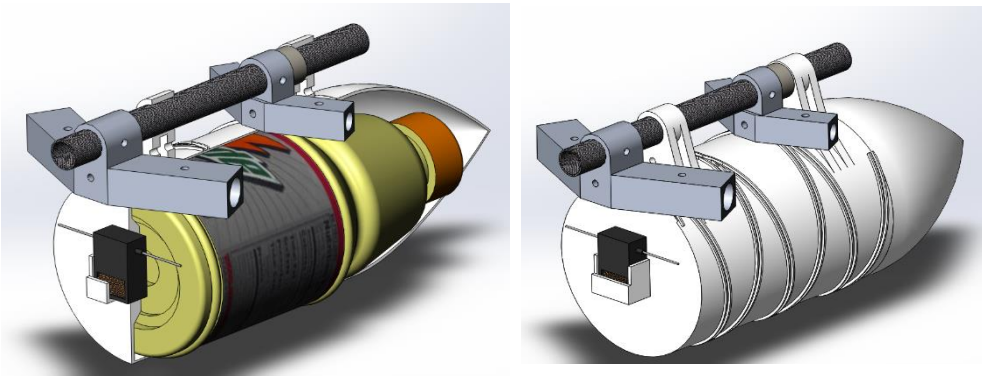

Figure 4.5-1 Section View and Entire View of 3D Printed Payload Case

After modifying the fuselage to contain two central spars and after testing the strength of the 3D printed case support hooks, two aluminum hoops were chosen to attach the case instead. These hoops were clamped to the two spars and were glued to the case. The updated model can be seen in the following figure:

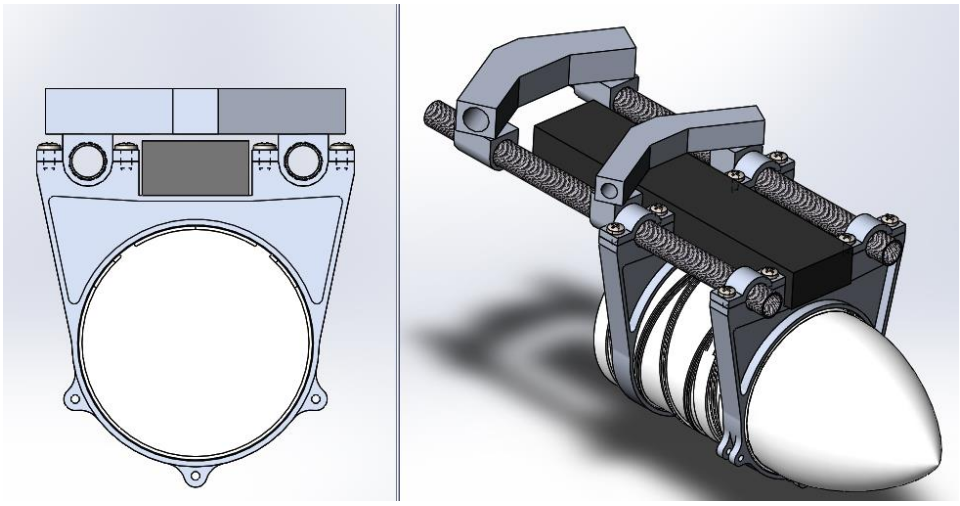

Figure 4.5-2 Updated Attachment of the 3D Printed Case

The top of each wing of the Manufacturing Support aircraft hinged upwards to nest the production aircraft inside. The foam fairing was designed to fully enclose the Production Aircraft.

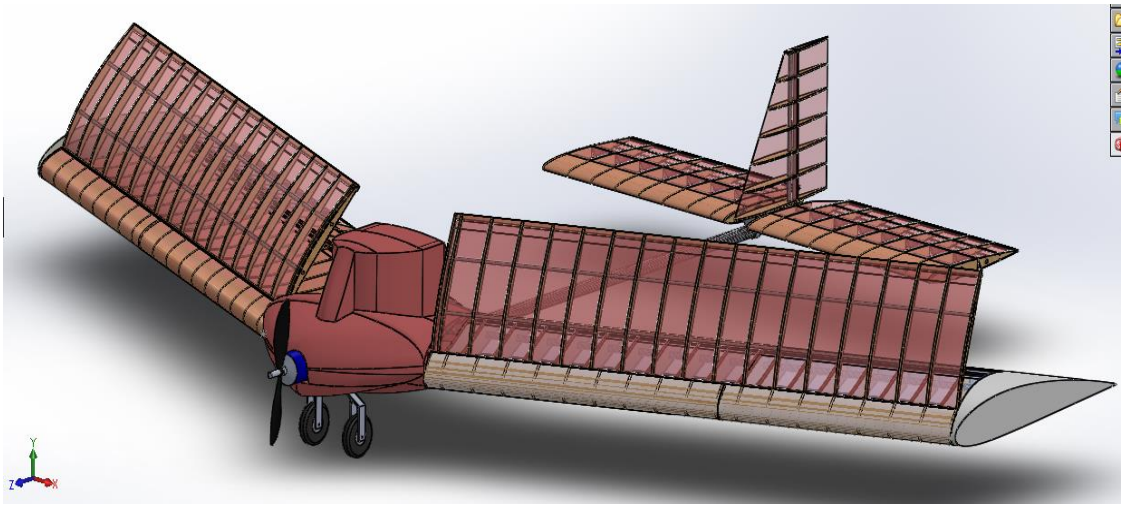

Figure 4.5-3 Manufacturing Support Aircraft with Wing Lids Open

4.6 Wings

The wings were designed to be as light as possible yet strong enough to resist to all aerodynamic forces in flight. Each wing consisted of an arrangement of laminated balsa ribs connected through two carbon fiber spars, with a balsa sheet placed at the leading edge along the length of the wing to maintain the airfoil shape and provide torsional strength. A heat-shrink MonoKote film was applied around the wings to give them a smooth surface. The wings were

attached to each other and the fuselage through aluminum fittings as described in section 4.3. Wing tips were cut out of foam to give the wing a tip parallel to the direction of the flow. The trailing edge was thickened and reinforced with a carbon fiber rod.

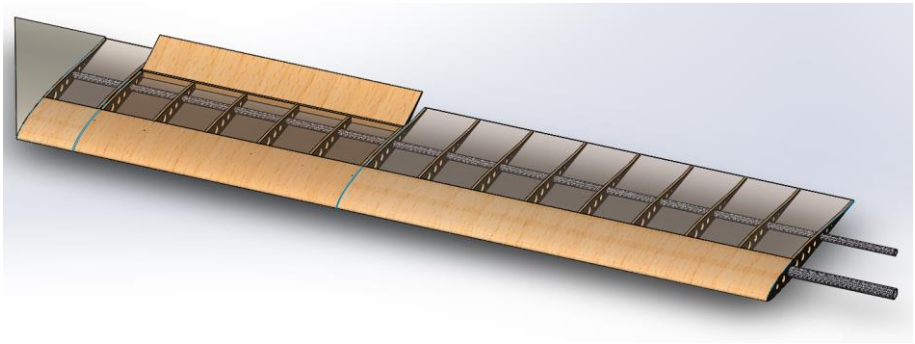

Figure 4.6-1 Production Aircraft Wing Design

The Manufacturing Support Aircraft wings were built in the same way as those of the Production Aircraft to ease the manufacturing process, with the only exception of the lid which was hinged to the main structure with sticky MonoKote

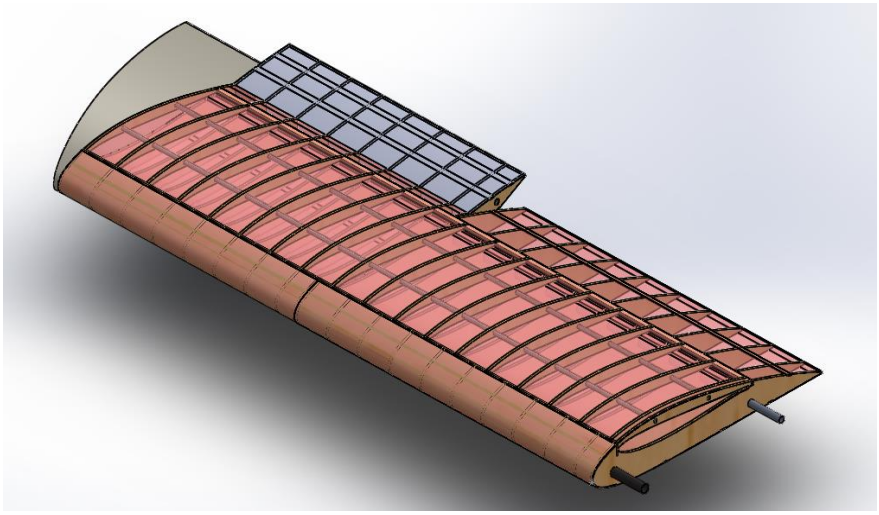

Figure 4.6-2 Manufacturing Support Aircraft Wing Design

4.7 Propulsion System Integration

Initially, our motor mount design included an aluminum and wooden plate attached to the central spar. The motor was screwed onto the plate to guarantee a flat surface and to help absorb motor vibrations, as seen in the following figure:

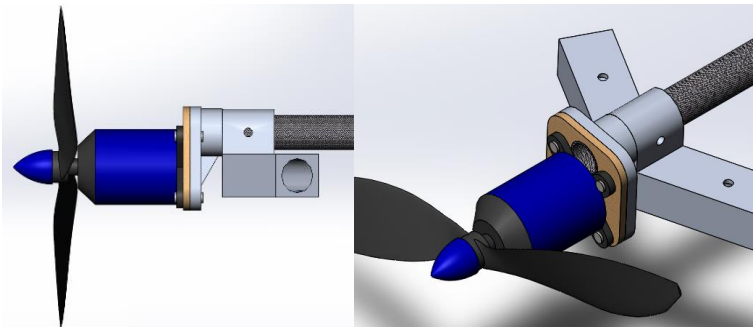

Figure 4.7-1 Initial Motor Mount for Production Aircraft

After our design was updated, a new aluminum motor plate was created. This new mount was attached and pinned to both central spars; it included a support for the nose wheel, as well as holes to mount the servo through L-brackets. The following figure shows this setup:

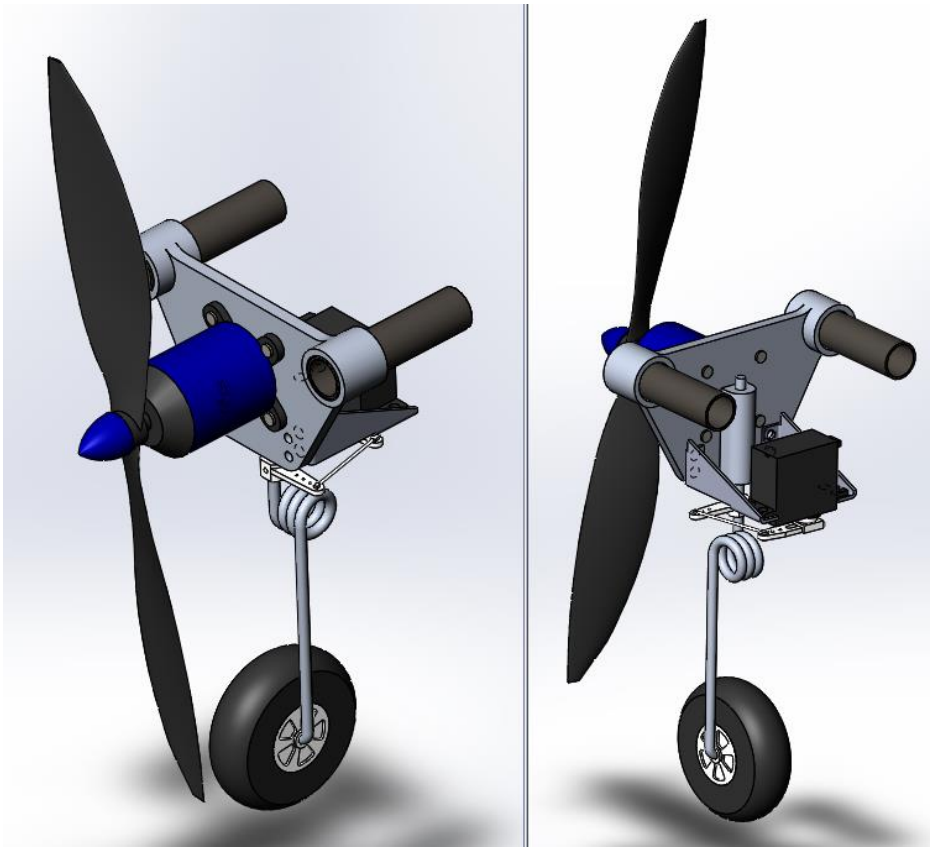

Figure 4.7-2 Final Motor Mount for Production Aircraft

The propulsion system components were originally selected using the analysis from the MATLAB program mentioned previously in sections 3 and 4. Following the wind tunnel test of the propulsion systems described in section 8, we confirmed that the original selected propulsion components had the proper characteristics for our Production flight mission. Though

it was found that the required battery capacity for the Production Aircraft decreased from 4200mAh to 2800mAh, this difference did not cause a need for modifications in our propulsion components. Therefore the AXI 2820/12 motor and 11X7” propeller selections remained unchanged. Based on the test data seen in section 8, we subsequently selected the propulsion components for the Manufacturing Support. The motor selected for the Manufacturing Support was an AXI Gold 4120/14 Outrunner with a 13X11” propeller with 4400mAh battery capacity.

The propulsion and electrical system for both the production and Manufacturing aircraft shown below, had an identical setup with the exception of a 40A electronic speed controller (ESC) for the Production Aircraft and a 65A ESC for the Manufacturing Support Aircraft. The separate amperage requirement was due to more power being needed for the Manufacturing Support Aircraft than for the Production Aircraft. The batteries were connected in parallel to increase the battery capacity for the missions. Also, there were three servos for both aircraft all having the same functionality, except the landing gear servo was also attached to the tail rudder in the Manufacturing Support Aircraft.

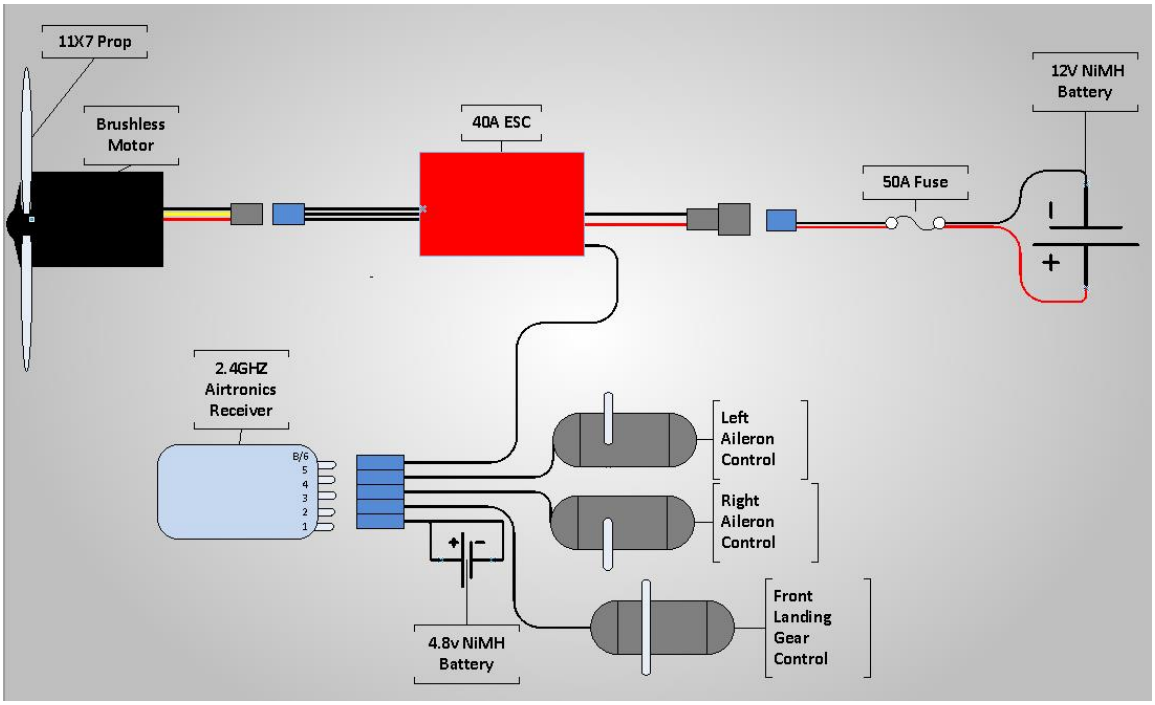

Figure 4.7-3 Production Aircraft Propulsion System Wiring Diagram

A combination of two batteries was used to power the motor in the Production Aircraft. The two batteries were attached to the wing spars with thin, aluminum fittings.

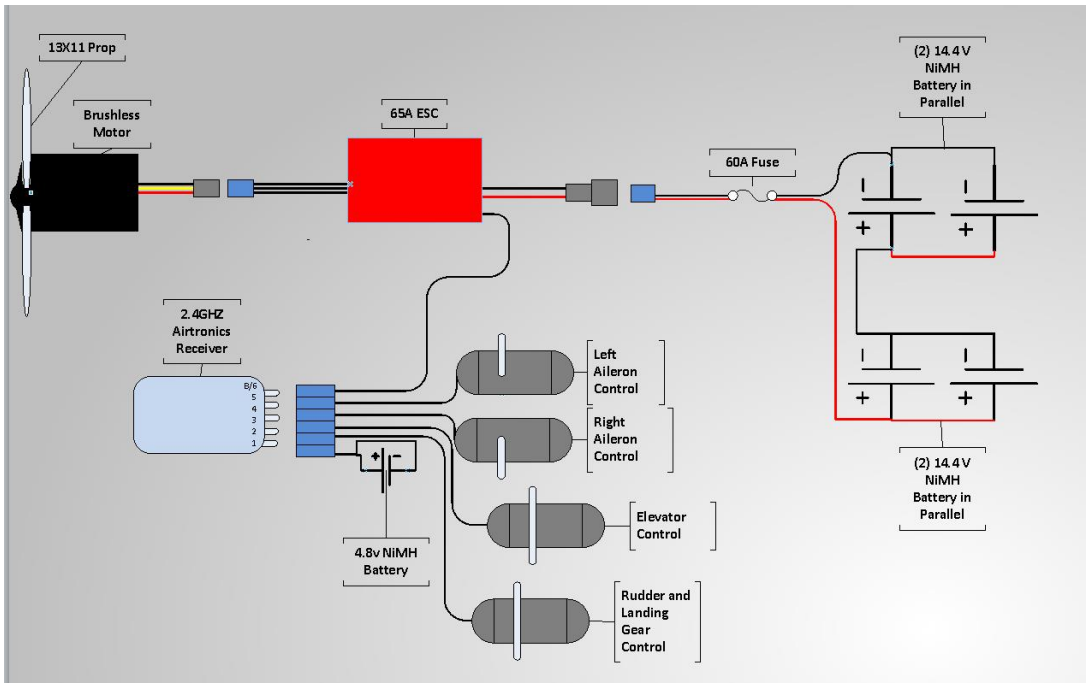

Figure 4.7-4 Manufacturing Support Aircraft Propulsion System Wiring Diagram

4.8 Landing Gear

The landing gear of the Production Aircraft was determined in the preliminary concept phase as composed of two wheels in the back and a steerable nose wheel. Since this aircraft was mounted upside down inside the Manufacturing Support Aircraft, the goal was to place the wheels as close to the fuselage as possible. The initial design included the back wheels mounted on an aluminum hoop designed to transfer shock away from the bottle casing to the central spar, as seen in the following figure:

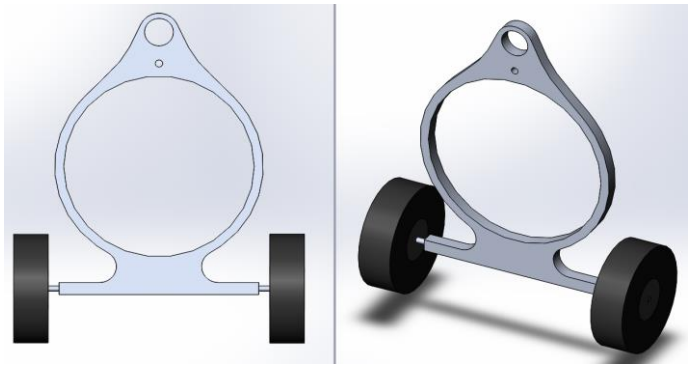

Figure 4.8-1 Initial Design of Production Aircraft Landing Gear

After changing the design of the fuselage to contain two tubes and two aluminum hoops, the landing gear design was simplified and mounted on the aft hoop as follows:

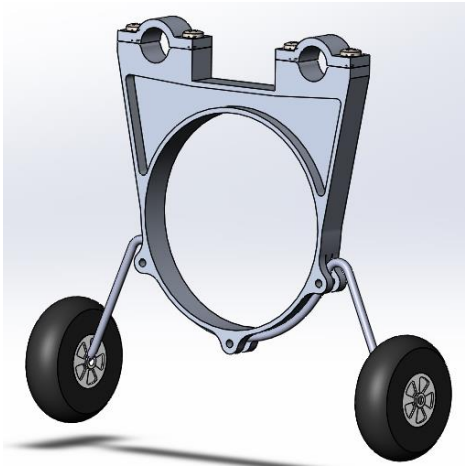

Figure 4.8-2 Final Design of Production Aircraft Landing Gear

The nose wheel was attached directly to the motor mount plate, which was another aluminum component. The servo that actuated the nose wheel was connected to the motor mount using two L-brackets. The following figure shows this layout:

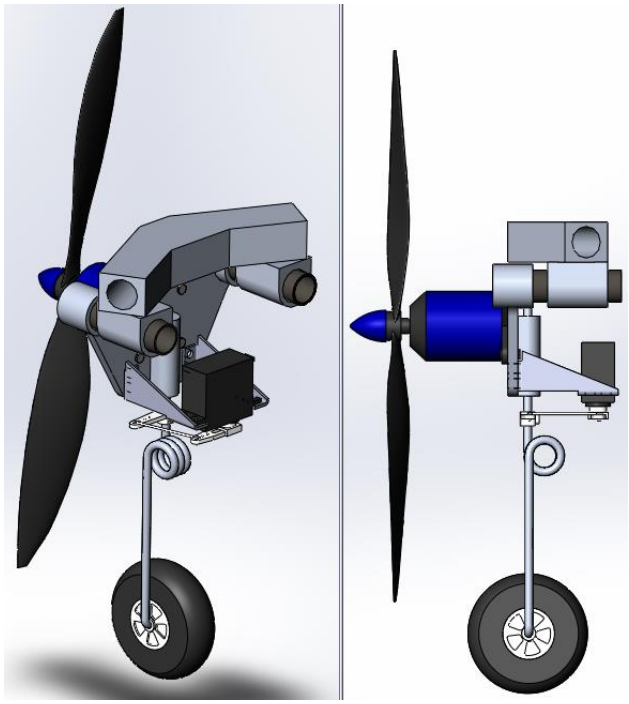

Figure 4.8-3 Nose Wheel and Servo Arrangement

Since a conventional layout was chosen for the Manufacturing Support Aircraft, a reversible tricycle landing gear layout was deemed most favorable. Therefore the front wheels

were designed to connect to the central spar and be able to move to a correct position according to the final CG. The rear wheel would be able to be steerable by connecting it to the rudder this would minimize the amount of servos on the tail.

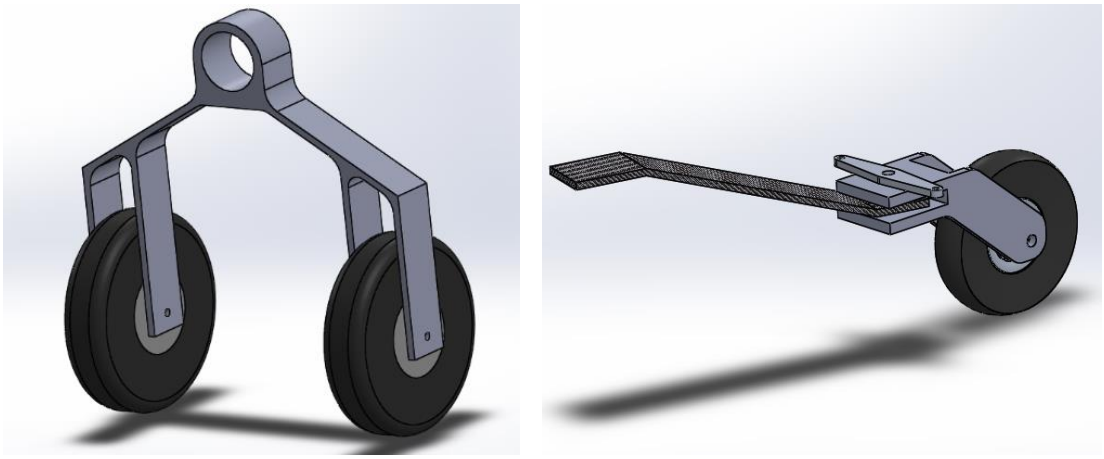

Figure 6.21 - Manufacturing Support Landing Gear

4.9 Expected Performance

Flight simulations conducted in MATLAB gave the following results:
Mission 1

- Takeoff distance: 63 ft
- Time to complete 3 laps: 207.4 seconds

Mission 2

- Takeoff distance: 83 ft
- Time to complete 3 laps: 220.4 seconds

Mission 3

- Takeoff distance: 57 ft
- Time to complete 3 laps: 173 seconds

4.10 Rated Aircraft Cost

Using pounds as the unit of weight, our aircraft's rated aircraft cost is as follows:

Table 4.10-1 Rated Aircraft Cost

Production Aircraft Weight	3.33lb
Production Aircraft Battery Weight	.661 lb
$N_{components}$ of the Production Aircraft	1
MS Aircraft Weight	10.472lb
MS Aircraft Battery Weight	1.5lb
Rated Aircraft Cost	**17.909**

5. Manufacturing

5.1 Materials Selected for Major Components

The manufacturing process selection was a significant factor in optimizing overall aircraft weight and total flight score. The selection of materials was determined based on research into materials used on previous winning aircraft. After extensive research the following materials were chosen for use in both of the aircraft: wood, composites, foam, and various plastics. These materials were used to create the major components of the aircraft, the fuselage, wings, tail and casing for our payload.

Laminated balsa plywood was selected for use in the ribs of both aircraft. This was due to balsa being a very light weight material which would result in a lightweight structure. As balsa sheets were not a strong material as they did not have a good strength to weight ratio, they were reinforced with plywood to ensure the material could withstand the weight of the aircraft. The laminated balsa plywood sheets were used to create the ribs of both the Production and Manufacturing Support Aircraft, and the tail of the Production Aircraft, with the use of a Laser-Cutting machine.

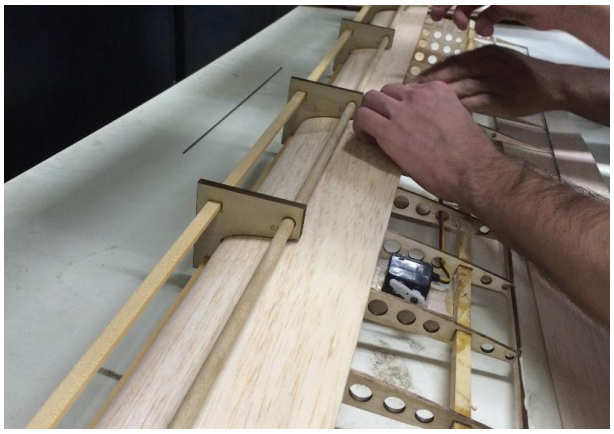

Figure 7.1 - Balsa Wood Ribs and Balsa Wood Leading Edge Wrap

Composites were chosen due to their high strength to low weight ratios. Carbon fiber was the backbone of lightweight composites and their tubes were made of carbon fiber, fiberglass and kevlar based composites. As a result, carbon fiber tubes were selected for the spars of the aircraft. The spars of an aircraft must hold the structure firmly together while avoiding cracks

and breaks in the ribs due to the load. Carbon fiber in the form of a unidirectional cloth was also used in to reinforce the casing for the Production payload.

Figure 7.2 - Carbon Fiber Wing Spars

Plastics are known for their low density and low electrical and thermal conductivity. Plastics are typically easier to manufacture and relatively less expensive than other materials. Both aircraft used MonoKote shrink wrap for the outer covering. MonoKote shrink wrap was lightweight, easy to use and very durable which made it a top choice for use in this competition. Plastics are also known to have a high strength to weight ratio when reinforced. As a result, a 3D printed case reinforced with carbon roving was used to carry the payload.

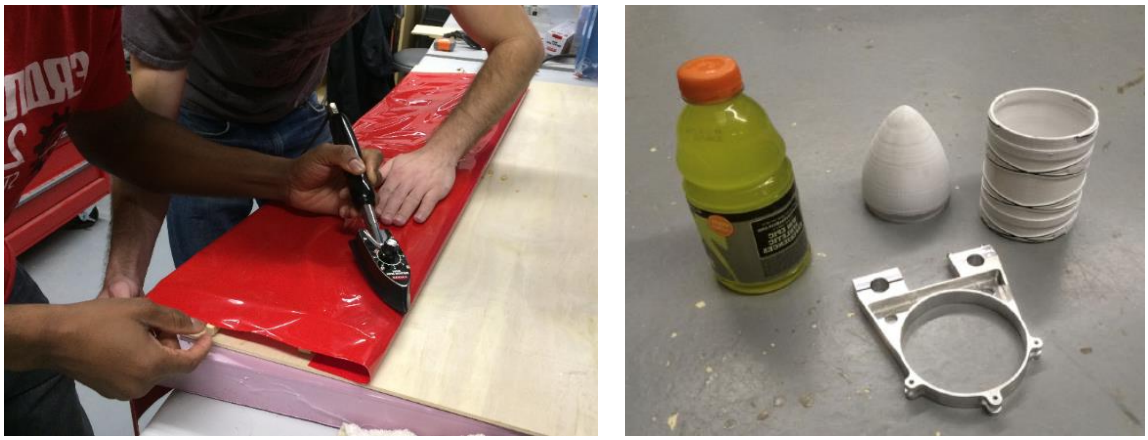

Figure 7.3 - Applying MonoKote Shrink Wrap (left); 3D Printed Bottle Case (right)

Foam is a popular material used when building RC aircraft as it is very inexpensive and its models can be made quickly and easily with the use of hot wire foam cutters. Foam structures are typically lightweight, durable and very flexible. For these reasons, the wingtips, control surfaces, and fuselage fairings of both aircraft were made out of foam.

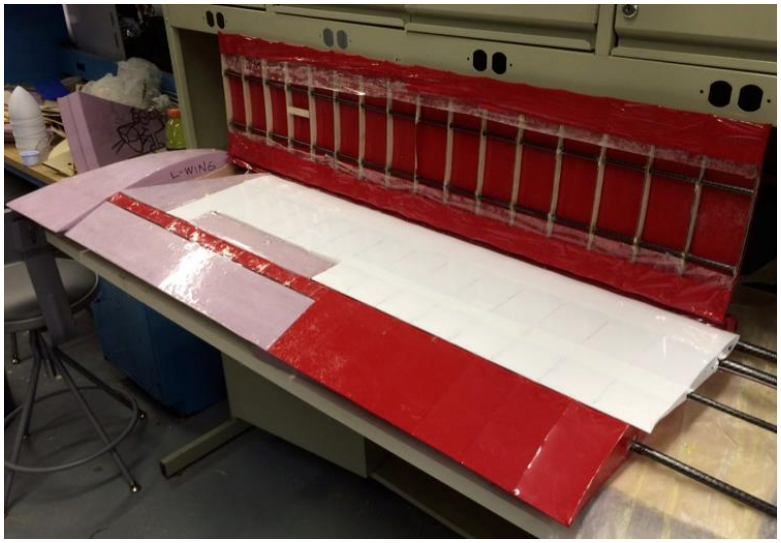

Figure 7.4 - Foam Wingtips abd Control Surfaces on Production Aicraft and Manufacturing Support Aicraft Wings

The detailed usage of these materials in constructing and testing our aircraft was as follows:

Table 5.1-1 Detailed Material Usage Description

Material	Component	Usage
Production Aircraft		
Balsa Plywood Sheets	Wings	Ribs
Carbon Fiber Tubes	Wings	Spars
Carbon Fiber Roving	Fuselage	Bottle Casing
MonoKote Shrink Wrap	Wings	Outer Covering
3D Printed material	Fuselage	Bottle Casing
Foam	Fuselage	Top Cover of Aircraft
Manufacturing Support Aircraft		
Balsa Plywood Sheets	Wings	Ribs
Carbon Fiber Tubes	Wings	Spars
Carbon Fiber Roving	Fuselage	Bottle Casing
MonoKote Shrink Wrap	Wings	Outer Covering
Foam	Fuselage	Top Cover of Aircraft

5.2 Manufacturing Processes

Although the aircraft was sized to be as light as possible, multiple manufacturing methods were explored in order find those that would conserve weight. The manufacturing plan for both the Production and Manufacturing Support Aircraft focused on the construction of three main components: fuselage, wings and landing gear.

Fuselage

The fuselage of the Production Aircraft was designed to hold the payload yet be as light as possible. The following three methods were investigated for the manufacturing of the fuselage:

- 3D Print – A payload case was manufactured via 3D printing. This case was able to hold the payload securely and featured a cone-shaped twist-off lid at the back end.
- Carbon Fiber Roving – carbon fiber roving was utilized in order to reinforce the 3D printed case. This was produced by wrapping the roving around the case until the structure was more durable.
- MonoKote – The fuselage's structure was wrapped with MonoKote shrink-wrap to serve as the aircraft's outer layer of skin.

The Manufacturing Support's fuselage was manufactured such that it was be able to carry the Production Aircraft's fuselage within it. This fuselage was manufactured using a foam casing large enough to withhold its payload and the Production Aircraft's landing gear.

Wings

Each wing consisted of a front and rear carbon fiber tube to serve as spars. Flexible balsa wood sheets were wrapped around the front of the wing ribs to form a leading edge while the trailing edge was created by a thin carbon fiber rod running along the rear end of each rib. The wing was built using a fixture created to ensure precision in rib spacing and movement. Each rib was laminated using three sheets of balsa wood in a zero-ninety-zero orientation and then cut using a laser cutter to create the desired airfoil shape. After the assembly of the wings was finished, plywood blocks were placed along the inner surface of the leading edge as a way to reinforce the structure along the leading edge of the wing. MonoKote was then applied to the wings to provide a smooth aerodynamic surface. The front and rear wing spars extended into the fuselage in order to promote structural efficiency.

One standout feature in the wings of the Manufacturing Support Aircraft was that they had to hold the Production Aircraft's wing internally. To account for this, the ribs were designed to with a cutout in the shape of the MH 45 airfoil so that the smaller wing could be nested into the larger wing. Additionally, a lid was created to fully enclose the nested Production Aircraft.

Figure 7.5 - Production Aircraft Wing Construction with Balsa Leading Edge Wrap and Laminated Balsa Plywood Ribs

Landing Gear

Different landing gear methods were used based on design specifications. On the Production Aircraft, the team manufactured the landing gear as close to the fuselage as possible to be able to be able to inversely mount the aircraft into the Manufacturing Support Aircraft. This process entailed a steerable nose wheel assembly and utilized a CNC milled aluminum plate to serve as mount for the main gear. The back wheels where mounted on a rod that was shaped and fixed around the aluminum hoop. This design allowed for the distribution of the landing impact around the plastic component and to the central spars, creating the necessary rigidity and strength for each gear.

Figure 7.6 - Production Aircraft with Landing Gear Mounted Inversely in the Manufacturing Support Aircraft

5.3 MANUFACTURING MILESTONES CHART

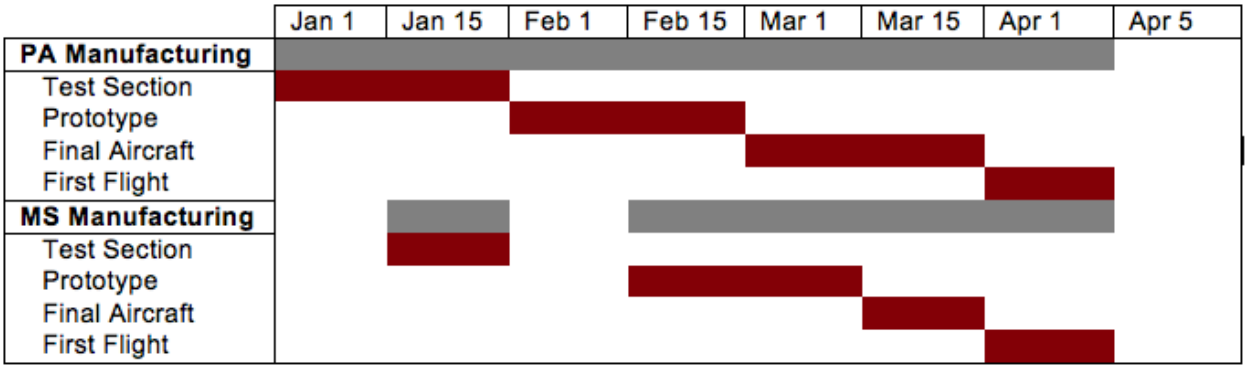

Figure 7.7 - Manufacturing Milestones Chart

6. Testing

The aircraft was tested in numerous different ways to analyze the difference between estimated and actual aircraft outputs. To begin testing the aircraft, individual components were tested to ensure that when assembled as a whole the airplanes would be able to sustain flight. Test sections of the wings of both aircraft were first created to ensure the airfoil selected met the design requirements; then, analysis was conducted to select the carbon fiber spar sizes which could sustain the load and maintain structural stability, and lastly the propellers and motors were tested to confirm that the propulsion system could provide the power needed for take-off. The results of these tests indicated the adjustments to be made to the designs before the manufacturing phase.

6.1 Structural Testing

To test the integrity of each structure, the yield strength of the carbon fiber spars was compared to the bending stress that resulted from the wings supporting the weight of the aircraft. To perform this comparison, the bending stress on the spars was calculated using the following formula for bending stress on a hollow tube. [6]

$$\sigma = \frac{WL^2}{2Z} \tag{22}$$

In this equation, W equals the distributive load, L equals the length of the tube, and Z equals the section modulus, which was calculated using the formula below. [6]

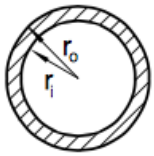

$$Z = \frac{0.78\,(r_o^4 - r_i^4)}{r_o} \tag{23}$$

These calculations revealed the bending stresses that wing spars were likely to experience in flight. After calculating the bending stresses for level flight and different load factors, and comparing these values to the yield strength of the spar material, it was determined that the material and diameter tubing that was chosen for the spars was sufficient to withstand the forces of flight that are expected for our aircraft.

6.2 Wind Tunnel Testing

To gain a more accurate understanding of the aerodynamics characteristics of the three dimensional wing, wing test sections were created and tested in a laminar flow wind tunnel. Each test section was 48 cm in length, contained between 8- 9 ribs, had two wooden dowels with diameter 2.095 cm, one inserted at the quarter chord and the other dowel inserted as close to the trailing edge as possible while still leaving enough room for the installation of control surfaces. Each test section was tested in a 60cm x 60cm wind tunnel to calculate the 3D lift on each wing. During this test, the theoretical lift versus angle of attack plot was attempted. The highest airspeed possible in the wind tunnel was approximately 146.65 ft/s; however, these tests were only conducted at a maximum of 25 m/s, which was the maximum cruise of both aircraft. By changing the airspeed and angle of attack, an experimental lift for the 3D wing was determined during multiple phases of flight. These results are discussed in Section 3.5.

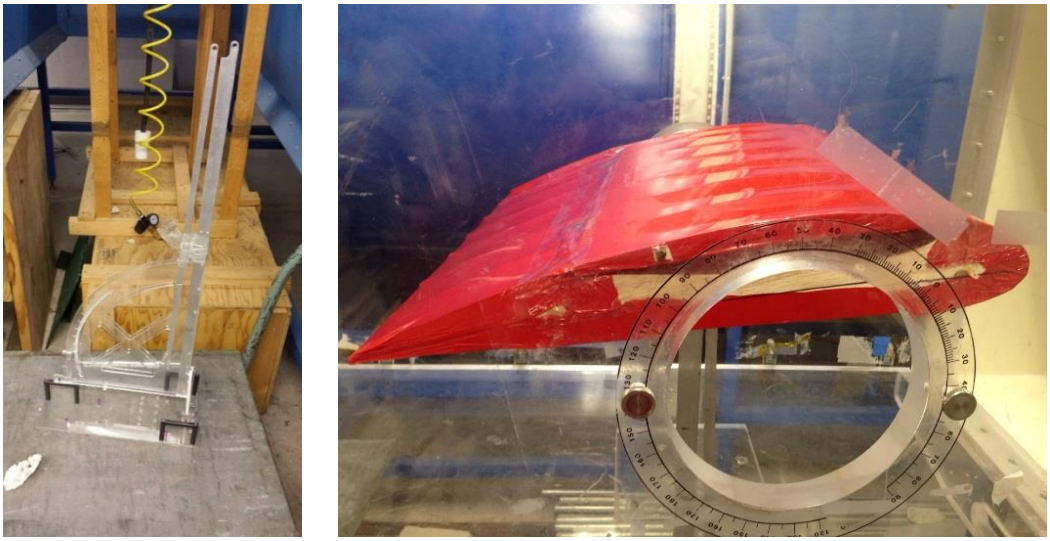

Figure 6.2-1 Wind Tunnel Testing of Wing Test Sections

The tests showed that the experimental lift curve slope for both aircraft was below the 2D calculated values, as seen in figures 3.5-1 and 3.5-2 in Section 3.5. However, this effect was taken into consideration when sizing both aircraft. A safety factor of 1.1 was added to the area calculations of both aircraft to generate the extra 4 N of lift for the Production; and 7.5 N for the Manufacturing Support Aircraft.

6.3 Battery and Propulsion Testing

A thrust test and an endurance test using the motor and batteries to be used in the competition were performed. The thrust test was conducted to measure the motor's actual thrust so we could compare it to the thrust stated on the motor's specifications sheet. An endurance test was done to verify that the batteries had enough capacity to run for the needed 5 minutes.

Tests on the propulsion system were completed to help identify the final motor and battery selection for both the Production and Manufacturing Support Aircraft. During the initial design phase, a motor, propeller and battery were selected as a baseline for our propulsion system and these components together created was the system that the propulsion tests were completed with. The tests were completed in a 60x60cm wind tunnel at speeds of 10, 15, 20 and 25 m/s. The two types of tests done were a thrust test and an endurance test. The setup consisted of the motor and propeller being attached to an arm that created moment about a pivot point which translates to another arm that has a scale on the end. Using statics, the thrust output of the motor was calculated. The test results can be seen below.

Table 6.3-1 Thrust Testing Results

Speed (m/s)	Thrust (N)	Current Draw (A)
10	10.26	24.6
15	7.94	24.2
20	7.30	25.6
25	5.61	23.4

From this data it was shown that the thrust at takeoff (10m/s) would be the limiting factor for the final motor selection. The Production Aircraft was calculated to need 9.53N (93% of tested value) of thrust from 0-10m/s in order to takeoff within the required 100ft, yet to only need 2.29N (41% of tested value) of thrust to hold at cruise speed (25m/s).

To test the battery endurance we ran the motor with the same current draw as the thrust test (~25A), starting from a fully charged battery and timed how long the battery lasted. Based on calculations using the battery capacity, the theoretical duration should have been 16 minutes, however the battery died at 12 minutes for the start of the test. This showed that the battery to be selected needed 33% more capacity than calculated.

The test results allowed the final motor/propeller/battery configurations to be chosen for both aircraft. An AXI 2820/12 motor with an 11x7 propeller (the motor/propeller used in the test) were selected for the Production Aircraft, with a battery pack consisting of (2) 12V 1400mAh battery packs connected in parallel. After comparing the thrust test results to the recommended aircraft size and appropriate usage data on the motor website, a motor was selected for the Manufacturing Support Aircraft. An AXI 4120/14 motor with a 13x11 propeller were selected, with a battery pack consisting of (2) 14V 2,200mAh battery packs connected in parallel.

6.4 Flight Checklist

A flight checklist was created to properly document the results of each flight test done on both our aircraft. Flight testing was done to evaluate the performance of the aircraft and its ability to complete each mission accordingly. Flight testing helped modify the design and manufacturing techniques to produce an aircraft capable to complete all 3 missions.

Flight Description		Weather Conditions	
Date:		Wind mph	
Time:		Humidity:	
Location:		Temperature	
Aircraft:		Cloud Cover	
Flight #:			
Mission Objectives:			
Configuration			
Weight(lb):		Propulsion Type:	
Payload:		Receiver Type:	
CG Location:		Propeller:	

Pre- Flight Checklist					
Structural Integrity		**Avionics**		**Propulsion**	
Wing		Power Test		Motor Wiring	
Control Surfaces/Linkages		Transmitter Test		Battery Connected	
Propeller		Receiver Test		Motor Test	
Landing Gear		Battery Test		Prop Clearance	
Fuselage		Servo Wiring			
Motor Mount					
Tail Section					
Final Comments:					
Pilot Signature:					
Advisor Signature:					

Figure 8.2 - Flight Checklist

6.5 Prototype

A preliminary foam prototype was created to test the basic concept and maneuverability of a small flying wing Production Aircraft. The foam airfoil was cut out using a hotwire setup and reinforced using wooden and carbon fiber spars. Elevons were added to the trailing edge of the prototype based on preliminary aerodynamic analysis in order to control the foam prototype. The foam prototype was hand launched down a steep hill and remotely controlled. This test revealed that the flying wing design was stable but pitch sensitive. The prototype was able to perform basic s-turns which were repeated several times. This preliminary model confirmed our proof of concept and encouraged further development of this design for the Production Aircraft. An image of our foam prototype is shown below.

Figure 9.1 - Foam Prototype of Production Aircraft

7. Final Results

7.1 Final Aircraft Performance

The testing process began by weighing the final aircraft to compare the actual aircraft weight to estimated aircraft weight. This was done first as the actual aircraft weights played an important role in the aircraft's ability to reach a speed sufficient for take-off, to sustain flight and to properly utilize the propulsion system created. It was found that the estimated weight for the Production Aircraft was 4 kg and the actual loaded weight was found to be 4.2 kg. Similarly the Manufacturing Support Aircraft was weighed and found to be 6.5 kg as opposed to its estimated weight of 7.3 kg. Since both the aircraft had exceeded their estimated weights, a safety factor was added for aerodynamic calculations.

Before leaving for the AIAA DBF 2016 competition, both aircraft were tested. The Production Aircraft was able to taxi very well and reach a speed fast enough for take-off, but was unable to fly. On each flight attempt, issues were encountered with the nose wheel and servo until, after multiple attempts, the nose wheel broke. This issue was further addressed on site at the competition.

Initially, the Manufacturing Support Aircraft was also unable to fly during the first tests. Unlike the Production Aircraft, this aircraft did not taxi well as too much drag was being created by the large fuselage. The tail wheel also proved problematic due to its inadequate size. Additionally, it could not take- off as it could not reach a speed fast enough for take- off. This plane was also slightly overweight for similar reasons as the Production Aircraft. As with the Production Aircraft, the problems were identified and further addressed on site at the competition.

7.2 Competition results

On site in Wichita, the main Production Aircraft issues were resolved. However, it was still unable to fly due to its extra weight, most likely due to adhesives and aluminum components as the extra sheets used when laminating the ribs. The Manufacturing Support Aircraft on the other

hand was able to fly in 30mph gusts and 20mph winds for a short period of time after some issues were addressed. Upon arrival in Wichita, the elevator range and power output were identified as main problems. The motor selected for the Manufacturing Support Aircraft required a voltage of approximately 24V but with the current circuit set up it was only receiving 14V and was unable to achieve a speed fast enough for take-off. The battery setup was adjusted by adding an additional battery in series to output a voltage suitable for the motor. Additionally, the position of the tail elevator could not be moved to allow more range and obtain stability. Although correcting these two issues allowed for a short flight, the addition of a battery increased the weight of the aircraft significantly and the additional range obtained by shifting the elevator position was still inadequate, leading to the plane crashing shortly after take-off. The damages sustained from the crash were irreparable and the two airplanes could not be used to participate in the AIAA DBF 2016 competition.

8. Conclusion

The goal of this MQP was to successfully compete in the 2016 AIAA/Cessna/Raytheon Design/Build/Fly competition, where teams were challenged to create two remote-controlled electrically powered aircraft. Both aircraft, the manufacturing support and production, were to achieve specific mission tasks as a part of receiving the highest total score. Although a score was not received by the team during the actual competition in Wichita, KS, the manufacturing of the project resulted in two aircraft capable of carrying their payloads based on their respective design.

8.1 Outcome

In order to create a viable design and prepare a building plan, research on different aircraft configurations, the study of aerodynamics, and the manufacturability and payload capabilities of these concepts were compiled. Quantitative decisions were made through the use of merit analyses and iterative design mechanisms. Final aircraft configurations selected by the team consisted of a flying wing design for the production aircraft nested inside the wings of a conventional design manufacturing support aircraft.

The production aircraft's flying wing design had the requirement of having to carry the payload of a 32oz Gatorade bottle during mission 3 of the competition. To satisfy this condition, this aircraft was designed to have a span of 2.150 m using an MH 45 airfoil and manufactured out of laser-cut laminated balsa plywood sheets, carbon fiber tubing, foam, MonoKote shrink wrap and 3D-printed material. The manufacturing support aircraft's conventional design was required to carry a payload of the production aircraft internally. A NACA 4418 airfoil and a span of 2.150 m was selected for the design of this aircraft. The manufacturing of this aircraft was completed using the same processes and materials as the production aircraft, with the exception of the 3D-printed casing. Additional wing lids were created for this aircraft as a way of securing the payload internally. Axi motors using nickel-metal hydride batteries powered both aircraft.

Unfortunately, adequate flight-testing of the final aircraft could not be performed by the team due to the lengthy time allotted to the design phase of the project. This resulted in the

realization that the production aircraft was unable to fly due to its heavy weight while attending the competition. Meanwhile, the manufacturing support aircraft was able to fly through 30mph gusts and 20 mph winds after for a short period of time before crashing and sustaining irreparable damages. Overall, the innovations in design and analysis as well as in the manufacturing techniques performed in this project can be of use for future WPI teams competing in the Design/Build/Fly competition.

8.2 RECOMMENDATIONS

Several unanticipated problems and setbacks that hindered the progress of the project were experienced by the team. These complications could have been avoided had the team had the following recommendations regarding the entire design, manufacturing and testing process prior to the start of the project.

The first recommendation is to recruit students who have experience with the design and building of radio-controlled aircraft. These students would be able to identify and clarify problems in the aircraft's design whereas students with less experience may not. They would also be of high use during times of manufacturing and purchasing parts.

With the addition of experienced members, the team should create a business-like structure consisting of sub-teams (propulsion, modeling, aerodynamics, etc.) who continuously meet throughout the week. Ideally, these sub-teams and the whole team would set strict deadlines for tasks that need to be completed through the use of a Gantt chart. This would allow the team to utilize their time appropriately so that the project gets sufficient flight-testing and remodeling time.

A third recommendation would be to seek funding from sponsors for this project, for the allotted budget provided may not be a sufficient amount if the team would like to create prototypes before the manufacturing of their final design, use good quality materials, purchase extra materials in the case of failures or allow the whole team to travel equally. Additionally, logistics for travel or team apparel should be planned well ahead of time.

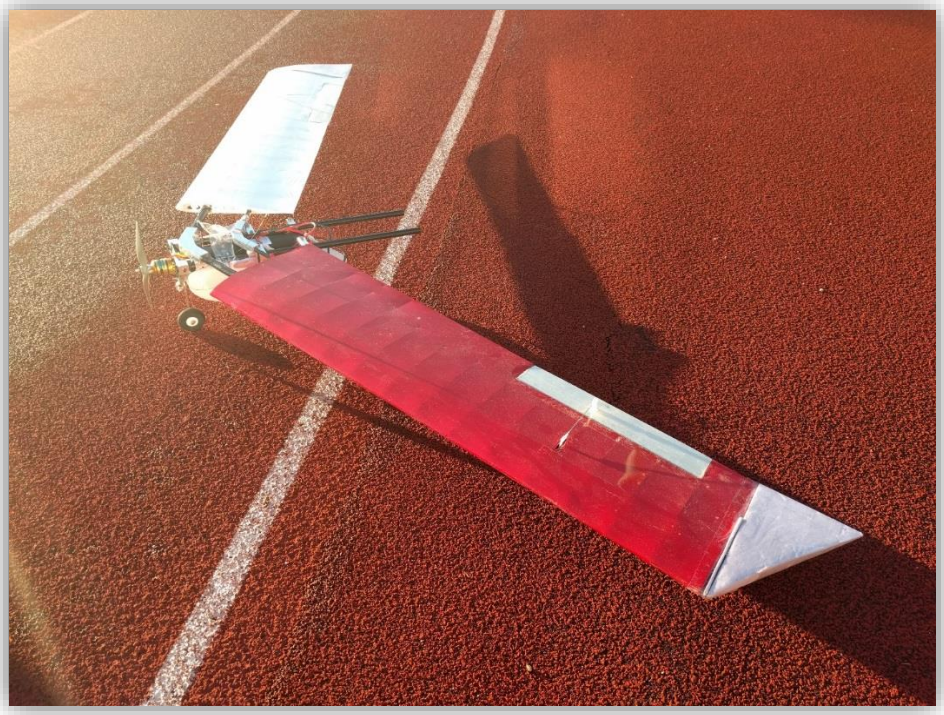

Appendix A – Aerodynamic Analyses Results

MH 114 – Coefficient of Lift vs Alpha / Moment, Drag, and Lift to Drag / Final Results

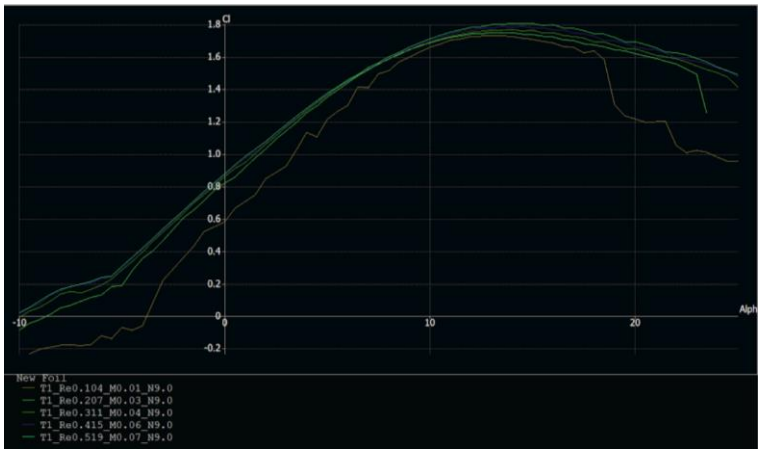

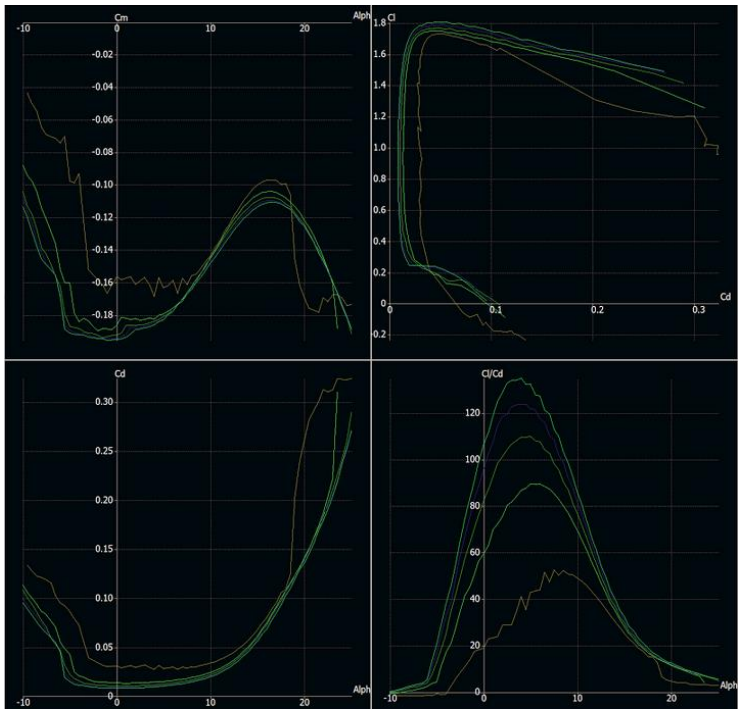

	Cruise Angle of Attack (α=0°)					Take-off Angle of Attack (α=10°)				
Airspeed	**5 m/s**	**10 m/s**	**15 m/s**	**20 m/s**	**25 m/s**	**5 m/s**	**10 m/s**	**15 m/s**	**20 m/s**	**25 m/s**
C_l	0.60	0.82	0.85	0.88	0.90	1.67	1.70	1.72	1.73	1.73
$C_{m,o}$	-0.16	-0.19	-0.19	-0.20	-0.20	-0.14	-0.14	-0.14	-0.15	-0.15
C_D	0.03	0.02	0.01	0.01	0.01	0.04	0.03	0.02	0.02	0.02
L/D	20.00	60.00	80.00	95.00	107.00	50.00	70.00	77.00	81.00	86.00

SD 7062 – Coefficient of Lift vs Alpha / Moment, Drag, and Lift to Drag / Final Results

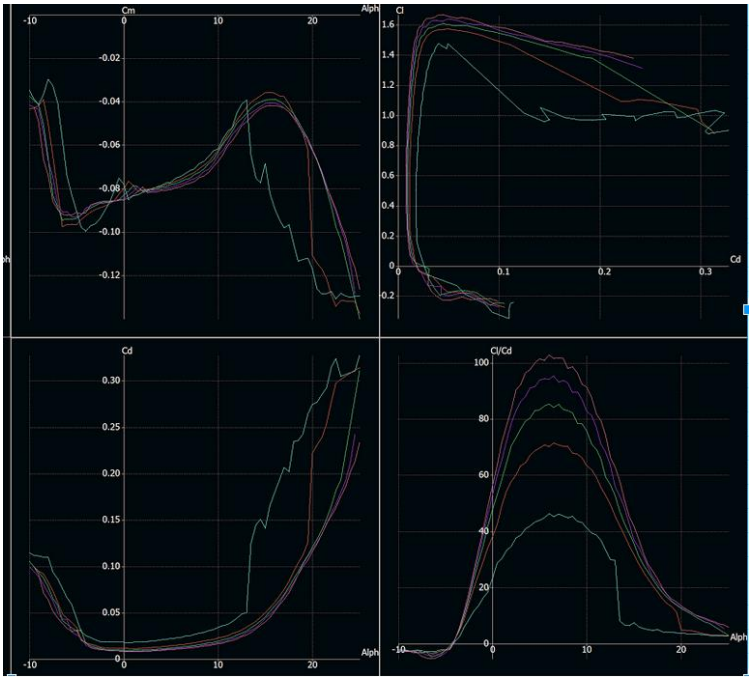

	Cruise Angle of Attack (α=0°)					Take-off Angle of Attack (α=10°)				
Airspeed	**5 m/s**	**10 m/s**	**15 m/s**	**20 m/s**	**25 m/s**	**5 m/s**	**10 m/s**	**15 m/s**	**20 m/s**	**25 m/s**
C_l	0.42	0.43	0.45	0.46	0.48	1.40	1.43	1.45	1.46	1.48
$C_{m,o}$	-0.08	-0.08	-0.08	-0.08	-0.09	-0.06	-0.06	-0.06	-0.07	-0.07
C_D	0.02	0.01	0.01	0.01	0.01	0.03	0.02	0.02	0.02	0.02
L/D	22.00	37.00	47.00	52.00	56.00	41.00	62.00	76.00	82.00	91.00

MH 83 – Coefficient of Lift vs Alpha / Moment, Drag, and Lift to Drag / Final Results

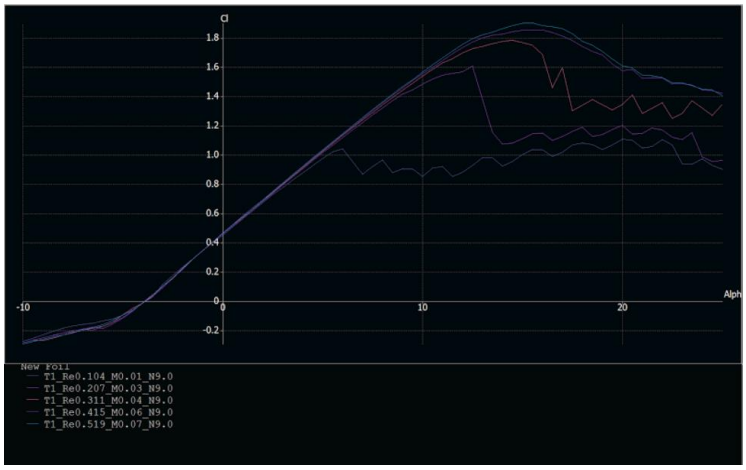

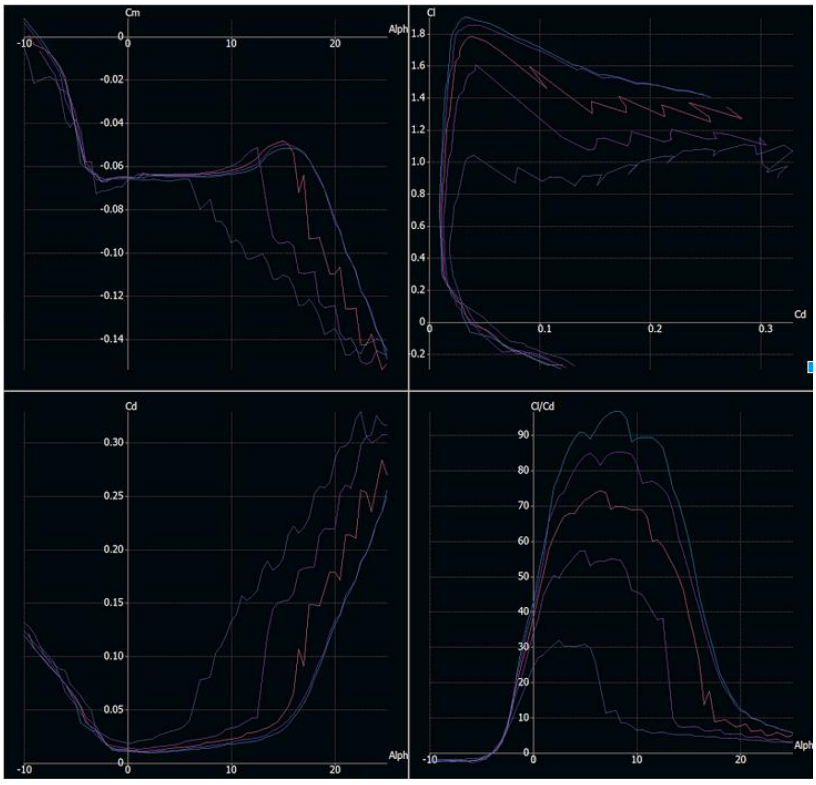

	Cruise Angle of Attack (α=0°)					Take-off Angle of Attack (α=10°)				
Airspeed	**5 m/s**	**10 m/s**	**15 m/s**	**20 m/s**	**25 m/s**	**5 m/s**	**10 m/s**	**15 m/s**	**20 m/s**	**25 m/s**
C_l	0.47	0.47	0.48	0.48	0.48	0.87	1.50	1.57	1.58	1.59
$C_{m,o}$	-0.07	-0.07	-0.07	-0.07	-0.07	-0.09	-0.06	-0.06	-0.06	-0.06
C_D	0.02	0.01	0.01	0.01	0.01	0.13	0.03	0.02	0.02	0.02
L/D	25.00	33.00	37.00	41.00	42.00	7.00	45.00	70.00	82.00	89.00

MHH 64 – Coefficient of Lift vs Alpha / Moment, Drag, and Lift to Drag / Final Results

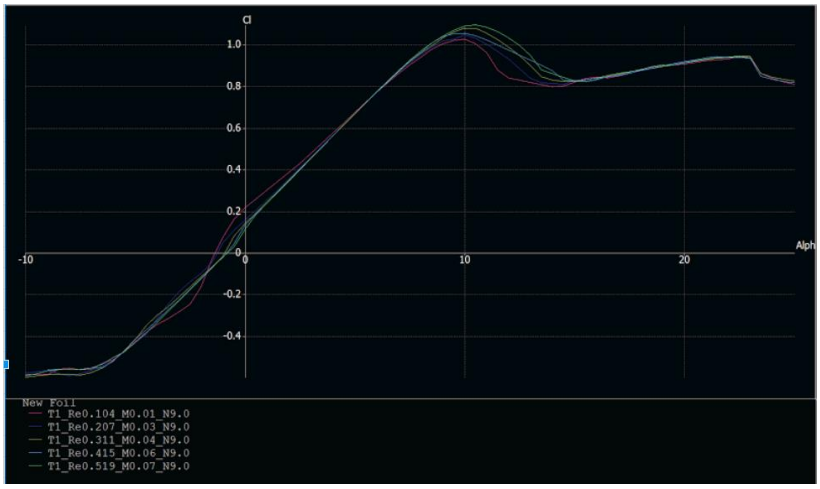

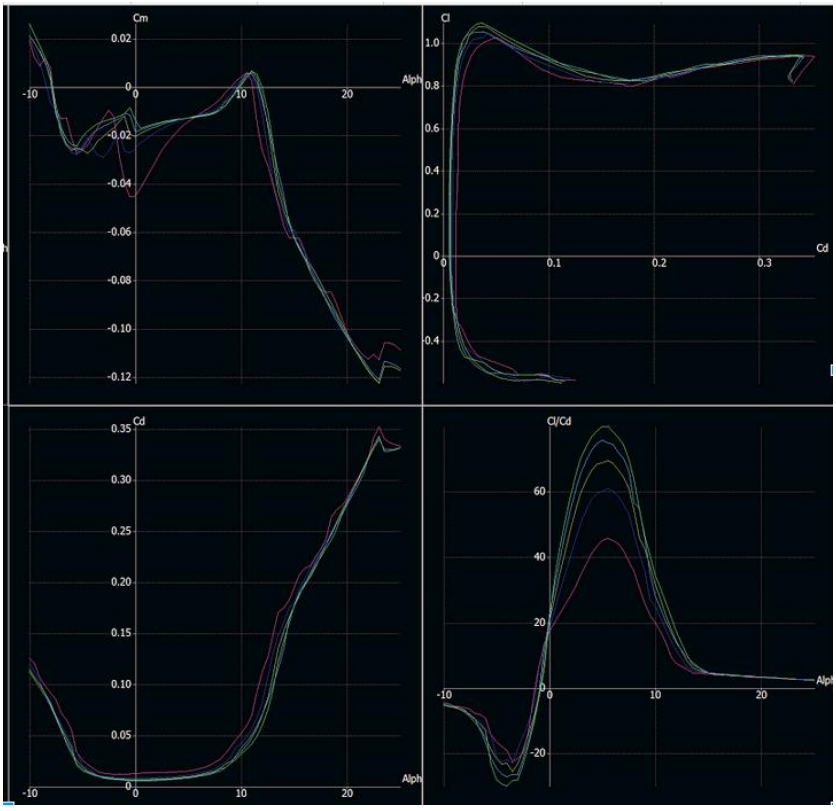

	Cruise Angle of Attack (α=0°)					Take-off Angle of Attack (α=10°)				
Airspeed	**5 m/s**	**10 m/s**	**15 m/s**	**20 m/s**	**25 m/s**	**5 m/s**	**10 m/s**	**15 m/s**	**20 m/s**	**25 m/s**
C_l	0.22	0.16	0.15	0.12	0.10	1.02	1.03	1.06	1.09	1.10
$C_{m,o}$	-0.04	-0.03	-0.02	-0.02	-0.01	0.01	0.00	0.00	0.00	0.00
C_D	0.01	0.01	0.01	0.01	0.01	0.05	0.04	0.04	0.04	0.03
L/D	17.00	18.00	21.00	21.00	21.00	20.00	25.00	28.00	32.00	35.00

S 1223 – Coefficient of Lift vs Alpha / Moment, Drag, and Lift to Drag / Final Results

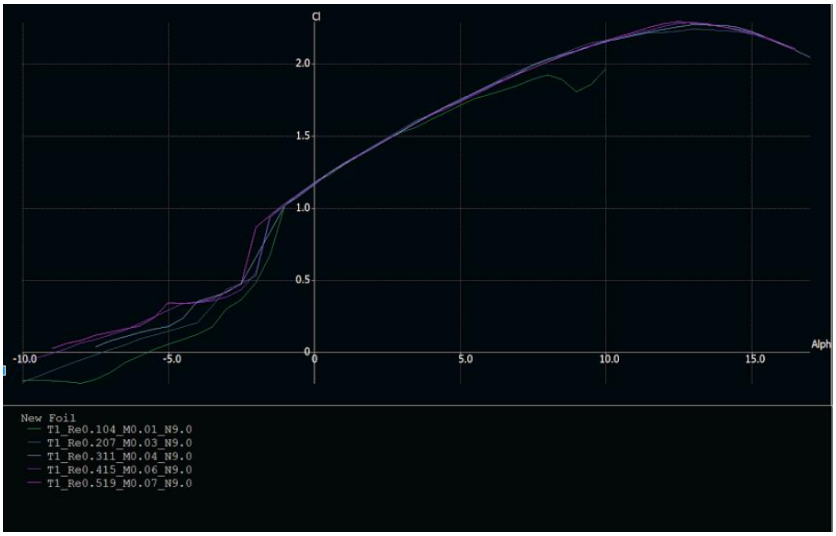

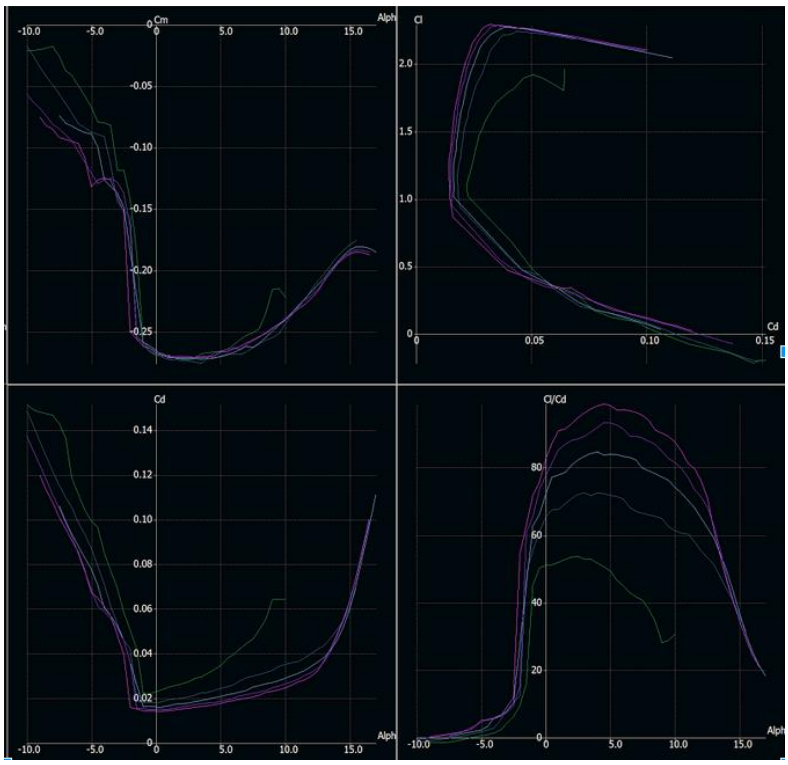

	Cruise Angle of Attack (α=0°)					Take-off Angle of Attack (α=10°)				
Airspeed	**5 m/s**	**10 m/s**	**15 m/s**	**20 m/s**	**25 m/s**	**5 m/s**	**10 m/s**	**15 m/s**	**20 m/s**	**25 m/s**
C_l	1.20	1.20	1.20	1.20	1.20	1.90	2.20	2.20	2.20	2.20
$C_{m,o}$	-0.27	-0.27	-0.27	-0.27	-0.27	-0.22	-0.23	-0.24	-0.24	-0.24
C_D	0.02	0.02	0.02	0.02	0.02	0.07	0.04	0.03	0.03	0.03
L/D	51.00	65.00	72.00	78.00	82.00	30.00	60.00	75.00	82.00	88.00

NACA 4424 – Coefficient of Lift vs Alpha / Moment, Drag, and Lift to Drag / Final Results

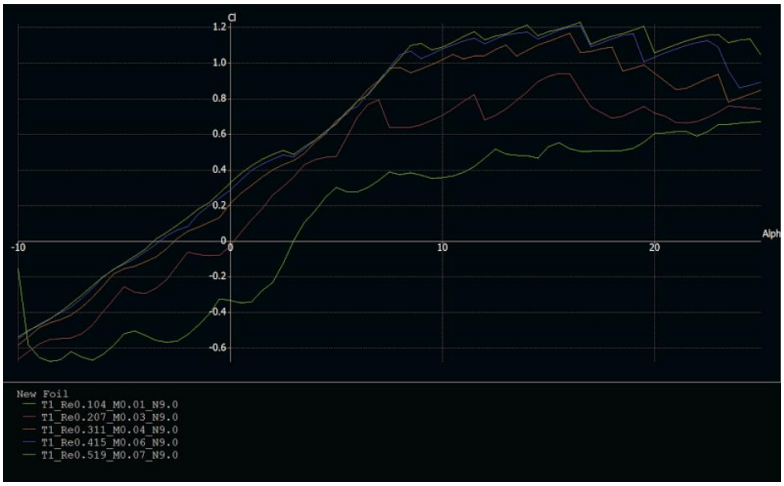

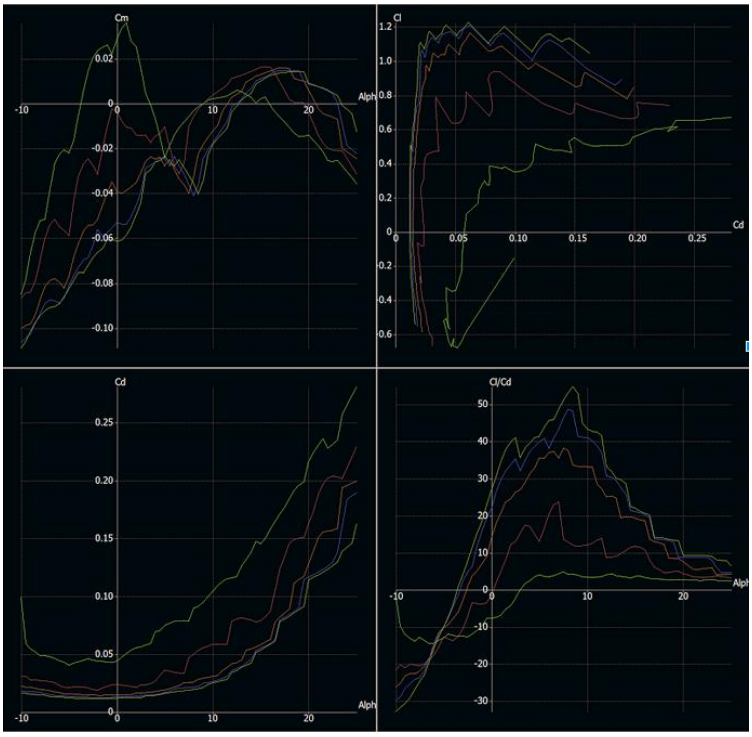

	Cruise Angle of Attack (α=0°)					Take-off Angle of Attack (α=10°)				
Airspeed	**5 m/s**	**10 m/s**	**15 m/s**	**20 m/s**	**25 m/s**	**5 m/s**	**10 m/s**	**15 m/s**	**20 m/s**	**25 m/s**
C_l	-0.32	0.00	0.20	0.30	0.34	0.38	0.71	1.01	1.09	1.10
$C_{m,o}$	0.03	0.00	0.00	-0.06	-0.06	0.00	0.00	-0.01	-0.02	-0.02
C_D	0.05	0.03	0.20	0.02	0.20	0.10	0.06	0.03	0.02	0.02
L/D	-7.00	0.00	15.00	22.00	28.00	4.00	12.00	33.00	40.00	43.00

MH 45 – Coefficient of Lift vs Alpha / Moment, Drag, and Lift to Drag / Final Results

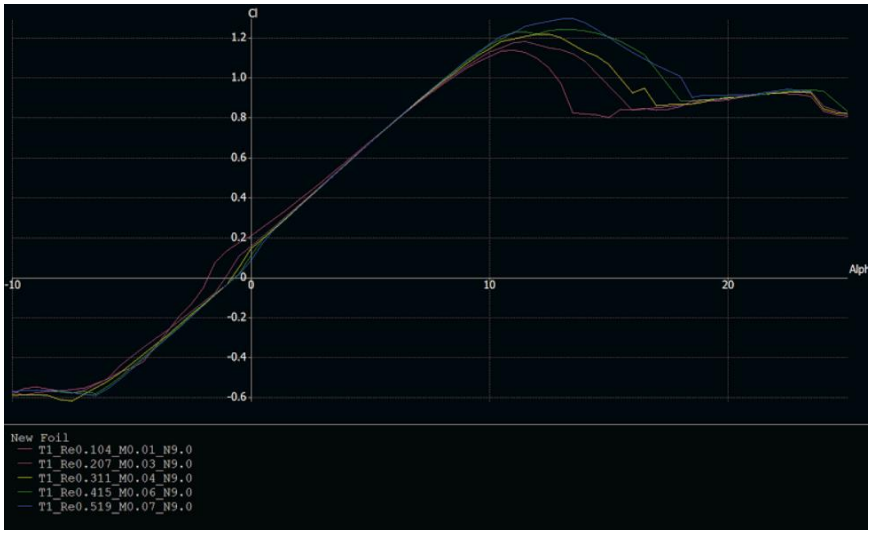

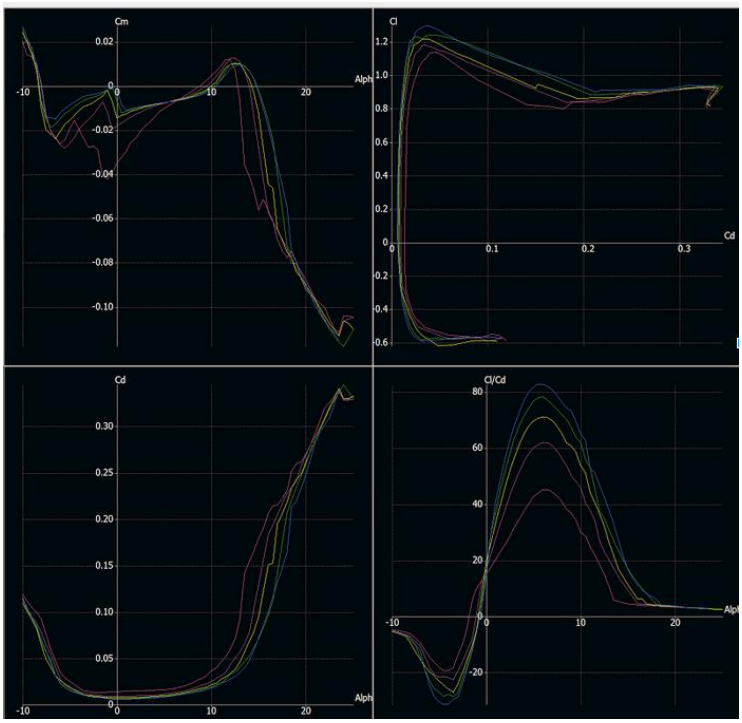

	Cruise Angle of Attack (α=0°)					Take-off Angle of Attack (α=10°)				
Airspeed	**5 m/s**	**10 m/s**	**15 m/s**	**20 m/s**	**25 m/s**	**5 m/s**	**10 m/s**	**15 m/s**	**20 m/s**	**25 m/s**
C_l	0.21	0.16	0.14	0.11	0.08	1.11	1.13	1.14	1.16	1.16
$C_{m,o}$	-0.04	-0.02	-0.01	-0.01	0.00	0.00	0.00	0.00	0.00	0.00
C_D	0.02	0.01	0.01	0.01	0.01	0.04	0.03	0.02	0.02	0.02
L/D	15.00	17.00	19.00	17.00	14.00	30.00	45.00	54.00	63.00	65.00

Appendix B – Initial Sizing Results

MH 114

	Cruise Angle of Attack (α=0°)					Take-off Angle of Attack (α=10°)				
Airspeed	**5 m/s**	**10 m/s**	**15 m/s**	**20 m/s**	**25 m/s**	**5 m/s**	**10 m/s**	**15 m/s**	**20 m/s**	**25 m/s**
b (m)	10.68	1.95	0.84	0.46	0.28	3.84	0.94	0.41	0.23	0.15
S (m^2)	3.26	0.60	0.26	0.14	0.09	1.17	0.29	0.13	0.07	0.05
AR	35.05	6.41	2.75	1.49	0.93	12.59	3.09	1.36	0.76	0.49
T/W	0.05	0.02	0.01	0.01	0.01	0.02	0.01	0.01	0.01	0.01
W/S	9.19	50.23	117.14	215.60	344.53	25.57	104.13	237.04	423.85	662.27

SD 7062

	Cruise Angle of Attack (α=0°)					Take-off Angle of Attack (α=10°)				
Airspeed	**5 m/s**	**10 m/s**	**15 m/s**	**20 m/s**	**25 m/s**	**5 m/s**	**10 m/s**	**15 m/s**	**20 m/s**	**25 m/s**
b (m)	15.26	3.73	1.58	0.87	0.53	4.58	1.12	0.49	0.27	0.17
S (m^2)	4.65	1.14	0.48	0.27	0.16	1.40	0.34	0.15	0.08	0.05
AR	50.08	12.23	5.19	2.86	1.75	15.02	3.68	1.61	0.90	0.57
T/W	0.05	0.03	0.02	0.02	0.02	0.02	0.02	0.01	0.01	0.01
W/S	6.43	26.34	62.02	112.70	183.75	21.44	87.59	199.83	357.70	566.56

MH 83

	Cruise Angle of Attack (α=0°)					Take-off Angle of Attack (α=10°)				
Airspeed	**5 m/s**	**10 m/s**	**15 m/s**	**20 m/s**	**25 m/s**	**5 m/s**	**10 m/s**	**15 m/s**	**20 m/s**	**25 m/s**
b (m)	13.64	3.41	1.48	0.83	0.53	7.37	1.07	0.45	0.25	0.16
S (m^2)	4.16	1.04	0.45	0.25	0.16	2.25	0.33	0.14	0.08	0.05
AR	44.75	11.19	4.87	2.74	1.75	24.17	3.51	1.49	0.83	0.53
T/W	0.04	0.03	0.03	0.02	0.02	0.14	0.02	0.01	0.01	0.01
W/S	7.20	28.79	66.15	117.60	183.75	13.32	91.88	216.37	387.10	608.67

MH 64

	Cruise Angle of Attack (α=0°)					Take-off Angle of Attack (α=10°)				
Airspeed	**5 m/s**	**10 m/s**	**15 m/s**	**20 m/s**	**25 m/s**	**5 m/s**	**10 m/s**	**15 m/s**	**20 m/s**	**25 m/s**
b (m)	29.14	10.02	4.75	3.34	2.56	6.28	1.56	0.67	0.37	0.23
S (m^2)	8.88	3.05	1.45	1.02	0.78	1.92	0.47	0.20	0.11	0.07
AR	95.60	32.86	15.58	10.95	8.41	20.62	5.10	2.20	1.21	0.76
T/W	0.06	0.06	0.05	0.05	0.05	0.05	0.04	0.04	0.03	0.03
W/S	3.37	9.80	20.67	29.40	38.28	15.62	63.09	146.08	267.05	421.09

S1223

	Cruise Angle of Attack (α=0°)					Take-off Angle of Attack (α=10°)				
Airspeed	**5 m/s**	**10 m/s**	**15 m/s**	**20 m/s**	**25 m/s**	**5 m/s**	**10 m/s**	**15 m/s**	**20 m/s**	**25 m/s**
b (m)	5.34	1.34	0.59	0.33	0.21	3.37	0.73	0.32	0.18	0.12
S (m^2)	1.63	0.41	0.18	0.10	0.07	1.03	0.22	0.10	0.06	0.04
AR	17.53	4.38	1.95	1.10	0.70	11.07	2.39	1.06	0.60	0.38

T/W	0.02	0.02	0.01	0.01	0.01	0.03	0.02	0.01	0.01	0.01
W/S	18.38	73.50	165.38	294.00	459.38	29.09	134.75	303.19	539.00	842.19

NACA 4424

	Cruise Angle of Attack (α=0°)					Take-off Angle of Attack (α=10°)				
Airspeed	**5 m/s**	**10 m/s**	**15 m/s**	**20 m/s**	**25 m/s**	**5 m/s**	**10 m/s**	**15 m/s**	**20 m/s**	**25 m/s**
b (m)	-20.03	0.00	3.56	1.34	0.75	16.87	2.26	0.71	0.37	0.23
S (m^2)	-6.11	0.00	1.09	0.41	0.23	5.14	0.69	0.21	0.11	0.07
AR	-65.73	0.00	11.68	4.38	2.47	55.35	7.41	2.31	1.21	0.76
T/W	-0.14	0.00	0.07	0.05	0.04	0.25	0.08	0.03	0.03	0.02
W/S	-4.90	0.00	27.56	73.50	130.16	5.82	43.49	139.19	267.05	421.09

MH 45

	Cruise Angle of Attack (α=0°)					Take-off Angle of Attack (α=10°)				
Airspeed	**5 m/s**	**10 m/s**	**15 m/s**	**20 m/s**	**25 m/s**	**5 m/s**	**10 m/s**	**15 m/s**	**20 m/s**	**25 m/s**
b (m)	30.53	10.34	5.09	3.64	3.21	5.78	1.42	0.62	0.35	0.22
S (m^2)	9.30	3.15	1.55	1.11	0.98	1.76	0.43	0.19	0.11	0.07
AR	100.15	33.92	16.69	11.95	10.52	18.95	4.65	2.05	1.13	0.73
T/W	0.07	0.06	0.05	0.06	0.07	0.03	0.02	0.02	0.02	0.02
W/S	3.22	9.49	19.29	26.95	30.63	17.00	69.21	157.11	284.20	444.06

Appendix C – Detailed Airfoil Results for Production Aircraft

MH 45						
Weight = Lift	40	N	4	kg		
Density of air	1.225	kg/m^3			Coeff of lift linearization	
Chord	0.2785	m			Cl = mx + b	
Area required at low speed	**0.60**	m^2			Cl = 0.092x + 0.1	
Frontal Area	0.06	m^2				

			Velocity (m/s)			
Parameter	**Notation**	**Units**	**10**	**15**	**20**	**25**
Reynolds Number	Re		207,000	311,000	415,000	519,000
Coeff of Lift	Cl		1.20	0.48	0.27	0.17
Angle of Attack	AoA	degrees	11.96	4.18	1.88	0.81
Span	b	meters	2.15	2.15	2.15	2.15
Aspect Ratio	AR		7.72	7.72	7.72	7.72
Coeff of Drag	Cd		0.03	0.02	0.01	0.01
Coeff of Moment	Cm		0.01	-0.01	-0.01	-0.01
Lift/Drag	L/D		40.00	70.00	50.00	20.00
Drag	D	Newtons	1.10	1.65	1.47	2.29
Power	P	Watts	11.00	24.75	29.33	57.29
Thrust/Weight Ratio	T/W		0.03	0.01	0.02	0.05
Wing Loading Factor	W/S	N/m^2	6.68	6.68	6.68	6.68

NACA 4412						
Weight = Lift	40	N	4	kg		
Density of air	1.225	kg/m^3			Coeff of lift linearization	
Chord	0.3048	m			Cl = mx +b	
Area required at low speed	**0.60**	m^2			Cl = 0.08x +0.5	
Frontal Area	0.07	m^2				

			Velocity (m/s)			
Parameter	**Notation**	**Units**	**10**	**15**	**20**	**25**
Reynolds Number	Re		207,000	311,000	415,000	519,000
Coeff of Lift Min	Cl		1.20	0.48	0.27	0.17
Angle of Attack	AoA	degrees	8.75	-0.19	-2.84	-4.07
Span	b	meters	1.96	1.96	1.96	1.96
Aspect Ratio	AR		6.44	6.44	6.44	6.44
Coeff of Drag	Cd		0.03	0.01	0.01	0.01
Coeff of Moment	Cm		-0.07	-0.10	-0.10	-0.10
Lift/Drag	L/D		50.00	60.00	55.00	55.00
Drag	D	Newtons	0.92	0.83	1.47	2.29
Power	P	Watts	9.17	12.38	29.33	57.29
Thrust/Weight Ratio	T/W		0.02	0.02	0.02	0.02
Wing Loading Factor	W/S	N/m^2	6.68	6.68	6.68	6.68

MH 114						
Weight = Lift	40	N	4	kg		
Density of air	1.225	kg/m^3			Coeff of lift linearization	
Chord	0.3048	m			Cl = mx +b	
Area required at low speed	**0.42**	m^2			Cl = 0.09x +0.8	
Frontal Area	0.05	m^2				

			Velocity (m/s)			
Parameter	**Notation**	**Units**	**10**	**15**	**20**	**25**
Reynolds Number	Re		207,000	311,000	415,000	519,000
Coeff of Lift	Cl		1.70	0.69	0.39	0.25
Angle of Attack	AoA	degrees	10.00	-1.26	-4.60	-6.14
Span	b	meters	1.39	1.39	1.39	1.39
Aspect Ratio	AR		4.55	4.55	4.55	4.55
Coeff of Drag	Cd		0.03	0.01	0.01	0.01
Coeff of Moment	Cm		-0.16	-0.19	-0.19	-0.19
Lift/Drag	L/D		70.00	80.00	95.00	105.00
Drag	D	Newtons	0.78	0.58	1.04	1.62
Power	P	Watts	7.76	8.74	20.71	40.44
Thrust/Weight Ratio	T/W		0.01	0.01	0.01	0.01
Wing Loading Factor	W/S	N/m^2	9.47	9.47	9.47	9.47

SD 7062						
Weight = Lift	40	N	4	kg		
Density of air	1.225	kg/m^3			Coeff of lift linearization	
Chord	0.3048	m			Cl = mx +b	
Area required at low speed	**0.45**	m^2			Cl = 0.08x +0.4	
Frontal Area	0.06	m^2				

			Velocity (m/s)			
Parameter	**Notation**	**Units**	**10**	**15**	**20**	**25**
Reynolds Number	Re		207,000	311,000	415,000	519,000
Coeff of Lift	Cl		1.60	0.65	0.36	0.23
Angle of Attack	AoA	degrees	15.00	3.08	-0.45	-2.09
Span	b	meters	1.47	1.47	1.47	1.47
Aspect Ratio	AR		4.83	4.83	4.83	4.83
Coeff of Drag	Cd		0.07	0.01	0.01	0.01
Coeff of Moment	Cm		-0.04	-0.08	-0.08	-0.08
Lift/Drag	L/D		30.00	70.00	70.00	70.00
Drag	D	Newtons	1.93	0.62	1.10	1.72
Power	P	Watts	19.25	9.28	22.00	42.97
Thrust/Weight Ratio	T/W		0.03	0.01	0.01	0.01
Wing Loading Factor	W/S	N/m^2	8.91	8.91	8.91	8.91

MH 83						
Weight = Lift	40	N	4	kg		
Density of air	1.225	kg/m^3			Coeff of lift linearization	
Chord	0.3048	m			Cl = mx +b	
Area required at low speed	**0.40**	m^2			Cl = 0.09x +0.45	
Frontal Area	0.05	m^2				

			Velocity (m/s)			
Parameter	**Notation**	**Units**	**10**	**15**	**20**	**25**
Reynolds Number	Re		207,000	311,000	415,000	519,000
Coeff of Lift	Cl		1.80	0.73	0.41	0.26
Angle of Attack	AoA	degrees	15.00	3.08	-0.45	-2.09
Span	b	meters	1.31	1.31	1.31	1.31
Aspect Ratio	AR		4.30	4.30	4.30	4.30
Coeff of Drag	Cd		0.15	0.01	0.01	0.01
Coeff of Moment	Cm		-0.05	-0.06	-0.06	-0.06
Lift/Drag	L/D		10.00	65.00	45.00	45.00
Drag	D	Newtons	3.67	0.55	0.98	1.53
Power	P	Watts	36.67	8.25	19.56	38.19
Thrust/Weight Ratio	T/W		0.10	0.02	0.02	0.02
Wing Loading Factor	W/S	N/m^2	10.02	10.02	10.02	10.02

MH 64						
Weight = Lift	40	N	4	kg		
Density of air	1.225	kg/m^3			Coeff of lift linearization	
Chord	0.3048	m			Cl = mx +b	
Area required at low speed	**0.62**	m^2			Cl = 0.1x +0.15	
Frontal Area	0.05	m^2				

			Velocity (m/s)			
Parameter	**Notation**	**Units**	**10**	**15**	**20**	**25**
Reynolds Number	Re		207,000	311,000	415,000	519,000
Coeff of Lift	Cl		1.15	0.46	0.26	0.17
Angle of Attack	AoA	degrees	10.00	3.15	1.11	0.17
Span	b	meters	2.05	2.05	2.05	2.05
Aspect Ratio	AR		6.72	6.72	6.72	6.72
Coeff of Drag	Cd		0.04	0.01	0.01	0.01
Coeff of Moment	Cm		0.00	-0.15	-0.15	-0.15
Lift/Drag	L/D		25.00	55.00	25.00	20.00
Drag	D	Newtons	1.53	0.86	1.53	2.39
Power	P	Watts	15.30	12.91	30.61	59.78
Thrust/Weight Ratio	T/W		0.04	0.02	0.04	0.05
Wing Loading Factor	W/S	N/m^2	6.40	6.40	6.40	6.40

S1223						
Weight = Lift	40	N	4	kg		
Density of air	1.225	kg/m^3			Coeff of lift linearization	
Chord	2	m			Cl = mx +b	
Area required at low speed	**0.32**	m^2			Cl = 0.07x +1.2	
Frontal Area	0.04	m^2				

			Velocity (m/s)			
Parameter	**Notation**	**Units**	**10**	**15**	**20**	**25**
Reynolds Number	Re		207,000	311,000	415,000	519,000
Coeff of Lift	Cl		2.25	0.91	0.51	0.33
Angle of Attack	AoA	degrees	15.00	-4.16	-9.84	-12.47
Span	b	meters	0.16	0.16	0.16	0.16
Aspect Ratio	AR		0.08	0.08	0.08	0.08
Coeff of Drag	Cd		0.06	0.02	0.02	0.02
Coeff of Moment	Cm		-0.17	-0.27	-0.27	-0.27
Lift/Drag	L/D		35.00	70.00	75.00	80.00
Drag	D	Newtons	1.17	0.88	1.56	2.44
Power	P	Watts	11.73	13.20	31.29	61.11
Thrust/Weight Ratio	T/W		0.03	0.01	0.01	0.01
Wing Loading Factor	W/S	N/m^2	12.53	12.53	12.53	12.53

Lissaman 7769						
Weight = Lift	40	N	4	kg		
Density of air	1.225	kg/m^3			Coeff of lift linearization	
Chord	0.3048	m			Cl = mx +b	
Area required at low speed	**0.55**	m^2			Cl = 0.1x + 0.3	
Frontal Area	0.06	m^2				

			Velocity (m/s)			
Parameter	**Notation**	**Units**	**10**	**15**	**20**	**25**
Reynolds Number	Re		207,000	311,000	415,000	519,000
Coeff of Lift	Cl		1.30	0.53	0.30	0.19
Angle of Attack	AoA	degrees	10.00	2.25	-0.05	-1.11
Span	b	meters	1.81	1.81	1.81	1.81
Aspect Ratio	AR		5.95	5.95	5.95	5.95
Coeff of Drag	Cd		0.02	0.02	0.02	0.02
Coeff of Moment	Cm		-0.02	-0.03	-0.03	-0.03
Lift/Drag	L/D		65.00	40.00	30.00	30.00
Drag	D	Newtons	0.68	1.52	2.71	4.23
Power	P	Watts	6.77	22.85	54.15	105.77
Thrust/Weight Ratio	T/W		0.02	0.03	0.03	0.03
Wing Loading Factor	W/S	N/m^2	7.24	7.24	7.24	7.24

Appendix D – Detailed Results for Manufacturing Support Aircraft

NACA 4418						
Weight = Lift	75	N	7.5	kg		
Density of air	1.225	kg/m^3			Coeff of lift linearization	
Chord	0.4826	m			Cl = mx +b	
Area required at low speed	**1.08**	m^2			Cl = 0.09x +0.5	
Frontal Area	0.10	m^2				

			Velocity (m/s)			
Parameter	**Notation**	**Units**	**10**	**15**	**20**	**25**
Reynolds Number	Re		207,000	311,000	415,000	519,000
Coeff of Lift	Cl		1.25	0.51	0.28	0.18
Angle of Attack	AoA	degrees	8.33	0.06	-2.40	-3.54
Span	b	meters	2.23	2.23	2.23	2.23
Aspect Ratio	AR		4.63	4.63	4.63	4.63
Coeff of Drag	Cd		0.02	0.01	0.01	0.01
Coeff of Moment	Cm		-0.08	-0.09	-0.09	-0.09
Lift/Drag	L/D		62.50	50.51	28.41	22.73
Drag	D	Newtons	1.32	1.49	2.64	3.30
Power	P	Watts	13.20	22.28	52.80	82.50
Thrust/Weight Ratio	T/W		0.02	0.02	0.04	0.04
Wing Loading Factor	W/S	N/m^2	6.96	6.96	6.96	6.96

NACA4412						
Weight = Lift	42.85	N	3.05	kg		
Density of air	1.225	kg/m^3	4.37244898		Coeff of lift linearization	
Chord	0.5588	m			Cl = mx +b	
Area required at low speed	**0.58**	m^2			Cl = 0.08x +0.5	
Frontal Area	0.07	m^2				

			Velocity (m/s)			
Parameter	**Notation**	**Units**	**10**	**15**	**20**	**25**
Reynolds Number	Re		207,000	311,000	415,000	519,000
Coeff of Lift Min	Cl		1.20	0.53	0.30	0.19
Angle of Attack	AoA	degrees	8.75	0.42	-2.50	-3.85
Span	b	meters	1.04	1.04	1.04	1.04
Aspect Ratio	AR		1.87	1.87	1.87	1.87
Coeff of Drag	Cd		0.03	0.01	0.01	0.01
Coeff of Moment	Cm		-0.07	-0.10	-0.10	-0.10
Lift/Drag	L/D		50.00	60.00	55.00	55.00
Drag	D	Newtons	0.89	0.80	1.43	2.23
Power	P	Watts	8.93	12.05	28.57	55.79
Thrust/Weight Ratio	T/W		0.02	0.02	0.02	0.02
Wing Loading Factor	W/S	N/m^2	5.23	5.23	5.23	5.23

MH 114						
Weight = Lift	42.85	N	3.05	kg		
Density of air	1.225	kg/m^3			Coeff of lift linearization	
Chord	0.5588	m			Cl = mx +b	
Area required at low speed	**0.41**	m^2			Cl = 0.09x +0.8	
Frontal Area	0.05	m^2				

			Velocity (m/s)			
Parameter	**Notation**	**Units**	**10**	**15**	**20**	**25**
Reynolds Number	Re		207,000	311,000	415,000	519,000
Coeff of Lift	Cl		1.70	0.76	0.43	0.27
Angle of Attack	AoA	degrees	10.00	-0.49	-4.17	-5.87
Span	b	meters	0.74	0.74	0.74	0.74
Aspect Ratio	AR		1.32	1.32	1.32	1.32
Coeff of Drag	Cd		0.03	0.01	0.01	0.01
Coeff of Moment	Cm		-0.16	-0.19	-0.19	-0.19
Lift/Drag	L/D		70.00	80.00	95.00	105.00
Drag	D	Newtons	0.76	0.57	1.01	1.58
Power	P	Watts	7.56	8.51	20.16	39.38
Thrust/Weight Ratio	T/W		0.01	0.01	0.01	0.01
Wing Loading Factor	W/S	N/m^2	7.41	7.41	7.41	7.41

MH 104						
Weight = Lift	42.85	N	4.368	kg		
Density of air	1.225	kg/m^3			Coeff of lift linearization	
Chord	0.5588	m			Cl = mx +b	
Area required at low speed	**0.58**	m^2			Cl = 0.11x +0.1	
Frontal Area	0.08	m^2				

			Velocity (m/s)			
Parameter	**Notation**	**Units**	**10**	**15**	**20**	**25**
Reynolds Number	Re		207,000	311,000	415,000	519,000
Coeff of Lift	Cl		1.20	0.53	0.30	0.19
Angle of Attack	AoA	degrees	10.00	3.94	1.82	0.84
Span	b	meters	1.04	1.04	1.04	1.04
Aspect Ratio	AR		1.87	1.87	1.87	1.87
Coeff of Drag	Cd		0.02	0.01	0.01	0.01
Coeff of Moment	Cm		-0.01	-0.02	0.00	0.00
Lift/Drag	L/D		62.50	53.00	30.00	20.00
Drag	D	Newtons	0.70	0.80	1.43	2.68
Power	P	Watts	6.96	12.05	28.57	66.95
Thrust/Weight Ratio	T/W		0.02	0.02	0.03	0.05
Wing Loading Factor	W/S	N/m^2	7.49	7.49	7.49	7.49

NACA2414						
Weight = Lift	42.85	N	4.368	kg		
Density of air	1.225	kg/m^3			Coeff of lift linearization	
Chord	0.4572	m			Cl = mx +b	
Area required at low speed	**0.56**	m^2			Cl = 0.077x +0.2	
Frontal Area	0.08	m^2				

			Velocity (m/s)			
Parameter	**Notation**	**Units**	**10**	**15**	**20**	**25**
Reynolds Number	Re		207,000	311,000	415,000	519,000
Coeff of Lift	Cl		1.25	0.56	0.31	0.20
Angle of Attack	AoA	degrees	13.64	4.62	1.46	0.00
Span	b	meters	1.22	1.22	1.22	1.22
Aspect Ratio	AR		2.68	2.68	2.68	2.68
Coeff of Drag	Cd		0.02	0.01	0.01	0.01
Coeff of Moment	Cm		-0.03	-0.05	-0.05	-0.05
Lift/Drag	L/D		62.50	56.00	31.00	20.00
Drag	D	Newtons	0.69	0.77	1.37	1.71
Power	P	Watts	6.86	11.57	27.42	42.85
Thrust/Weight Ratio	T/W		0.02	0.02	0.03	0.05
Wing Loading Factor	W/S	N/m^2	7.80	7.80	7.80	7.80

S8036						
Weight = Lift	42.85	N	3.05	kg		
Density of air	1.225	kg/m^3			Coeff of lift linearization	
Chord	0.5588	m			Cl = mx +b	
Area required at low speed	**0.56**	m^2			Cl = 0.059x +0.2	
Frontal Area	0.07	m^2				
			0.029	0.044	0.058	0.073

			Velocity (m/s)			
Parameter	**Notation**	**Units**	**10**	**15**	**20**	**25**
Reynolds Number	Re		207,000	311,000	415,000	519,000
Coeff of Lift	Cl		1.25	0.56	0.31	0.20
Angle of Attack	AoA	degrees	17.80	6.03	1.91	0.00
Span	b	meters	1.00	1.00	1.00	1.00
Aspect Ratio	AR		1.79	1.79	1.79	1.79
Coeff of Drag	Cd		0.03	0.01	0.01	0.01
Coeff of Moment	Cm		0.00	-0.05	-0.03	-0.03
Lift/Drag	L/D		42.67	56.00	31.00	20.00
Drag	D	Newtons	0.86	0.77	1.37	2.14
Power	P	Watts	8.57	11.57	27.42	53.56
Thrust/Weight Ratio	T/W		0.02	0.02	0.03	0.05
Wing Loading Factor	W/S	N/m^2	5.45	5.45	5.45	5.45

Appendix E – MATLAB Code for Power Requirement Calculation

Stage_1_inputs:

```
%% Takeoff parameter calculator for RC aircraft
% To be used by WPI AIAA Design, Build, Fly teams only

% Used in conjunction WPI_DBF_flight_analysis
% Calculates
%   -If plane will take off within takeoff field length
%   -Takeoff velocity taking into account a 25% buffer to account for
%    uncontrollable factors

function flight_output_values = stage_1_inputs(mass, weight, density, Cd0, A_drag, Cl, A_wing, prop_diam,
prop_RPM, prop_pitch)

%% Uncomment when using inputs from WPI_DBF_flight_analysis to analyze results
mass = 2.5;
v_cruise = 160;
weight = 2.5*9.8;
density = .957*1.255;
Cd0 = .021;
A_drag = .03;
A_wing = .34;
Cl = 1.20;
prop_diam = 11;
prop_RPM = 8490;
prop_pitch = 7;

%% Calculates necessary velocity for liftoff
V_takeoff = sqrt((2*weight)/(density*A_wing*Cl));

%% Calculating propeller static thrust
```

```
static_thrust =
(1.225*(pi*((0.0254*prop_diam)^2))/4)*((prop_RPM*.0254*prop_pitch*(1/60))^2)*((prop_diam/(3.29546*prop_pi
tch))^1.5);
thrust_initial = static_thrust;

%% Finding acceleration and velocity as a function of time
%takes into account decreasing value of dynamic thrust

%initializing variables
current_accel_value = zeros(1,500);
current_vel = zeros(1,500);
new_thrust = 0;
t_liftoff = 0;
t_count = 0;
timestep = 0.1;

%loop to find time to liftoff and t_count, a count of total recursions
for t=1:1:500
   if t == 1
      current_accel_value(t) = thrust_initial/mass;
      current_vel(t) = current_accel_value(t)*timestep;
      new_thrust = (1.225*(pi*((0.0254*prop_diam)^2))/4)*(((prop_RPM*.0254*prop_pitch*(1/60))^2)-
(prop_RPM*.0254*prop_pitch*(1/60)*current_vel(t)))*((prop_diam/(3.29546*prop_pitch))^1.5);
   else
      current_accel_value(t) = (new_thrust/mass) - (.5*density*A_drag*Cd0*(current_vel(t-1)^2)/mass);
      current_vel(t) = current_vel(t-1)+current_accel_value(t)*timestep;
      new_thrust = (1.225*(pi*((0.0254*prop_diam)^2))/4)*(((prop_RPM*.0254*prop_pitch*(1/60))^2)-
(prop_RPM*.0254*prop_pitch*(1/60)*current_vel(t)))*((prop_diam/(3.29546*prop_pitch))^1.5);
   end
   if current_vel(t) > 1.25*V_takeoff
      t_liftoff=t*0.1;
      t_count = t;
      break
   end
end

%% Calculates position of aircraft at moment of liftoff
```

```
Pos_at_liftoff = 0;
accel_total = 0;
for y = 1:1:t_count
   if y == 1
      Pos_at_liftoff = 0.5*current_accel_value(y)*timestep^2;
   else
      Pos_at_liftoff = Pos_at_liftoff + current_vel(y-1)*timestep + 0.5*current_accel_value(y)*timestep^2;
   end
end

%% Outputs
flight_output_values = [Pos_at_liftoff; current_vel(t_count); t_liftoff; t_count; static_thrust];
```

WPI_DBF_Flight_Analysis

```
%% Flight Analysis Program for RC Aircraft
% To be used by WPI AIAA Design, Build, Fly teams only
%
% Used in conjunction with stage_1_inputs
% Calculates
%   -If plane will take off within takeoff field length
%   -Max velocity based on generated thrust
%   -Power required to maintain cruising velocity
%   -Total flight time

% Breaks flight into four stages
%   - 1. Takeoff
%   - 2. Climb
%   - 3. Cruise
%   - 4. Turn

% ALL VALUES EXCEPT PROP SPECS TO BE ENTERED IN METRIC UNITS
% prop thrust equation accounts for conversions

%Perameter to show liftoff failure, or failure if max_v is less than
%v_cruise
takeoff_outcome = 'Successful takeoff within prescribed field length';
%% Insert aircraft perameters
```

```
% weight = ;              % N
% mass = weight/9.8;
% density = ;            % kg/m^3
% bank_angle = ;         % deg
% A_wing = ;             % m^2
% A_drag = ;             % m^2
% cruise_Cd0 = ;
% cruise_Cl = ;
% v_cruise = ;           % desired cruise velocity
% cruise_alt = ;         % m
% max_liftoff_x = ;      % m
% prop_diam = ;          % in
% prop_RPM = ;           % rotations per minute
% prop_pitch = ;         % in

% Values based upon MH45 airfoil data found by Aerodynamics team
mass = 3.5;
v_cruise = 21.5;
cruise_Cl = 0.27;
takeoff_Cl = 1.2;
weight = mass*9.8;
cruise_alt = 17;
density = .957*1.255;
Cd0 = .03;
cruise_Cd0 = 0.1;
M1_Cd = cruise_Cd0;
A_drag = .03;
A_wing = .34;
prop_diam = 11;
climb_aoa = 15;
prop_RPM = 8490;
prop_pitch = 7;
AR = 5;
max_liftoff_x = 33;

%% Stage 1: Start to takeoff time calculations, does aircraft take off in time?
```

```
stage_1_outputs = stage_1_inputs(mass, weight, density, M1_Cd, A_drag, takeoff_Cl, A_wing, prop_diam,
prop_RPM, prop_pitch);
takeoff_dx = stage_1_outputs(1);
takeoff_vel = stage_1_outputs(2);
t_takeoff = stage_1_outputs(3);
t_count = stage_1_outputs(4);
thrust_initial = stage_1_outputs(5)

%Liftoff space defined as liftoff_max_x - x_liftoff, must be positive for
%legal takeoff

liftoff_space = max_liftoff_x - takeoff_dx;
if liftoff_space < 10
   takeoff_outcome = 'Aircraft does not take off within set takeoff area'
else
   takeoff_outcome
end

%% Stage 2: Climb
%Time assuming v_climb_initial = 1.25*V_takeoff

%Part B: finding t_climb and total dx after climb
t_climb = cruise_alt/((takeoff_vel)*sin(climb_aoa*pi/180));
climb_dx = t_climb*(takeoff_vel)*cos(climb_aoa*pi/180);

%% Stage 3: Cruise

%Initializing variables
accel_value = zeros(1,500);
current_vel = zeros(1,500);
max_velocity = 0;
n_thrust = zeros(1,500);
time_to_cruiseV = 0;
t_cruiseV_count = 0;
timestep = 0.1;
thrust_cruise_v = 0;
```

```
%Loop to populate acceleration matrix and find aircraft max velocity
for t=1:1:500
   if t == 1
      accel_value(t) = thrust_initial/mass;
      current_vel(t) = accel_value(t)*timestep;
      n_thrust(t) = (1.225*(pi*((0.0254*prop_diam)^2))/4)*(((prop_RPM*.0254*prop_pitch*(1/60))^2)-
(prop_RPM*.0254*prop_pitch*(1/60)*current_vel(t)))*((prop_diam/(3.29546*prop_pitch))^1.5);
   else
      accel_value(t) = (n_thrust(t-1)/mass) - (.5*density*A_drag*Cd0*(current_vel(t-1)^2)/mass);
       if accel_value(t) < 0
          max_velocity = current_vel(t-1)
          break
       end
      current_vel(t) = current_vel(t-1)+accel_value(t)*timestep;
      if current_vel(t) > v_cruise
         time_to_cruiseV = t*0.1;
         t_cruiseV_count = t;
         thrust_cruise_v = n_thrust(t-1);
         current_vel(t);
         break
      end
      n_thrust(t) = (1.225*(pi*((0.0254*prop_diam)^2))/4)*(((prop_RPM*.0254*prop_pitch*(1/60))^2)-
(prop_RPM*.0254*prop_pitch*(1/60)*current_vel(t)))*((prop_diam/(3.29546*prop_pitch))^1.5);
   end
end

%Power (in watts) required for cruising velocity
power_for_cruise = n_thrust(1)*current_vel(t_cruiseV_count)
% %Finding if max velocity is greater than desired cruising velocity
% if max_velocity < v_cruise
%     fail = 1;
%     break
% end

%Time required to accelerate to cruise V
t_accel_2_cruiseV = time_to_cruiseV - t_takeoff;
%Finding distance covered while accelerating to cruise_V
```

```
cruiseV_accel_dx = 0;
accel_total = 0;
for y = t_count:1:t_cruiseV_count
   if y == 1
      cruiseV_accel_dx = 0.5*accel_value(y)*timestep^2;
   else
      cruiseV_accel_dx = cruiseV_accel_dx + current_vel(y-1)*timestep + 0.5*accel_value(y)*timestep^2;
   end
end
cruiseV_accel_dx
%Total dx when cruise velocity is reached
dx_total_preCruise = cruiseV_accel_dx + takeoff_dx + climb_dx;

%Calculating total time during cruise phase
t_cruise = ((6000*12*2.54/100)-dx_total_preCruise)/v_cruise;

%% Stage 4: Turns
%assuming level turn
%order or operaions
% 1. Choose appripriate radius of turn
% 2. Use this value and your chosen cruising velocity to calculate load
%    factor (should be around 1.3-1.5)
% 3. Determine the necessary bank angle of the aircraft

% Enter desired radius of turn
r_turn = 50;
turn_length = pi*r_turn;

%Calculating load factor
n = sqrt(((v_cruise^2)/(9.8*r_turn))^2 + 1)

%Calculating bank angle
bank_angle = asind(sqrt(1-(1/(n^2))))

%Calculating time spent turning
t_turn = turn_length/current_vel(t_cruiseV_count);
total_t_turn = 12*t_turn;
```

```
% %calculating total time of flight
t_total = t_takeoff + time_to_cruiseV + t_climb + +t_cruise + total_t_turn
```

Appendix F – CAD Package

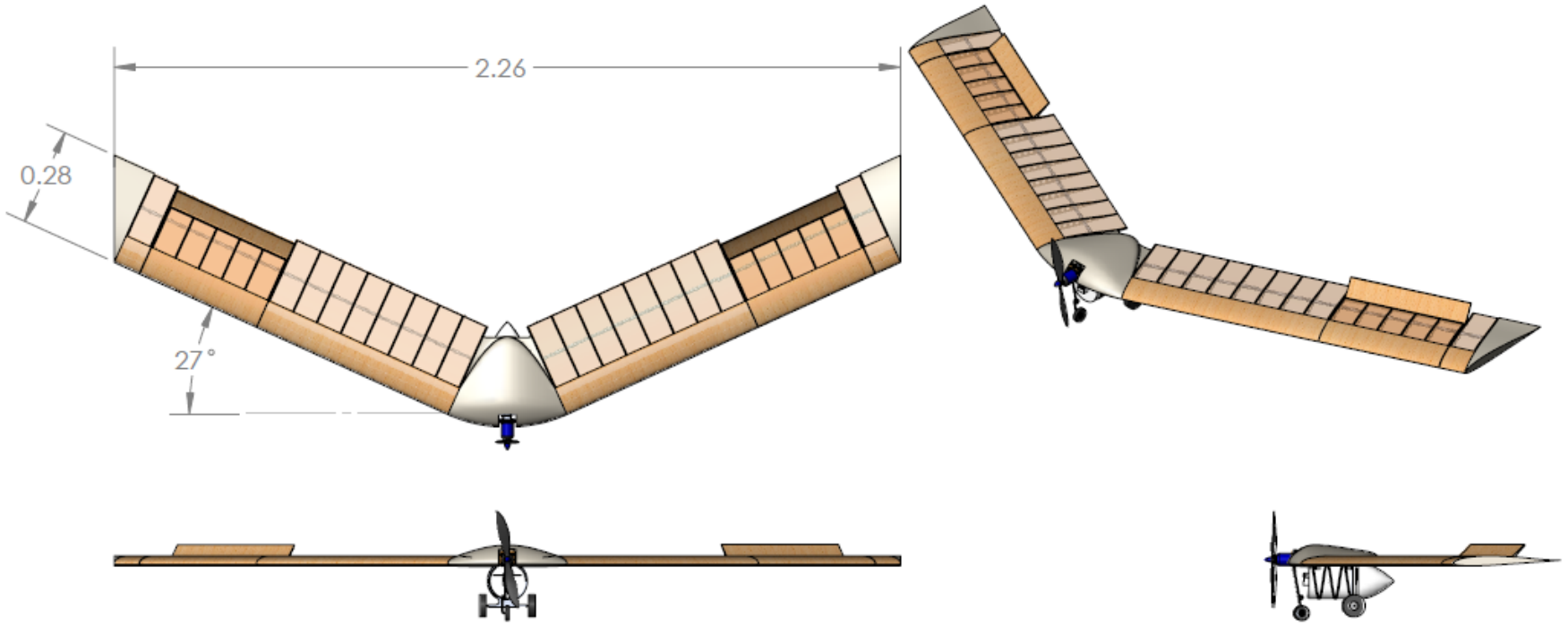

		UNLESS OTHERWISE SPECIFIED:		NAME	DATE
		DIMENSIONS ARE IN METERS TOLERANCES: FRACTIONAL ± .01 ANGULAR: MACH ± .01 TWO PLACE DECIMAL ± .01	DRAWN	RD	2/21/16
			CHECKED		
			ENG APPR.		
			MFG APPR.		
		INTERPRET GEOMETRIC TOLERANCING PER: ANSI Y14.5	Q.A.		
		MATERIAL	COMMENTS:		
NEXT ASSY	USED ON	FINISH			
APPLICATION		DO NOT SCALE DRAWING			

WPI DBF 2016

TITLE:
Production A/C
3 Views

SIZE	DWG. NO.	REV
A	All_drawings	
SCALE: 1:18	WEIGHT:	SHEET 1 OF 7

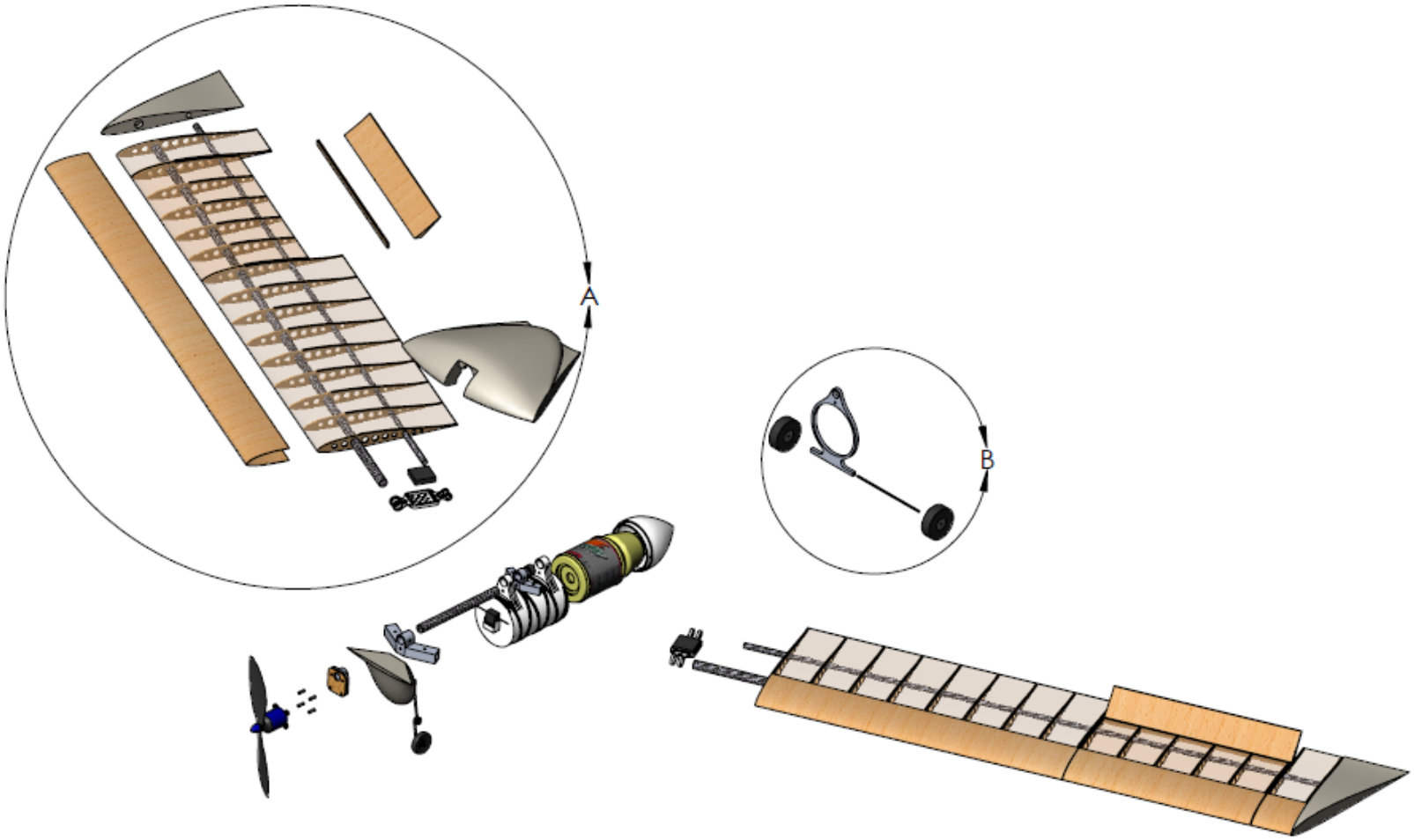

		UNLESS OTHERWISE SPECIFIED:		NAME	DATE
		DIMENSIONS ARE IN METERS TOLERANCES: FRACTIONAL± .01 ANGULAR: MACH± .01 TWO PLACE DECIMAL ± .01	DRAWN	RD	2/21/16
			CHECKED		
			ENG APPR.		
			MFG APPR.		
		INTERPRET GEOMETRIC TOLERANCING PER: ANSI Y14.5	Q.A.		
		MATERIAL	COMMENTS:		
NEXT ASSY	USED ON	FINISH			
APPLICATION		DO NOT SCALE DRAWING			

WPI DBF 2016

TITLE:

Production A/C Exploded View

SIZE	DWG. NO.	REV
A	All_drawings	

SCALE: 1:12 | WEIGHT: | SHEET 2 OF 7

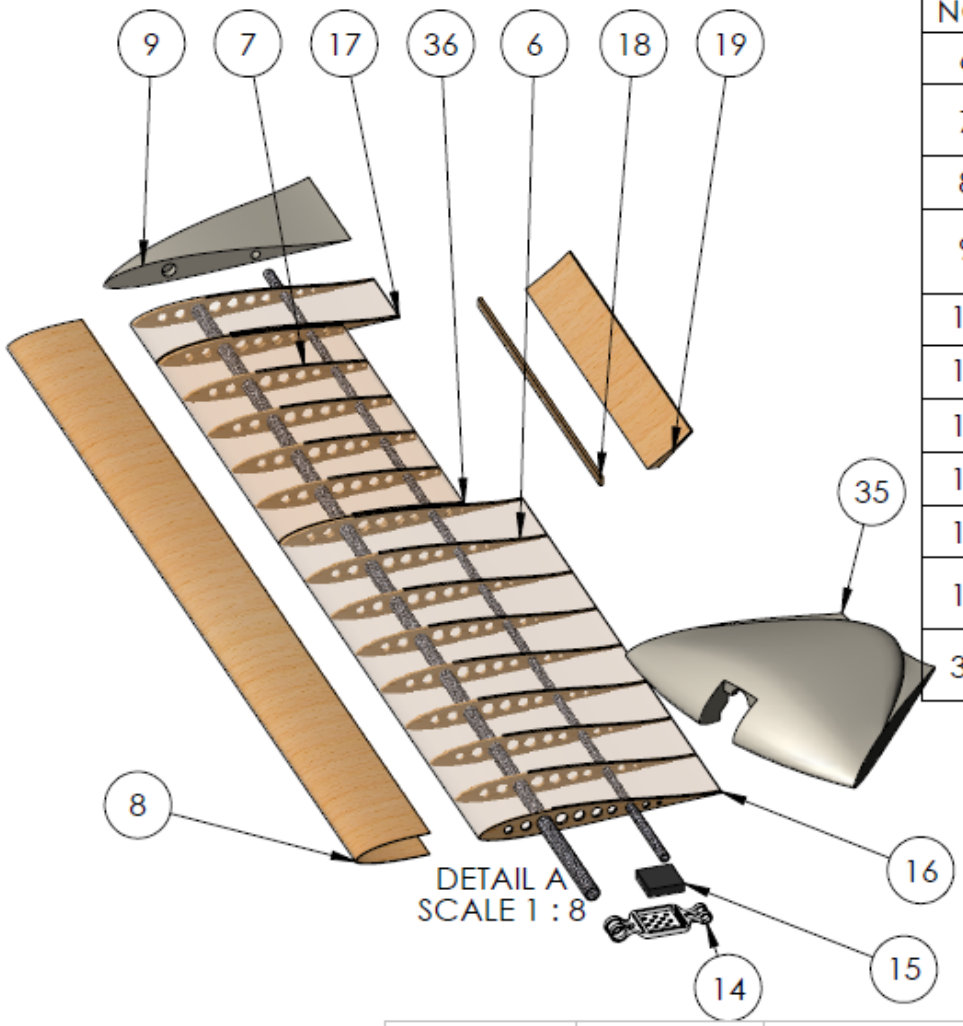

ITEM NO.	PART NAME	MATERIAL	QTY.
6	RIB_MH45_28cm	Balsa	22
7	RIB_MH45_28cm_ControlSurface	Balsa	12
8	Balsa_Sheet_LE	Balsa	2
9	Foam_Wingtip_Right	Polyurethane Foam Rigid	1
14	Battery_case	ABS	2
15	Battery_half		2
16	Heat_Shrink		2
17	Heat_Shrink_small		2
18	Control_Surface_Plate	Balsa	2
19	Elevon		2
36	Heat_Shrink_ControlRibs		2

UNLESS OTHERWISE SPECIFIED:

DIMENSIONS ARE IN METERS
TOLERANCES:
FRACTIONAL ± .01
ANGULAR: MACH ± .01
TWO PLACE DECIMAL ± .01

INTERPRET GEOMETRIC TOLERANCING PER: ANSI Y14.5

MATERIAL

FINISH

DO NOT SCALE DRAWING

	NAME	DATE
DRAWN	RD	2/21/16
CHECKED		
ENG APPR.		
MFG APPR.		
Q.A.		

COMMENTS:

NEXT ASSY | USED ON | APPLICATION

WPI DBF 2016

TITLE:

Wing Detail

SIZE	DWG. NO.	REV
A	All_drawings	

SCALE: 1:8 | WEIGHT: | SHEET 3 OF 7

ITEM NO.	PART NUMBER	MATERIAL	QTY.
29	Hoop	6061 Alloy	1
30	LandingGearRod	6061 Alloy	1
31	BackWheel		2

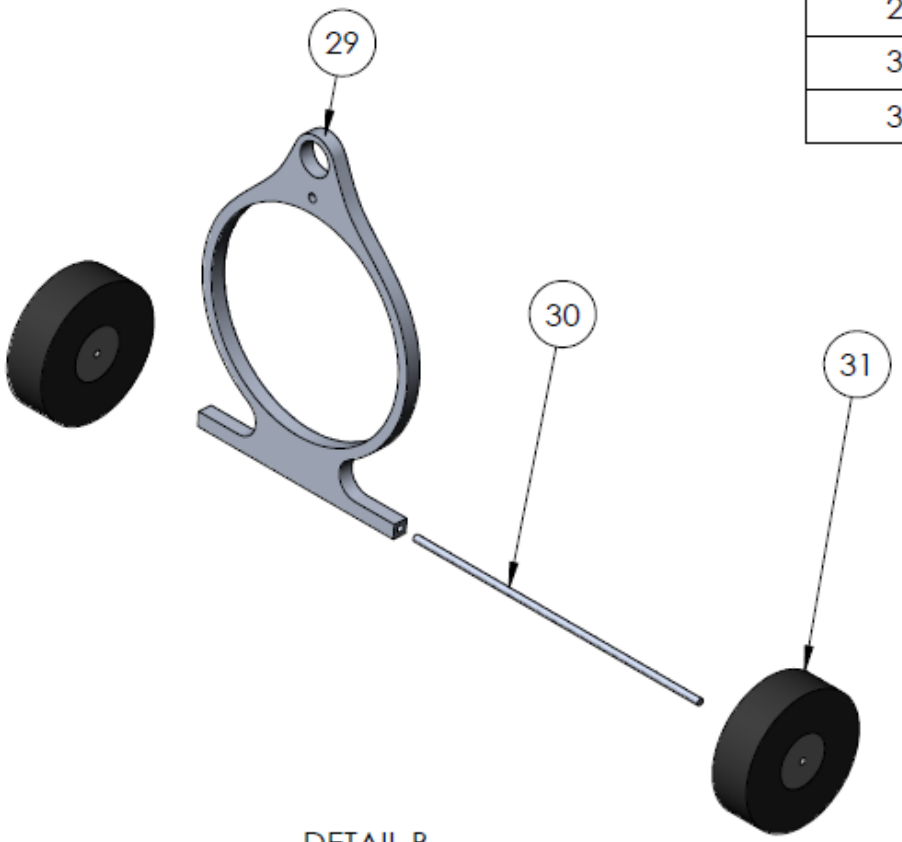

DETAIL B
SCALE 1 : 3

		UNLESS OTHERWISE SPECIFIED:		NAME	DATE
		DIMENSIONS ARE IN METERS TOLERANCES: FRACTIONAL± .01 ANGULAR: MACH± .01 TWO PLACE DECIMAL ± .01	DRAWN	RD	2/21/16
			CHECKED		
			ENG APPR.		
			MFG APPR.		
		INTERPRET GEOMETRIC TOLERANCING PER: ANSY Y14.5	Q.A.		
		MATERIAL	COMMENTS:		
NEXT ASSY	USED ON	FINISH			
APPLICATION		DO NOT SCALE DRAWING			

WPI DBF 2016

TITLE:

Landing Gear Detail

SIZE	DWG. NO.	REV
A	All_drawings	
SCALE: 1:3	WEIGHT:	SHEET 4 OF 7

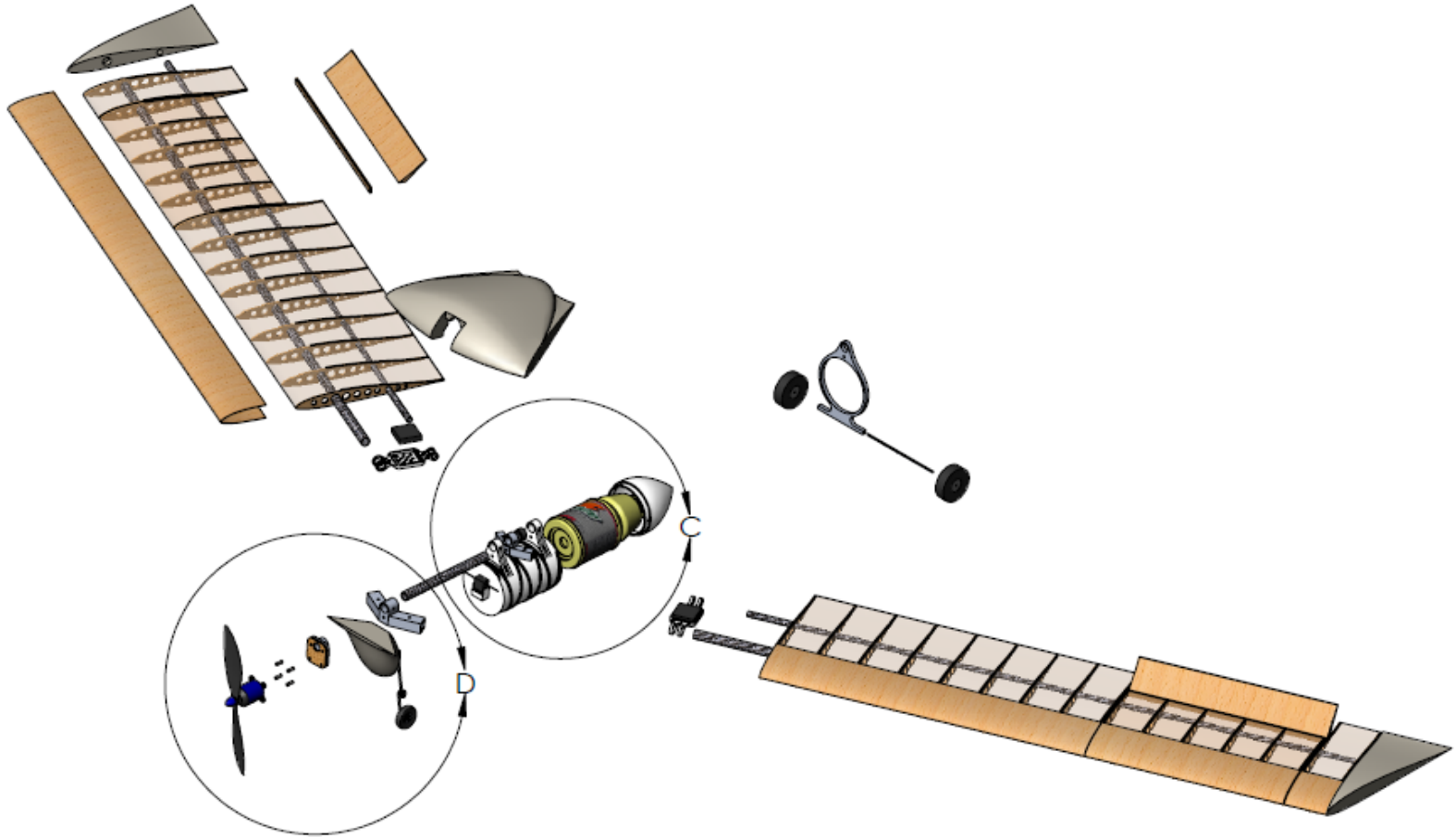

		UNLESS OTHERWISE SPECIFIED:		NAME	DATE
		DIMENSIONS ARE IN METERS TOLERANCES: FRACTIONAL± .01 ANGULAR: MACH± .01 TWO PLACE DECIMAL ± .01	DRAWN	RD	2/21/16
			CHECKED		
			ENG APPR.		
			MFG APPR.		
		INTERPRET GEOMETRIC TOLERANCING PER: ANSI Y14.5	Q.A.		
		MATERIAL	COMMENTS:		
NEXT ASSY	USED ON	FINISH			
APPLICATION		DO NOT SCALE DRAWING			

WPI DBF 2016

TITLE:

Production A/C Exploded View

SIZE	DWG. NO.	REV
A	All_drawings	

SCALE: 1:12 | WEIGHT: | SHEET 5 OF 7

ITEM NO.	PART NUMBER	MATERIAL	QTY.
1	CF Central Spar	Thornel Mat VMA	1
4	Al_fitting_aft	6061 Alloy	1
11	Bottle_Case	ABS	1
12	GatBottle1		1
13	Cone	ABS	1
21	Receiver		1
22	Aft_Bushing	Rubber	1

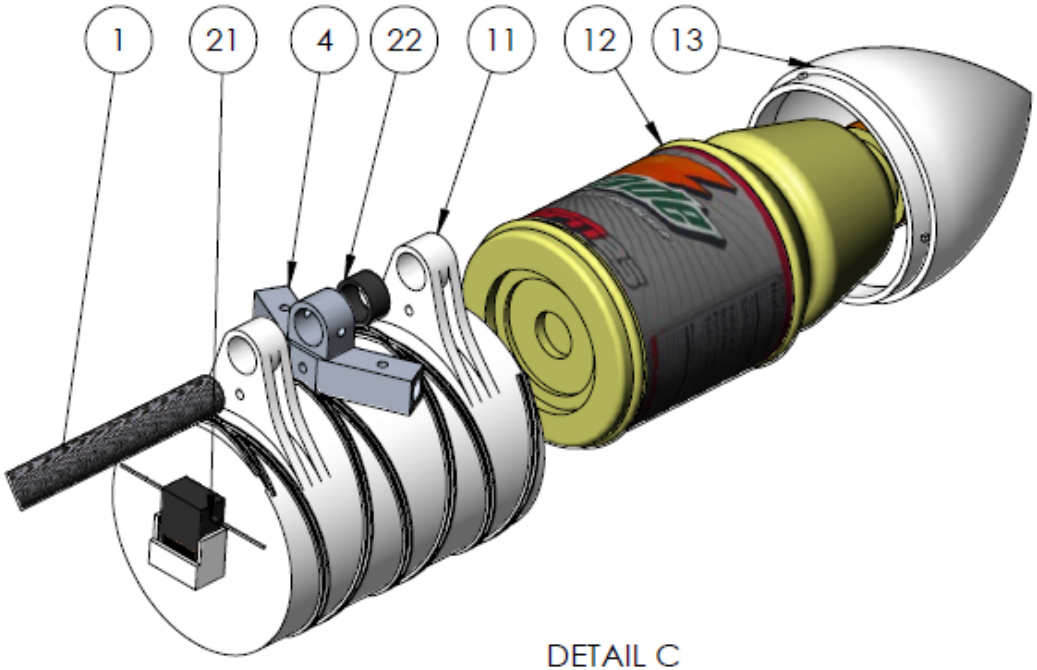

DETAIL C
SCALE 1 : 3

		UNLESS OTHERWISE SPECIFIED:		NAME	DATE
		DIMENSIONS ARE IN METERS TOLERANCES: FRACTIONAL± .01 ANGULAR: MACH± .01 TWO PLACE DECIMAL ± .01	DRAWN	RD	2/21/16
			CHECKED		
			ENG APPR.		
			MFG APPR.		
		INTERPRET GEOMETRIC TOLERANCING PER: ANSI Y14.5	Q.A.		
		MATERIAL	COMMENTS:		
NEXT ASSY	USED ON	FINISH			
APPLICATION		DO NOT SCALE DRAWING			

WPI DBF 2016

TITLE:
Fuselage Detail

SIZE	DWG. NO.	REV
A	All_drawings	
SCALE: 1:3	WEIGHT:	SHEET 6 OF 7

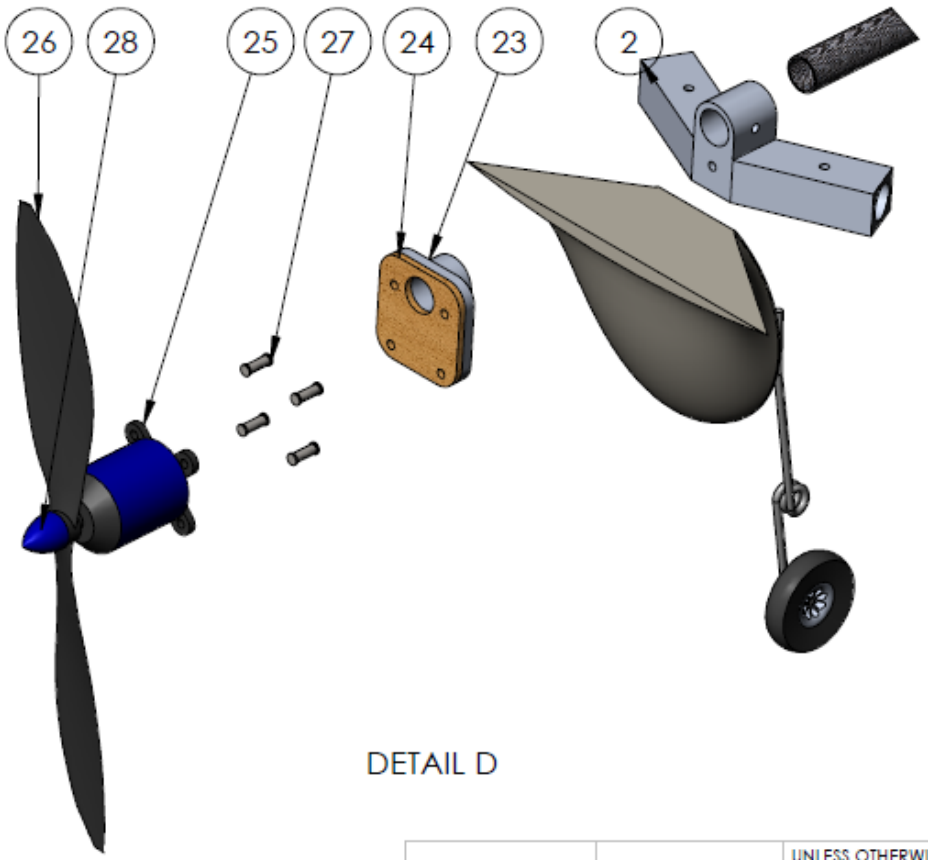

DETAIL D

ITEM NO.	PART NUMBER	MATERIAL	QTY.
2	Al_fitting_front	6061 Alloy	1
23	Motor_Plate_MetalPiece	6061 Alloy	1
24	Motor_Plate	Oak	1
25	Motor		1
26	11inch_Prop	PE High Density	1
27	Motor_Bolt		4
28	Motor_tip	ABS	1

UNLESS OTHERWISE SPECIFIED:

DIMENSIONS ARE IN METERS
TOLERANCES:
FRACTIONAL ± .01
ANGULAR: MACH ± .01
TWO PLACE DECIMAL ± .01

INTERPRET GEOMETRIC TOLERANCING PER: ANSI Y14.5

MATERIAL

FINISH

DO NOT SCALE DRAWING

NEXT ASSY | USED ON | APPLICATION

	NAME	DATE
DRAWN	RD	2/21/16
CHECKED		
ENG APPR.		
MFG APPR.		
Q.A.		

COMMENTS:

WPI DBF 2016

TITLE:

Propulsion System Detail

SIZE: A | DWG. NO.: All_drawings | REV:

SCALE: 1:3 | WEIGHT: | SHEET 7 OF 7

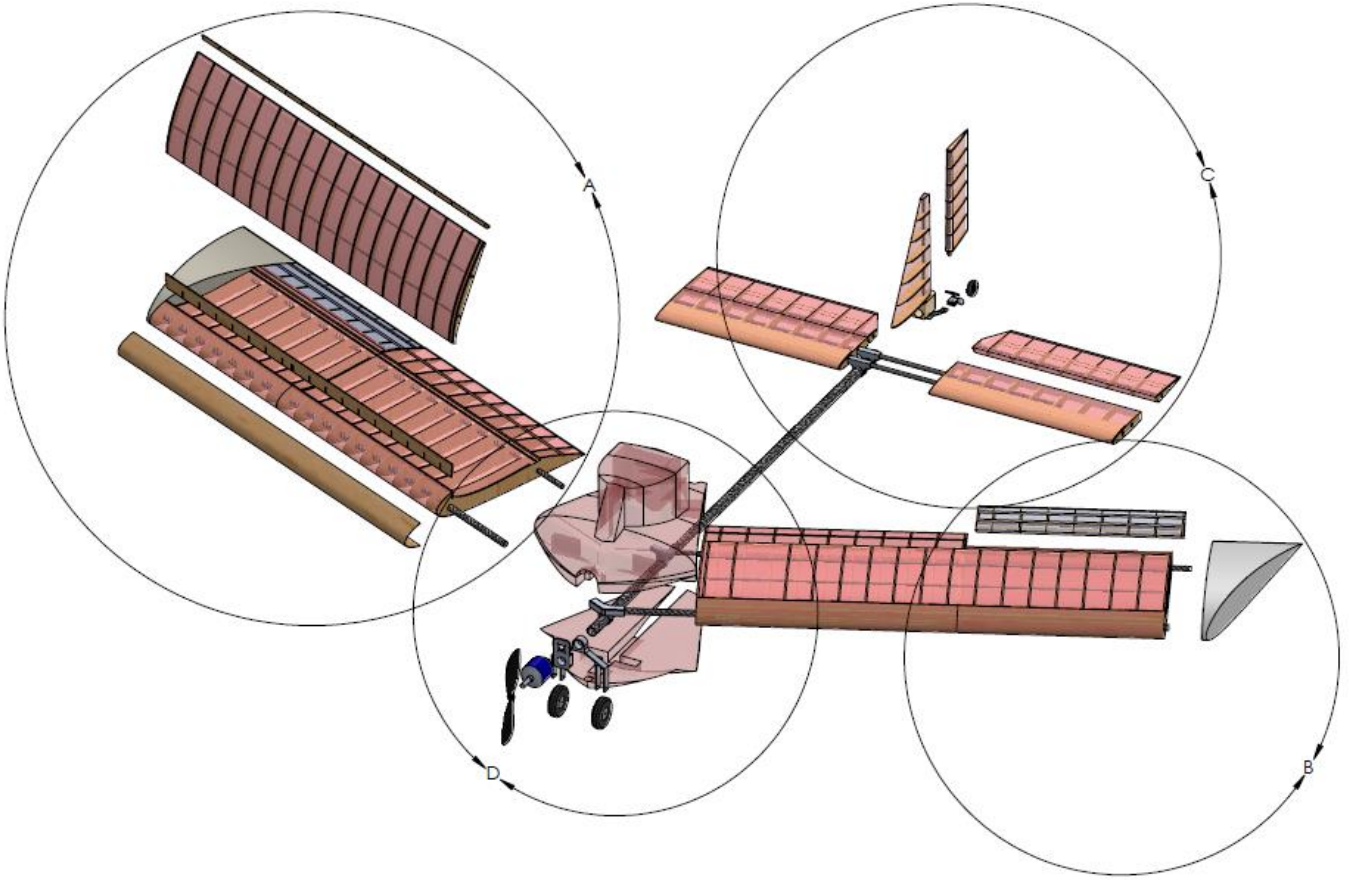

		UNLESS OTHERWISE SPECIFIED:		NAME	DATE
		DIMENSIONS ARE IN METERS TOLERANCES: FRACTIONAL ±.0.1 ANGULAR: ±.01° TWO PLACE DECIMAL ±.01	DRAWN	LDP	2/21/16
			CHECKED		
			ENG APPR.		
			MFG APPR.		
		INTERPRET GEOMETRIC TOLERANCING PER: ASME Y14.5	Q.A.		
		MATERIAL	COMMENTS:		
NEXT ASSY	USED ON	FINISH			
APPLICATION		DO NOT SCALE DRAWING			

TITLE:
Goats on Parade -
Exploited View Manufacturing Support

SIZE	DWG. NO.	REV
B	2016DBF_WPI_THREE_VIEW	A

SCALE: 1:12	WEIGHT:	SHEET 2 OF 6

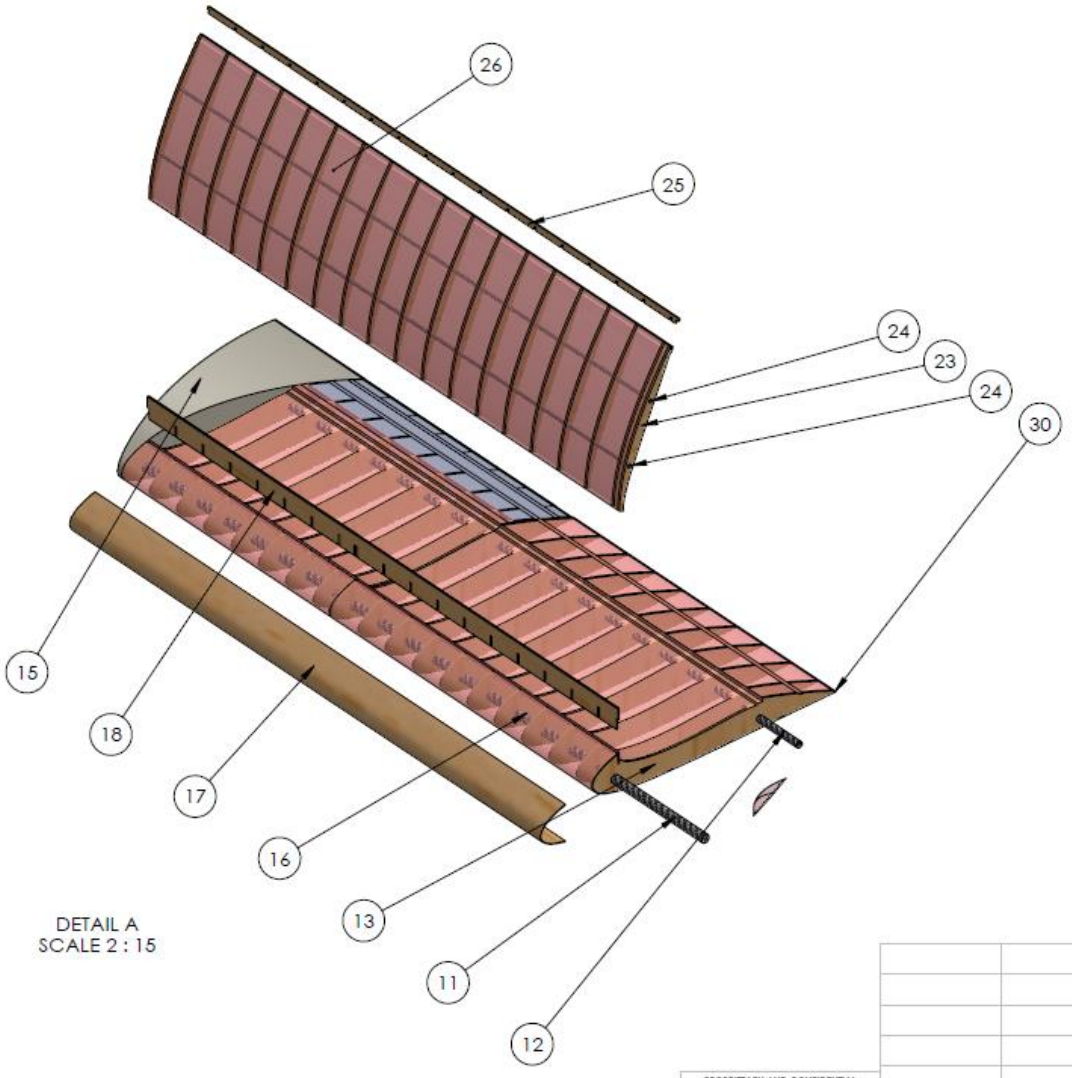

DETAIL A
SCALE 2 : 15

ITEM NO.	PART NUMBER	MATERIAL	QTY.
11	MSWingFrontRod	Custom Carbon Fiber Tube	2
12	MSWingBackRod	Custom Carbon Fiber Tube	2
13	NACA4418 Rib	Balsa	22
15	WingTipRight	Polyurethane Foam Rigid	1
16	Wing Skin	Monokote	2
17	NACA4418 Leading Edge	Balsa	2
18	NACA4418 LE Vertical Spar	Balsa	2
23	NACA4418 Lid	Balsa	38
24	LidRod	Custom Carbon Fiber Tube	4
25	NACA4418 LID Horizontal Spar	Balsa	2
26	Lid Skin	Monokote	2
30	TE Rod	Custom Carbon Fiber Tube	2

UNLESS OTHERWISE SPECIFIED:
DIMENSIONS ARE IN METERS
TOLERANCES:
FRACTIONAL ±.0.1
ANGULAR: ±.01°
TWO PLACE DECIMAL ±.01
INTERPRET GEOMETRIC TOLERANCING PER: ASME Y14.5
MATERIAL
FINISH
NEXT ASSY | USED ON
APPLICATION | DO NOT SCALE DRAWING

	NAME	DATE
DRAWN	LDP	2/21/16
CHECKED		
ENG APPR.		
MFG APPR.		
Q.A.		
COMMENTS:		

TITLE:
Goats on Parade -
Detail View A
Manufacturing Support

SIZE B | DWG. NO. 2016DBF_WPI_THREE_VIEW | REV A
SCALE: 1:15 | WEIGHT: | SHEET 3 OF 6

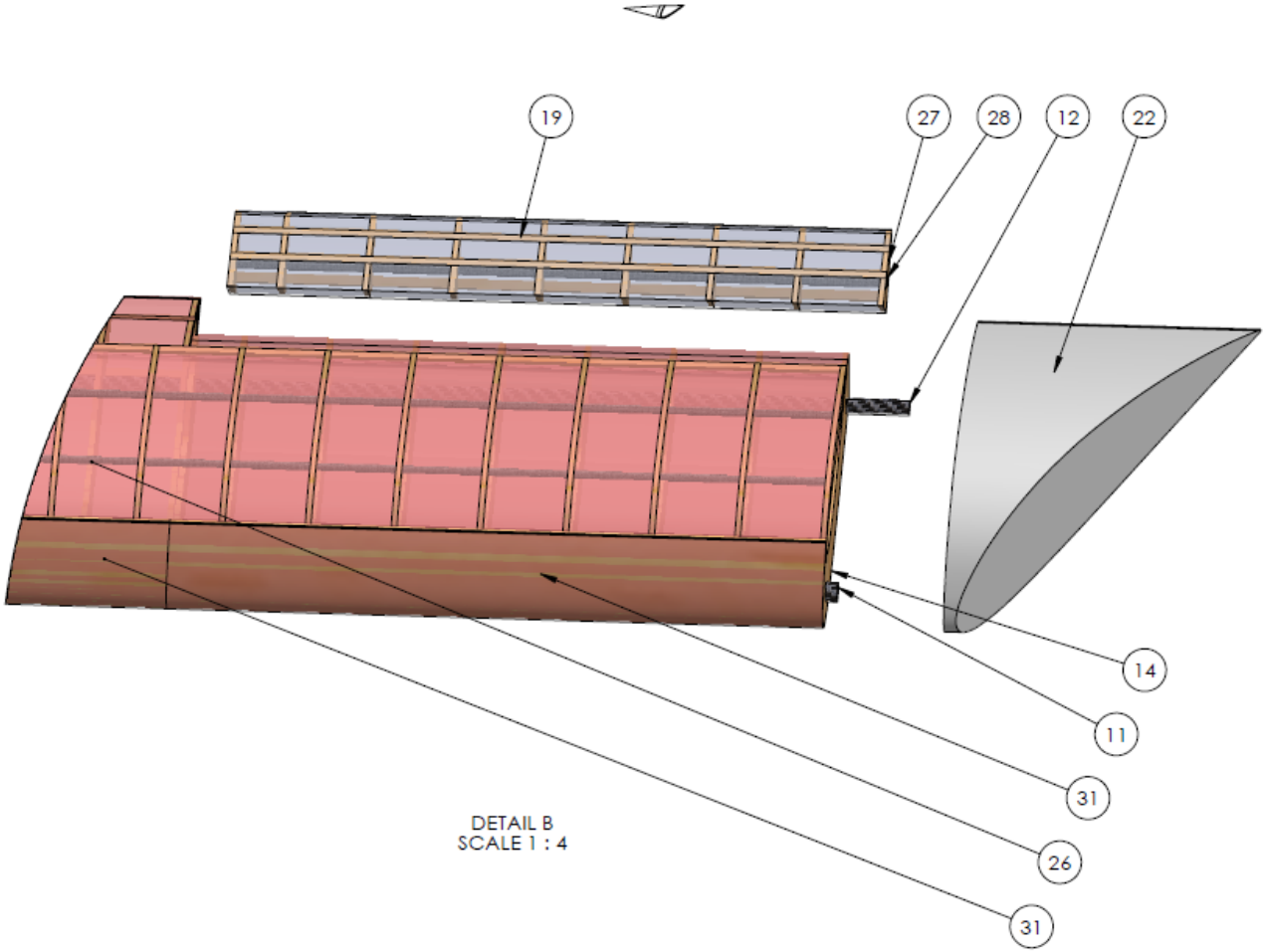

DETAIL B
SCALE 1 : 4

ITEM NO.	PART NUMBER	MATERIAL	QTY.
11	MSWingFrontRod	Custom Carbon Fiber Tube	2
12	MSWingBackRod	Custom Carbon Fiber Tube	2
13	NACA4418	Balsa	22
14	NACA4418 aileron	Balsa	18
15	WingTipRight	Polyurethane Foam Rigid	1
17	NACA4418 Leading Edge2	Balsa	2
18	NACA4418 LE VERTICAL SPAR	Balsa	2
19	Aileron skin	Monokote	2
22	WingTipLeft	Polyurethane Foam Rigid	1
23	NACA4418 Lid	Balsa	38
24	LidRod	Custom Carbon Fiber Tube	4
25	NACA4418 LID Horizontal SPAR	Balsa	2
26	Lid Skin	Monokote	2
27	Aileron	Balsa	18
28	Aileron Rod	Custom Carbon Fiber Tube	2
30	TE Rod	Custom Carbon Fiber Tube	2
31	Wing Skin	Monokote	2

UNLESS OTHERWISE SPECIFIED:
DIMENSIONS ARE IN METERS
TOLERANCES:
FRACTIONAL ±.0.1
ANGULAR: ±.01°
TWO PLACE DECIMAL ±.01
INTERPRET GEOMETRIC TOLERANCING PER: ASME Y14.5
MATERIAL
FINISH
DO NOT SCALE DRAWING

	NAME	DATE
DRAWN	LDP	2/21/16
CHECKED		
ENG APPR.		
MFG APPR.		
Q.A.		
COMMENTS:		

NEXT ASSY | USED ON | APPLICATION

TITLE:
Goats on Parade -
Detail View B
Manufacturing Support

SIZE	DWG. NO.	REV
B	2016DBF_WPI_THREE_VIEW	A

SCALE: 1:15 | WEIGHT: | SHEET 4 OF 6

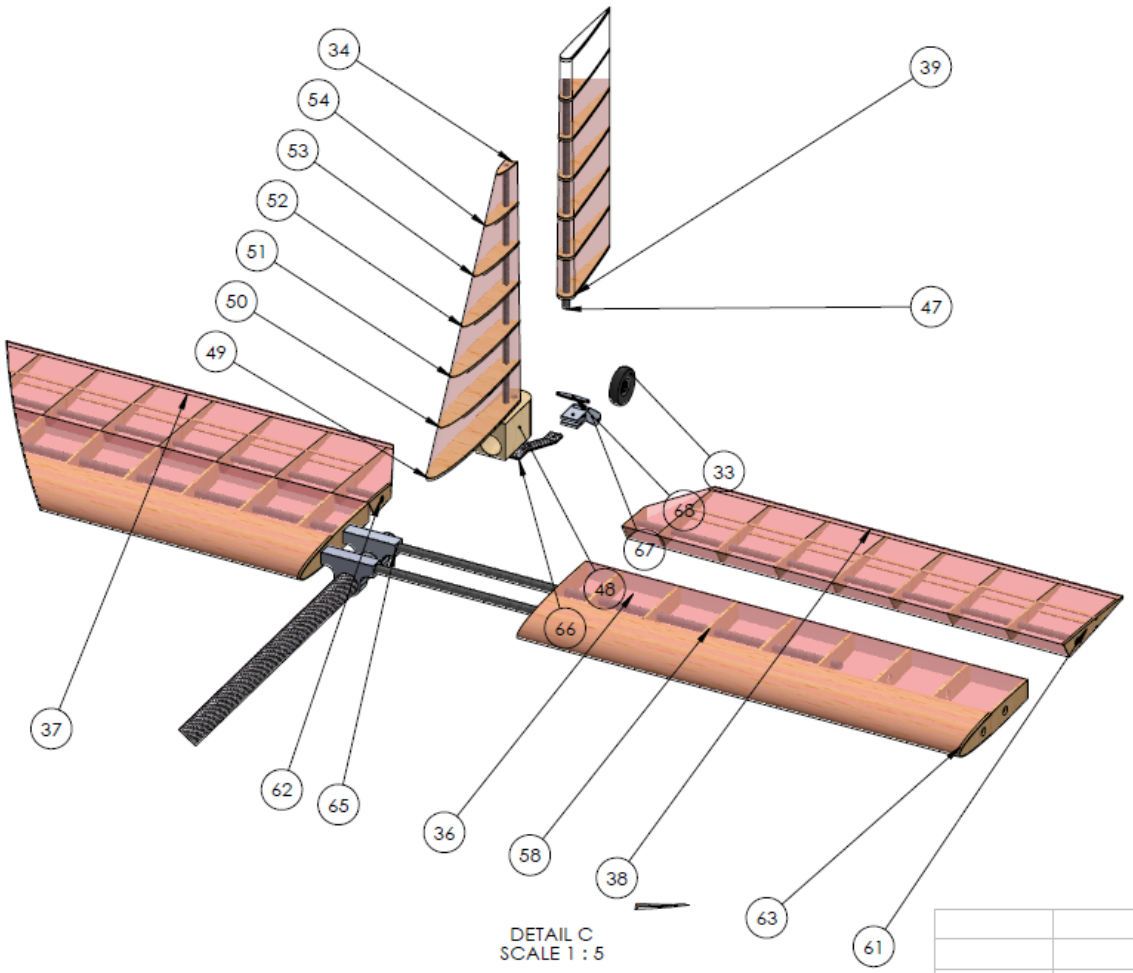

DETAIL C
SCALE 1 : 5

ITEM NO.	PART NUMBER	MATERIAL	Default/ QTY.
33	Back_Wheel_tire	Rubber	1
34	Tail Vertical Skin	Monokote	1
36	Tail Horizontal Skin	Monokote	2
37	Elevator Skin	Monokote	1
38	Elevator Skin Left	Monokote	1
39	Rudder rib	Balsa	6
46	Vertical tail rod	Custom Carbon Fiber Tube	1
47	Vertical Rudder rod	Custom Carbon Fiber Tube	1
48	Tail Fuselage Fitting	Pine	1
49	Tail Vertical Front 1	Balsa	1
50	Tail Vertical Front 2	Balsa	1
51	Tail Vertical Front 3	Balsa	1
52	Tail Vertical Front 4	Balsa	1
53	Tail Vertical Front 5	Balsa	1
54	Tail Vertical Front 6	Balsa	1
58	Tail Horizontal front	Balsa	18
61	Elevator Rib	Balsa	16
62	Elevator Smaller Rib	Balsa	2
63	Tail Horizontal LE	Balsa	2
65	Back Horizontal Tail fitting	6061 Alloy	1
66	Tail Wheel bracket	Thornel Mat VMA	1
67	Tail Wheel bracket extra piece	6061 Alloy	1
68	Wheel Bracket Rudder adapter	6061 Alloy	1

		UNLESS OTHERWISE SPECIFIED:		NAME	DATE
		DIMENSIONS ARE IN METERS TOLERANCES: FRACTIONAL ±.0.1 ANGULAR: ±.01° TWO PLACE DECIMAL ±.01	DRAWN	LDP	2/21/16
			CHECKED		
			ENG APPR.		
			MFG APPR.		
		INTERPRET GEOMETRIC TOLERANCING PER: ASME Y14.5	Q.A.		
		MATERIAL	COMMENTS:		
NEXT ASSY	USED ON	FINISH			
APPLICATION		DO NOT SCALE DRAWING			

TITLE:
Goats on Parade -
Detail View C
Manufacturing Support

SIZE	DWG. NO.	REV
B	2016DBF_WPI_THREE_VIEW	A
SCALE: 1:15	WEIGHT:	SHEET 5 OF 6

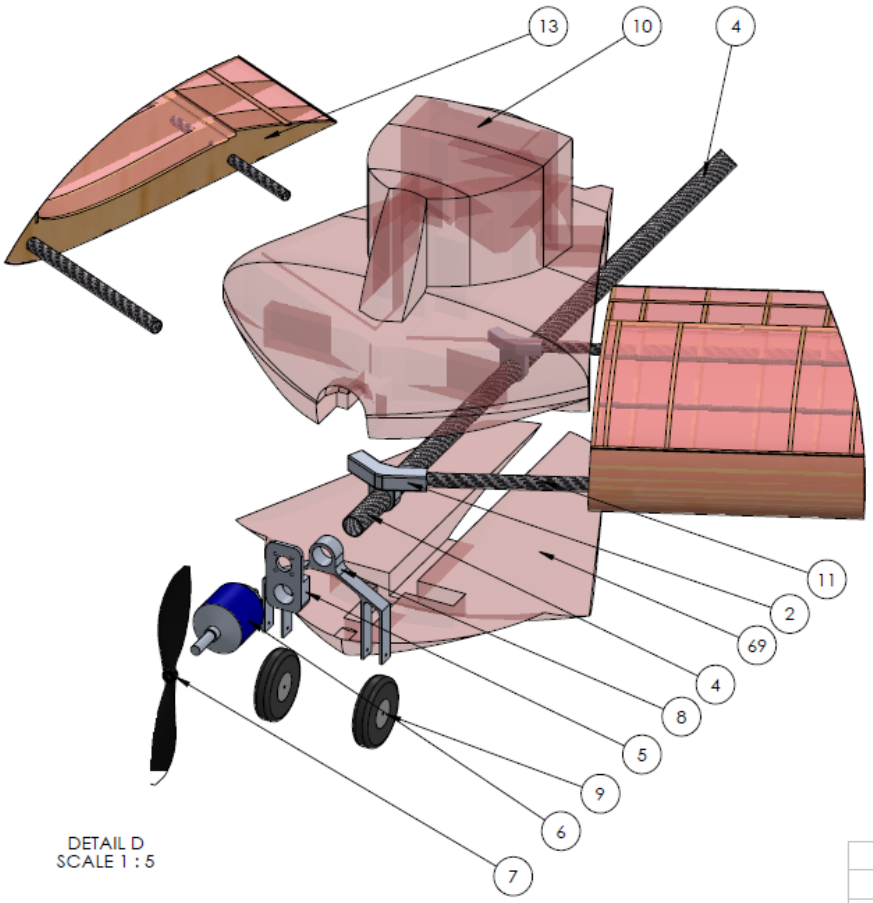

DETAIL D
SCALE 1 : 5

ITEM NO.	PART NUMBER	MATERIAL	QTY.
2	FrontMS_fitting_AlBox MS	6061 Alloy	1
3	BackMS_Aft_fitting_Al Box	6061 Alloy	1
4	Central Carbon FiberTube	Custom Carbon Fiber Tube	1
5	MS_Motor_Mount Plate	6061 Alloy	1
6	MS_Motor		1
7	Propeller 13in		1
8	Front gear	6061 Alloy	1
9	FrontWheel	Rubber	2
10	Fuselage Top	Polyurethane Foam Rigid	1
11	MSWingFrontRod	Custom Carbon Fiber Tube	2
12	MSWingBackRod	Custom Carbon Fiber Tube	2
13	NACA4418	Balsa	22
69	Fuselage Bottom	Polyurethane Foam Rigid	1

UNLESS OTHERWISE SPECIFIED:
DIMENSIONS ARE IN METERS
TOLERANCES:
FRACTIONAL ±.0.1
ANGULAR: ±.01°
TWO PLACE DECIMAL ±.01
INTERPRET GEOMETRIC TOLERANCING PER: ASME Y14.5
MATERIAL
FINISH
DO NOT SCALE DRAWING

NEXT ASSY | USED ON
APPLICATION

	NAME	DATE
DRAWN	LDP	2/21/16
CHECKED		
ENG APPR.		
MFG APPR.		
Q.A.		
COMMENTS:		

TITLE:
Goats on Parade -
Detail View D
Manufacturing Support

SIZE B | DWG. NO. 2016D8F_WPI_THREE_VIEW | REV A
SCALE: 1:15 | WEIGHT: | SHEET 6 OF 6

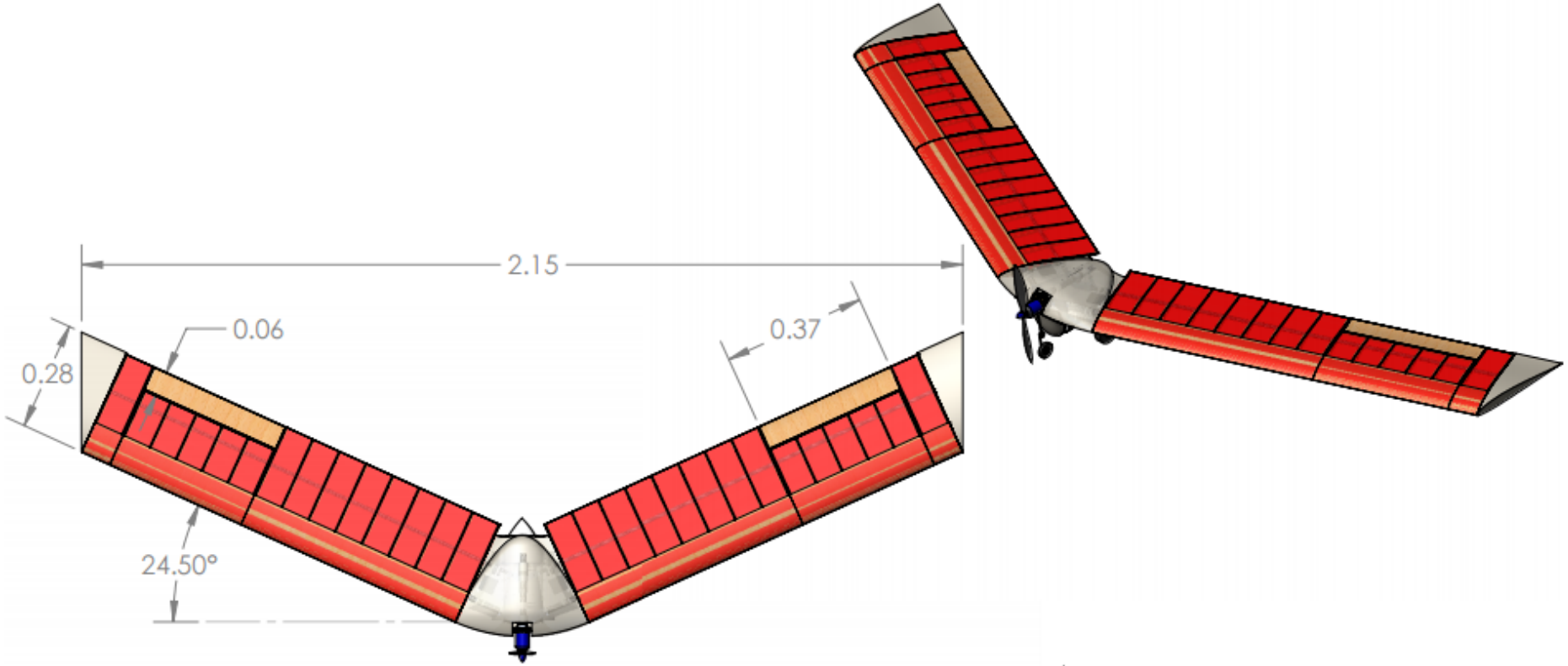

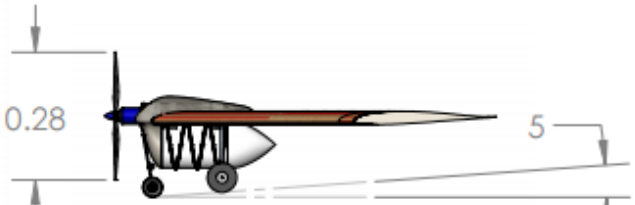

UNLESS OTHERWISE SPECIFIED:		NAME	DATE	UNIVERSITY AND TEAM: WPI Goats on Parade	
DIMENSIONS ARE IN METERS TOLERANCES: FRACTIONAL ± .01 ANGULAR: ± .01° TWO PLACE DECIMAL ± .01	DRAWN	RD	2/21/16		
	CHECKED	LDP	2/22/16	TITLE: PRODUCTION AIRCRAFT	
	ENG APPR.				
	MFG APPR.				
INTERPRET GEOMETRIC TOLERANCING PER: ASME Y14.5	Q.A.				
MATERIAL	COMMENTS:			SIZE A	DWG. NO. 2016DBF_WPI_THREE_VIEW
FINISH					REV
NEXT ASSY / USED ON				SCALE: 1:16	SHEET 1 OF 2
APPLICATION	DO NOT SCALE DRAWING				

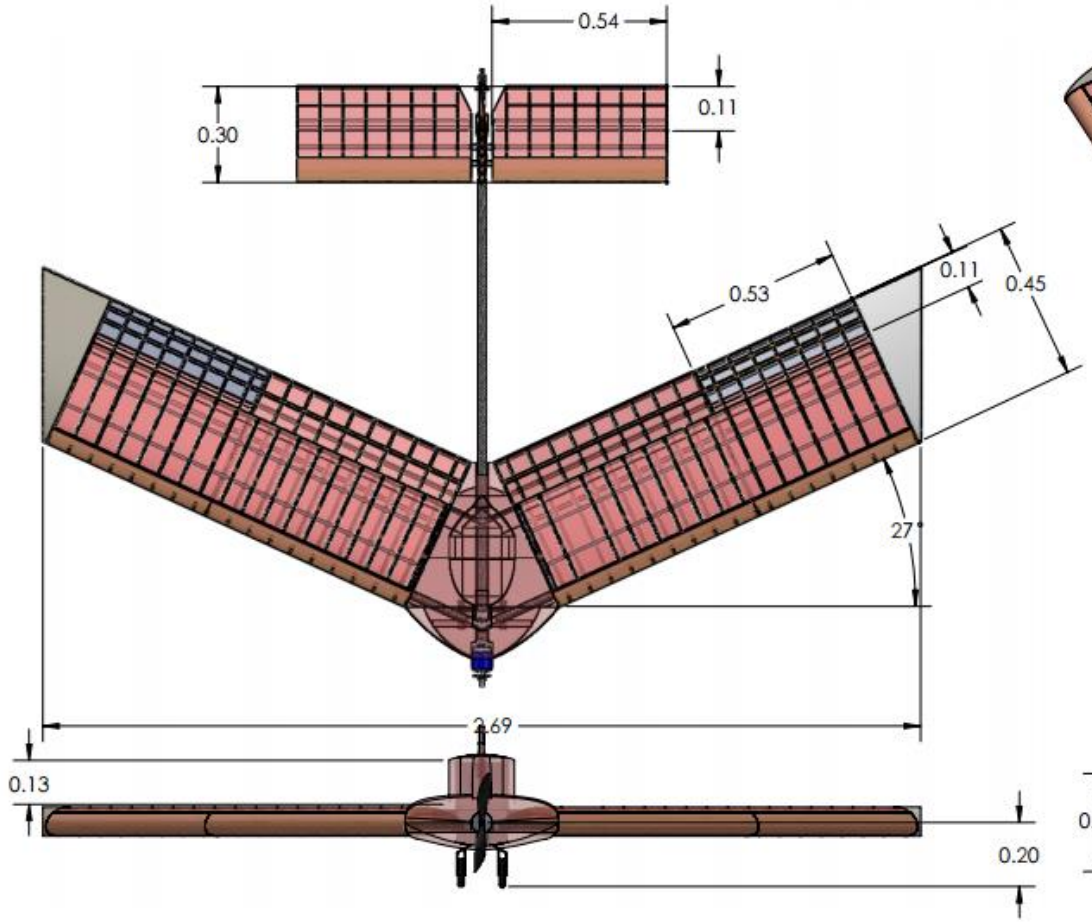

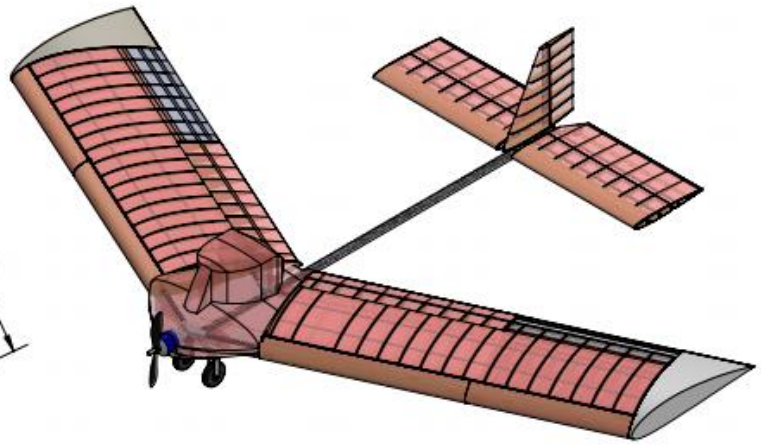

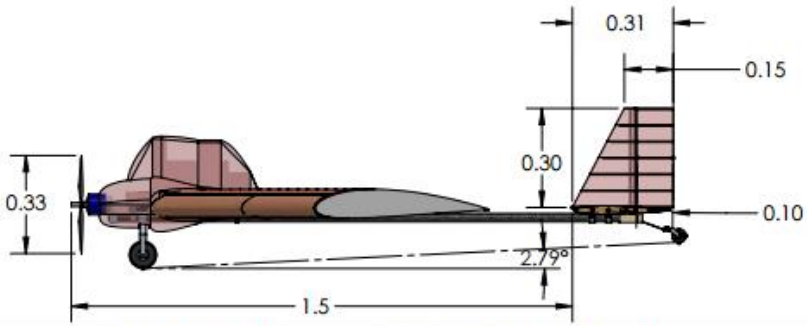

SOLIDWORKS Student Edition.
For Academic Use Only.

UNLESS OTHERWISE SPECIFIED:
DIMENSIONS ARE IN METERS
TOLERANCES:
FRACTIONAL ± 0.1
ANGULAR: ± .01°
TWO PLACE DECIMAL ± .01
INTERPRET GEOMETRIC TOLERANCING PER: ASME Y14.5
MATERIAL
FINISH
NEXT ASSY | USED ON
APPLICATION | DO NOT SCALE DRAWING

	NAME	DATE
DRAWN	RD	2/21/16
CHECKED	BA	2/22/16
ENG APPR.		
MFG APPR.		
Q.A.		
COMMENTS:		

University and team:
WPI Goats on Parade

TITLE:
MANUFACTURING SUPPORT

SIZE	DWG. NO.	REV
B	2016DBF_WPI_THREE_VIEW	A
SCALE: 1:15	WEIGHT:	SHEET 2 OF 2

References

[1] Newcome, Lawrence. *Unmanned Aviation: A Brief History of Unmanned Aerial Vehicles*. Reston: American Institute of Aeronautics and Astronautics, 2004. Web

[2] "Design, Build, Fly Competition." AIAA Shaping the Future of Aerospace. American Institute of Aeronautics and Astronautics, 2015. Web. 24 Apr. 2016.

[3] "2015/16 Rules and Vehicle Design." Design Build Fly 2015/16 Contest Year 20th Annual Event. AIAA, Oct. 2015. Web. 31 Oct. 2015.

[4] Raymer, Daniel P. *Aircraft Design: A Conceptual Approach*. 5th ed. Reston: American Institute of Aeronautics and Astronautics, 2012. Print.

[5] Crathern, Kyle, Reinaldo Fonseca Vieira Lopes, Timothy Momose, and Neil Pomerleau. *Micro Aircraft Competition Design: Flying Wing*. Worcester: Worcester Polytechnic Institute, 2013. Web.

[6] "Bending Thermal Stresses in Plates." Design for Thermal Stresses Barron/Design for Thermal Stresses (2011): 264-316. Web.

[7] *CES EduPack.* Computer software. Granta Material Intelligence, n.d. Web. Sept. 2015.

[8] *DBF Logo*. N.d. *Design Build Fly 2015/16 Contest Year 20th Annual Event*. Web. 10 Sept. 2015.